The impacts of volcanism on hydrocarbon-bearing sedimentary basins - Examples from the world-class Neuquén Basin case study, Argentina

Olivier Galland[1], Sabina Chiacchiera[2], Hernán de la Cal[2,3], Dougal A. Jerram[1,4], Ezequiel Lombardo[5,6], J. Octavio Palma[2], Gisel Peri[6], Ole Rabbel[1], Juan B. Spacapan[7], Maria Dolores Vallejo[5], Daniel Yagupsky[6,8], Alain Zanella[9]

[1] Njord Center, Department of Geosciences, University of Oslo, Oslo, Norway
[2] Facultad de Ciencias Naturales y Museo, Universidad Nacional de La Plata, La Plata, Argentina
[3] ROCH S.A.
[4] DougalEARTH Ltd., Solihull, UK
[5] Chevron Argentina
[6] Departamento de Ciencias Geológicas, Facultad de Ciencias Exactas y Naturales, Universidad de Buenos Aires, Buenos Aires, Argentina
[7] Y-TEC S A, Av del Petróleo Argentino, Buenos Aires, Argentina
[8] Instituto de Estudios Andinos Don Pablo Groeber (IDEAN), CONICET – Universidad de Buenos Aires, Buenos Aires, Argentina
[9] Laboratoire de Planétologie et Géosciences, LPG – UMR 6112 CNRS, Le Mans Université, Université d'Angers, Nantes Université, Le Mans Université, Le Mans, France

This paper is a non-peer reviewed preprint submitted to EarthArXiv. This preprint was submitted to peer-review journal Global and Planetary Change.

Abstract

The last two decades of research have highlighted that volcanism occurring in sedimentary basins can have substantial effects on sedimentary formations. In particular, igneous intrusions can trigger the generation of large amounts of greenhouse gases in organic-rich host rocks, leading to dramatic climate change and mass extinctions. Volcanism can also have significant impacts on hydrocarbon-bearing sedimentary basins. The Neuquén Basin, Argentina, is an outstanding example of hydrocarbon-producing sedimentary basin hosting massive volcanism. The combination of substantial industry subsurface data and outstanding outcrops makes the Neuquén Basin a world-class geological object to study magma-sedimentary rock interactions and their implications to hydrocarbon systems. This contribution reviews well-studied examples from the Neuquén Basin that illustrate: (1) thermal effects of sills on maturation of the organic matter of the source rock, (2) fracturing processes in igneous intrusions and the host rock, (3) sills as producing fractured reservoirs, (4) intrusion-induced doming as structural trap or as potential fractured reservoir, (5) fluid migration along igneous intrusions, (6) reservoir compartmentalization induced by dykes, (7) generation of bitumen dykes in vicinity of intrusions, and (8) improvement of geophysical imaging using large-scale outcrops.

All in all, our review (1) documents various effects of magma-rock interactions in hydrocarbon-bearing sedimentary basins, and (2) highlights the great scientific value of the Neuquén Basin as a world-class case study for unravelling processes of magma-rock interactions in hydrocarbon-bearing sedimentary basins.

1 Introduction

Sedimentary basins have been major providers of geological resources for mankind, such as oil, gas, coal, drinking water, geothermal warm water, minerals, building materials (e.g., Kilhams et al., 2024, and references therein). Conventional geological knowledge motivating resource exploration in sedimentary basins principally involves sedimentology and tectonics (Howell et al., 2005; Hudec and Jackson, 2007). Nevertheless, research has highlighted that numerous sedimentary basins host significant volcanic activity, the so-called volcanic basins (Rohrman, 2007; Senger et al., 2017; Jerram et al., 2022; Kilhams et al., 2024; and references therein). The impacts of volcanism on sedimentary basins are tremendous, with implications for hydrocarbons exploration (Petford and McCaffrey, 2003; Schutter, 2003; Rohrman, 2007; Delpino and Bermúdez, 2009; Senger et al., 2017), groundwater (Chevallier et al., 2001; Chevallier et al., 2004), geothermal energy (e.g., Bischoff et al., 2025) and carbon storage (e.g., Schmitt et al., 2023; Johannesen et al., 2025). In addition, the magma/sediment interactions during the Earth's history lead to the release of large amounts of greenhouse and poisonous gases in the atmosphere, leading to dramatic climate changes and mass extinctions (Courtillot and Renne, 2003; Svensen et al., 2004; Svensen et al., 2007; Svensen et al., 2009).

This paper focuses on the impacts of volcanism on hydrocarbon-bearing sedimentary basins. Hydrocarbon accumulations are associated with igneous rocks in more than 100 countries across the globe (Schutter, 2003), however very few volcanic basins have been subject to commercial production. Examples include the Mesozoic-Cenozoic basins of eastern China (Gu et al., 2002; Wu et al., 2006; Jiaqi et al., 2012), the Mesozoic Neuquén Basin in Argentina (e.g., Rodriguez Monreal et al., 2009; Witte et al., 2012; Spacapan et al., 2020a), tuffaceous reservoirs in Tierra del Fuego, Argentina (Feinstein et al., 2022; D'Elia et al., 2023) and West Java (Farooqui et al., 2009), intrusion hosted reservoirs in Thailand (Schutter, 2003), and the Parnaiba Basin, Brazil (de Miranda et al., 2018). In addition, magmatic activity has played a key role in the petroleum systems of many other basins worldwide (Senger et al., 2017).

Delpino and Bermúdez (2009) defined two main types of petroleum systems associated with igneous rocks. Type I igneous petroleum system corresponds to igneous rocks intruded into a potential source rock. Type I includes three sub-types corresponding to the degree of maturation of the source rock at the time of

emplacement of the magma. In Type IA, the source rock is immature to early mature, in Type IB the source rock is mature, whereas in Type IC the host rock is postmature when magma is emplaced. These different subtypes lead to different scenarios in terms of hydrocarbon generation. Type II igneous petroleum systems are defined when the igneous rocks are intruded in host rock layers that are not source rocks. Similarly to Type I, Type II igneous petroleum systems are subdivided in three subtypes. In Type IIA, sills and laccoliths were emplaced in host rocks that are well known productive formations in the basin, generally sandstones or carbonates. In Type IIB, the host rock is a tight formation, and the intrusion-related fracturing can improve reservoir quality. In Type IIC, feeders such as dykes can act as barriers that can be part of a trap or compartmentalise a reservoir. We will see in this paper that this classification is incomplete, as intermediate scenarios can also be documented.

There are numerous challenges for studying the impacts of volcanism on hydrocarbon-bearing sedimentary basins. First, numerous volcanic basins are offshore (Senger et al., 2017), e.g. the North Atlantic Margin (e.g., Svensen et al., 2004; Thomson, 2007; Fjeldskaar et al., 2008; Rateau et al., 2013; Mark et al., 2018), offshore Australia (Jackson et al., 2013b; Magee and Jackson, 2020), South Atlantic (Abdelmalak et al., 2025), offshore New Zealand (Bischoff et al., 2017; Morley, 2018; Bischoff et al., 2020) and China Sea (Liu et al., 2017; Sun et al., 2019), such that geological processes can only be studied through seismic data or borehole data. The resolution of, and imaging challenges associated with, seismic data are insufficient to address the complex structure geometries and processes of volcanic features emplaced in sedimentary basins, and borehole data only provide 1D, very expensive data. Similar challenges are faced in onshore volcanic basins that are not exhumed, such as the Tarim Basin, China (Yao et al., 2018) and the Parnaiba Basin, Brazil (de Miranda et al., 2018). Other volcanic basins are well exposed, such as the Karoo-Ferrar Basins (e.g., Svensen et al., 2007; Jerram et al., 2010; Polteau et al., 2010; Muirhead et al., 2012; Svensen et al., 2012), the Tunguska Basin, Siberia (Svensen et al., 2009), Utah-Colorado (Gilbert, 1877; Jackson, 1997; de Saint-Blanquat et al., 2006; Wilson et al., 2016; Kjenes et al., 2024), Namibia (Jerram D et al., 2000; Bauer et al., 2003), the Oslo Rift, Norway (Poppe et al., 2020; Neumann et al., 2025), such that geological field studies can be conducted. However, these basins have not been prospective for hydrocarbons, so that very limited subsurface data have been collected.

The Neuquén Basin, Argentina, is a unique hydrocarbon-bearing volcanic basin that provides both (1) large subsurface seismic and borehole data thanks to commercial hydrocarbon production from igneous petroleum systems and (2) exceptional outcrop analogues resulting from the combination of Andean tectonics and semi-arid climate. In this paper, we provide a review of geological case studies in the Neuquén Basin that illustrate numerous aspects of the impacts of volcanism on hydrocarbon-bearing sedimentary basin. Our review shows that the Neuquén Basin is an easily accessible, world-class case study for studying the impacts of volcanism on hydrocarbon systems, with values for academic and applied research, as well as for education of geoscientists.

The described case study examples will allow addressing the following processes and challenges (Figure 1):

- the thermal impacts of igneous intrusions on source rock formations, based on (i) subsurface data from productive oil fields and (ii) surface geological observations from an exhumed field analogue;
- The structural impacts of igneous intrusions. We will describe (i) how sills can be complex fractured reservoirs, (ii) how an intrusive complex generated crustal doming that acts as hydrocarbon trap, and (iii) how faulting along the edge of a laccolith-induced doming can be a target for a fractured reservoir;
- The impacts of igneous intrusions on fluid migrations. We will describe (i) how cooling igneous intrusions generate high-grade hydrocarbons and affect their migration, (ii) how cooled, fractured igneous intrusions represent long-term high-permeability pathways that may control large-scale hydrocarbon migration, and (iii) how impermeable igneous intrusions may represent seals and barriers that can compartmentalise conventional reservoirs;
- The role of volcanism on the formation of bitumen veins, which are peculiar geological structures that accommodate sudden migration of large volumes of hydrocarbons;
- The impacts of volcanism on geophysical imaging in volcanic basins. We will describe examples of (i) how realistic seismic modelling of sill complexes can help interpreting seismic data of basins hosting igneous sills, (ii) how to image subvertical igneous dykes from 3D seismic data, (iii) how to improve

subvolcanic seismic imaging, and (iv) how to use AMT surveys to image igneous intrusions emplaced in source rock formations.

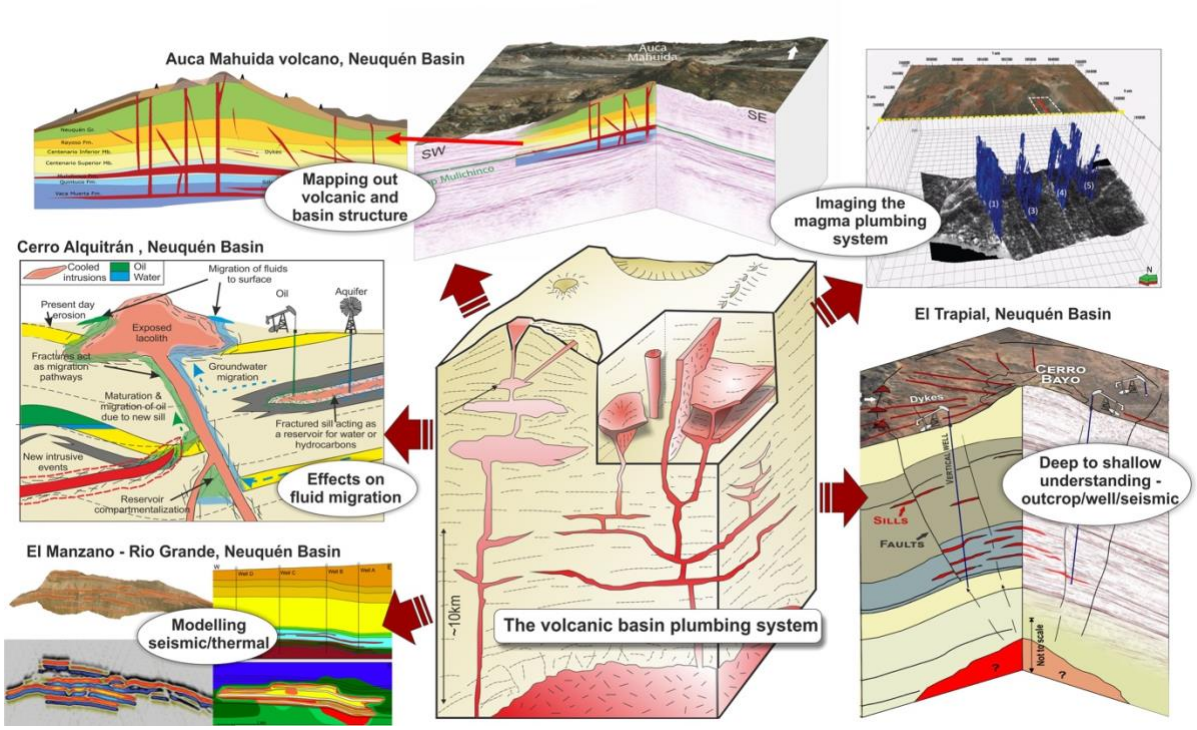

Figure 1. The volcanic plumbing system from the deep intrusive roots to the shallow intrusions and eruptive products (modified from Jerram, 2021). The Neuquén Basin provides a number of windows into the aspects of the volcanic plumbing system. The magma pathway through a sedimentary basin will permanently alter the basin's structure and properties. Modelling of the effects of intrusions and their seismic expression can help understand this impact (e.g. El Manzano – Rio Grande; Rabbel et al., 2018; see Section 7; Spacapan et al., 2018; see Section 3). There is a direct effect on the porosity and permeability pathways through igneous effected basin, as highlighted at Cerro Alquitrán and surrounding intrusions (Galland et al., 2023; Galland et al., 2024; see Section 5). Active volcanoes such as Auca Mahuida are shown to have domed structures linked to their shallow and deep plumbing systems (Delpino et al., 2014b; Basaldúa and Cristallini, 2022; see Section 5). In eroded volcanic centres such as El Trapial, the detail provided by both surface and subsuface data can reveal key elements of the structure and intrusive network beneath such volcanoes (Lombardo et al., 2024; see Section 4; Lombardo et al., under review; see Section 7).

2 Geological setting: the Neuquén Basin

2.1 Formation and evolution of the Neuquén Basin

The Neuquén Basin is located on the eastern flank of the Andes in Argentina and central Chile, between latitudes 32°S and 40°S (Figure 2). The basin encompasses sedimentary sequences dating from Late Triassic to early Cenozoic (Figure 3), covering an area of more than 120 000 km^2, and containing up to 6000 m of preserved marine and continental deposits (Gulisano and Gutiérrez Pleimling, 1995; Vergani et al., 1995; Cobbold and Rossello, 2003). The marine sedimentary layers consist primarily of shale, sandstone and carbonate (Figure 3), reflecting the varying depositional environments in the basin over time. Extensive volcanic deposits and intrusive complexes developed primarily in the back-arc region during the evolution of the Andean subduction zone throughout the Eocene and Miocene (Kay et al., 2006a).

The evolution of the Neuquén Basin can be summarized in three stages (Vergani et al., 1995; Howell et al., 2005; Veiga et al., 2020): (1) rift stage or synrift stage (Late Triassic–Early Jurassic), (2) thermal subsidence stage (sag stage) or postrift phase (late Early Jurassic–Early Cretaceous), and (3) foreland stage (Late Cretaceous-Neogene), related to Andean uplift (Figure 3). The rift stage is characterized by the formation of isolated rift depocenters during the Late Triassic, which were filled with synrift deposits associated with the Precuyano Cycle. During the subsequent sag stage, the previously isolated depocenters merged, forming a more extensive basin that was filled with characteristic sedimentary deposits of the Neuquén Basin. This sag phase led to the deposition of the Cuyo, Lotena, and Mendoza Groups (Figure 3). The Mendoza Group comprises: the early Tithonian-early Valanginian Vaca Muerta Formation (~1,250–1,400 m thick), characterized by bituminous mudstones deposited under anoxic conditions (Sylwan, 2014; Brisson et al., 2020; Minisini et al., 2020), and the late Valanginian-early Barremian Agrio Formation (~2,509–3,000 m thick), consisting of transgressive, organic-rich marlstones (Sylwan, 2014). Note that locally the Agrio Formation is deposited directly upon the Vaca Muerta Formation, however usually the middle Valanginian Mulichinco or Chachao Formations is intercalated between them (Figure 3). The Mulichinco Formation, found in central and southern part of the basin, are sandstone deposited in a mixed wave and tidal flat environment (Schwarz and Howell, 2005; Sleveland et al., 2020). Conversely, the

Chachao Formation, found in the northern part of the basin, represents a carbonate ramp rich in biogenic material (Kozlowski et al., 1993b; Brisson and Veiga, 1998). Subsequent deposition occurred in restricted hypersaline marine environments, resulting in the evaporitic Huitrín Formation, followed by continental fluvial and lacustrine deposits of the Rayoso Formation (Figure 3)(Vergani et al., 1995). During the Early Cretaceous, the tectonic regime gradually shifted to a compressive setting due to a decrease in the subduction angle of the Nazca Plate. This marked the end of the retroarc-sag stage and the onset of the foreland phase associated with the Andean orogeny (Cobbold and Rossello, 2003; Ramos et al., 2010), evidenced by the deposition of the Late Cretaceous synorogenic continental red beds of the Neuquén Group unconformably overlying previous Mesozoic units (Tunik et al., 2010; Fennell et al., 2017).

2.2 The petroleum systems of the Neuquén Basin

From the Lower Jurassic to the Lower-Late Cretaceous, three main petroleum systems developed (Urien and Zambrano, 1994). Their names are derived from the formation of the source rock, followed by the name of the major reservoir rock. In chronological order, they are: Los Molles-Lajas (Cuyo Group), Vaca Muerta-Tordillo, and Agrio-Avilé (Figure 3).

According to Villar et al. (2005), the source rocks of the Los Molles, Vaca Muerta, and Agrio formations primarily consist of organic-rich black shales deposited in basinal and outer-shelf marine environments, each with varying hydrocarbon generation potential. The clastic rocks of the Lajas, Tordillo, and Avilé formations are predominantly sandstones deposited in shallow-water deltaic and marine settings (Maretto et al., 2002; Masarik, 2002; McHilroy et al., 2005). These sandstone bodies, together with shallow-marine carbonate rocks, constitute most of the reservoir rock. Thick evaporite deposits, mainly gypsum and halite, frequently act as regional seals. The Vaca Muerta Formation is the main source rock in the Neuquén Basin. Together with the Quintuco Formation, it forms the Vaca Muerta-Quintuco system, which has attracted increasing interest due to its quality as an unconventional reservoir (Sagasti et al., 2014; Zeller et al., 2015; Acevedo and Bande, 2018; Estrada et al., 2018; Ukar et al., 2020).

The numerous andesitic to basaltic sills, predominantly emplaced in the source rock formations of the Mendoza Group, serve as the main fractured reservoirs of the hydrocarbon fields along the Río Grande Valley (Schiuma, 1994; Witte et al., 2012; Spacapan et al., 2020a; Rabbel et al., 2021). Meanwhile, in the Huantraico region, large-scale doming of the Mesozoic strata associated with magma emplacement forms the structural trap of the El Trapial oil field, one of the most prolific in the Neuquén Basin (González and Aragón, 2000; Orchuela et al., 2003; Lombardo et al., 2024).

2.3 Cenozoic igneous activity in the Neuquén Basin

Over the past 65 million years, the evolution of the active Andean convergent margin has played a key role in shaping the timing and distribution of igneous activity throughout the Neuquén Basin. The subduction of the oceanic Nazca Plate beneath the continental South American Plate has produced a magmatic arc that runs roughly parallel to the margin. At the surface, this subduction-driven volcanism forms a volcanic arc, whose width has shifted multiple times in an east–west direction, as well as voluminous back-arc volcanism (Kay et al., 2006a). Kay et al. (2006a) attribute these variations to changes in the age and subduction angle of the oceanic plate. In the subsurface, this volcanic activity is expressed through a series of shallow intrusive bodies with diverse compositions and geometries, including dioritic and granodioritic laccoliths, doleritic sills, and swarms of both felsic and mafic dykes.

The first significant episode of volcanic activity spread between Chos Malal and Zapala, and west of Chos Malal during Eocene. This episode resulted in the diorite intrusive complexes of the Collipilli Formation (Llambías and Rapela, 1988), consisting of dykes, sills, laccoliths and plugs emplaced in the source rock formations of the Mendoza Group, and the andesitic volcanic deposits of the Cayanta Formation (Kay et al., 2006a). The geochemistry of the igneous rocks emplaced during this episode exhibits characteristic arc composition. Given the location of these arc-related igneous rocks, the subducting slab was interpreted to dip 30 degrees (Kay et al., 2006a).

In Lower Miocene, an active volcanic arc remained at a similar position as that in the Eocene (Kay et al., 2006a). However, extensive retro-arc magmatism occurred through large portions of the Neuquén Basin. In the northern sector of the basin (Figure 2), volcanism produced extensive lava flow sequences (Nullo et al., 2002; Dyhr et al., 2013b; Søager et al., 2013) along with numerous basaltic to andesite sills, dikes and

laccoliths (e.g. Pampa Amarilla laccolith, see sections 4.3 and 7.4)(Barrionuevo et al., 2019; Galland et al., 2022), primarily intruded into the source rock formations of the Mendoza Group. The sills hosted within these organic-rich formations represent the primary fractured reservoirs for hydrocarbon fields along the Río Grande Valley (Schiuma, 1994; Witte et al., 2012; Spacapan et al., 2020a) and at the Altiplanicie del Payún (Rodriguez Monreal et al., 2009; Delpino et al., 2014a). Exposed analogues of these igneous petroleum systems are found at El Manzano (Rabbel et al., 2018; Rabbel et al., 2023)(see sections 3.1, 4.1, 5.1 and 7.1), the Sierra de Cara Cura (Palma et al., 2024b)(see sections 3.2 and 5.1) and the Cuesta del Chihuido intrusive complexes (Spacapan et al., 2016, 2017; Barrionuevo et al., 2019). In this area, this volcanism has been assigned to a volcanic cycle named Molle Volcanic Cycle (Nullo et al., 2002).

South of Río Colorado, in the northern part of Neuquén Province, significant Lower Miocene retroarc volcanism occurs within the Huantraico region (Ramos and Barbieri, 1988), situated between the Tromen volcanic massif to the west and the Auca Mahuida volcano to the east (Figure 2). The first volcanic activity of the area resulted in felsic tuff, followed by thick intercalations of basalts and tuffs that constitute the volcanic pile of the Sierra de Huantraico (Palaoco Formation; Groeber, 1946; Holmberg, 1975; Ramos and Barbieri, 1988). These eruptive products were likely fed, at least partly, by large radial dyke swarms of Cerro Bayo de la Sierra Negra (CBSN, also called Cerro Bayo Trapial; see section 4.2) and around Sierra de Huantraico (Ramos and Barbieri, 1988). During the Lower Miocene, the geochemical compositions of the basalts exhibit an upward increasing arc component in the volcanostratigraphy, suggesting a gradual shallowing of the subducting slab (Kay and Copeland, 2006; Dyhr et al., 2013a; Dyhr et al., 2013b).

During Upper Miocene, the shallowing of the subducting slab resulted in arc, typical andesitic volcanism. In the southern part of the Neuquén Basin, this activity resulted in the build-up of Chachahuén Volcano (Holmberg, 1962; Kay et al., 2006b; Palma et al., 2024a) and an intrusive complex north of Chos Malal (Cerro Negro de Tricao Malal; Kay et al., 2006a; Gürer et al., 2015). In the northern sector of the Neuquén Basin, this Upper Miocene arc volcanism resulted in shallow laccoliths of the La Brea andesitic formation (Nullo et al., 2002), which includes the Cerro Alquitrán and Cerro La Paloma intrusions, from which large amounts of bitumen seep naturally (see section 5.2)(Galland et al. 2023; 2024). The volcanic activity associated with the La

Brea andesitic magmatism has been assigned to a volcanic cycle named Huincán Volcanic Cycle (Nullo et al., 2002).

Finally, widespread Pliocene–Quaternary back-arc volcanism, associated with the steepening of the slab, spread through the Neuquén Basin with the build-up of the Auca Mahuida (see section 5.3)(Rossello et al., 2002; Pallares et al., 2016; Basaldúa and Cristallini, 2022), Payun Matrú (Ramos and Folguera, 2011; Søager et al., 2013) and Tromen volcanoes (Galland et al., 2007). The emplacement of these large back-arc volcanic systems lead to the emplacement of sills and laccoliths within the organic-rich shale formations of the basin (Rossello et al., 2002; Basaldúa and Cristallini, 2022) and likely large dyke complexes.

Note that the Neogene volcanism is restricted to the north of a crustal-scale structural lineament, the so-called Cortaderas Lineament (Figure 2)(Cobbold and Rossello, 2003; Kay et al., 2006a).

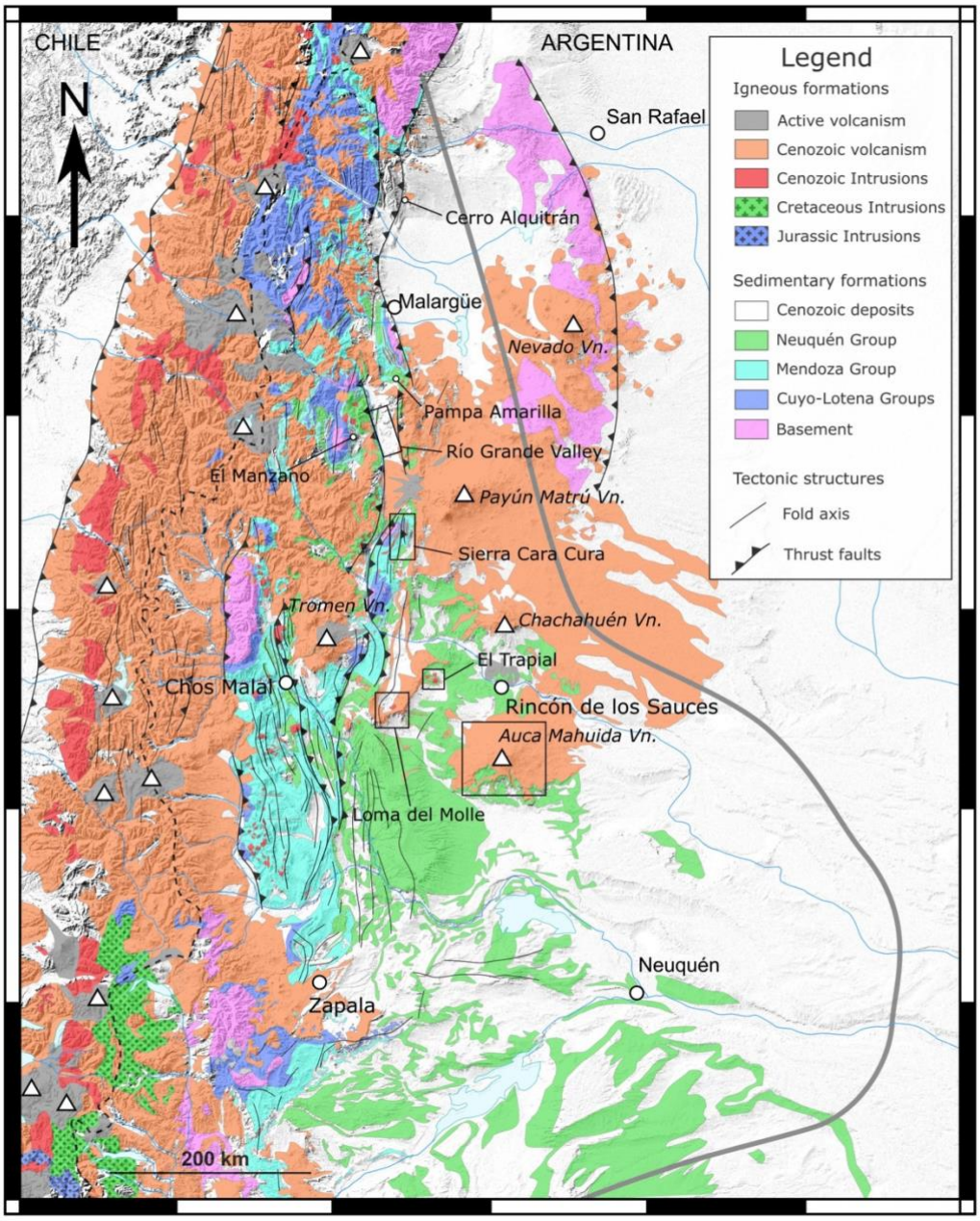

315

316 Figure 2. Simplified geological map of the Neuquén Basin locating main volcanic systems and
317 case studies developed in this paper. Modified from Palma et al. (2024b).

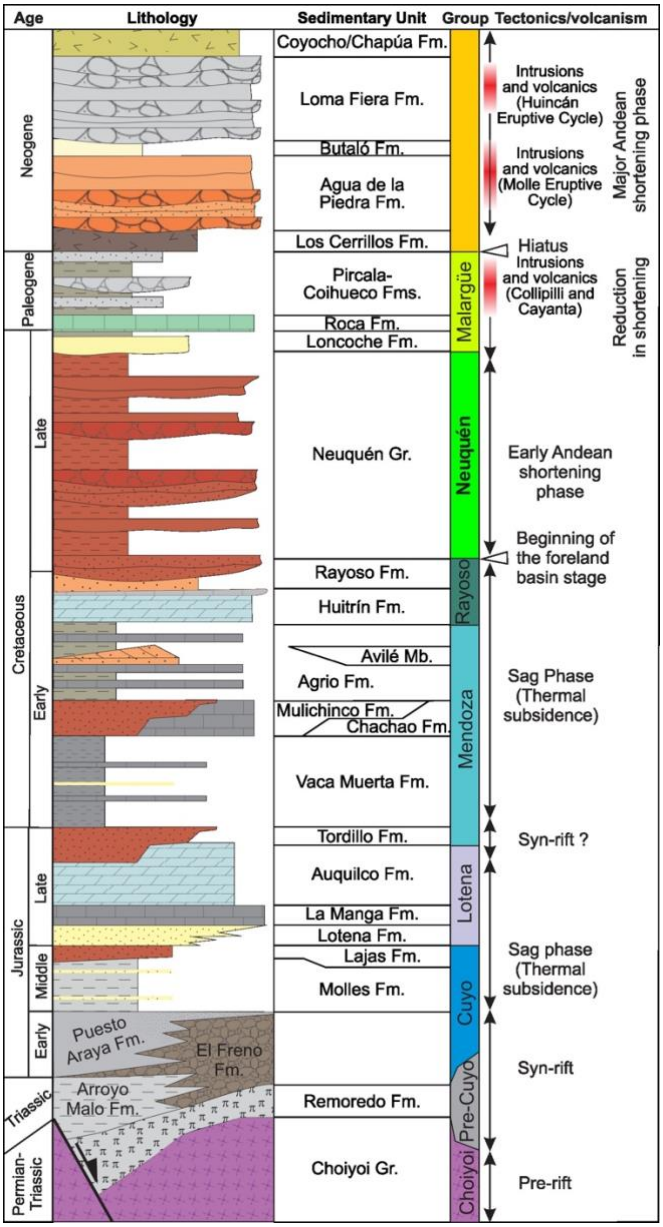

Figure 3. Synthetic stratigraphic column of the Neuquén Basin. Modified from Barrionuevo et al. (2019) and Galland et al. (2022).

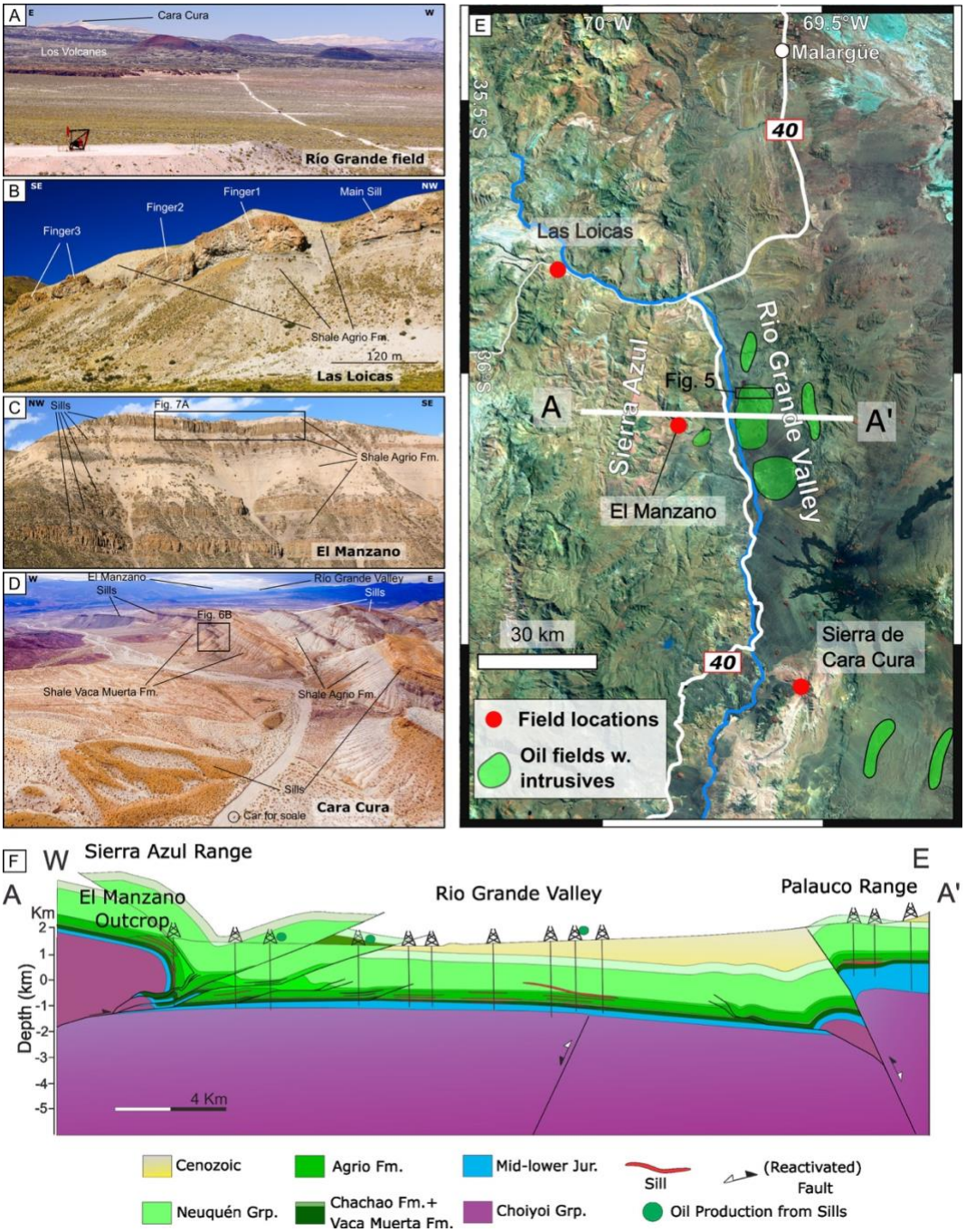

Figure 4. A. Field photograph of oil field of the Río Grande Valley (see sections 3.1, 4.1 and 7.1). B. Field photograph of sills emplaced in organic-rich shale of Agrio Formation, Las Loicas (modified from Galland et al., 2019). C. Field photograph of andesitic sills emplaced in organic-rich shale of Agrio Formation, El Manzano (see sections 5.1, **Error! Reference source not found.** and 7.1). D. Drone photograph of part of Cara Cura range (see section 3.2). Locations of field localities are indicated in map of Figure 2. E. Satellite image locating localities of A-D and oil fields with igneous intrusions. F. Geological cross section across Sierra Azul and Río Grande Valley, located in E (Spacapan et al., 2018; Rabbel et al., 2023).

3 Thermal impact of igneous intrusions on source rock maturation

3.1 Maturation at producing hydrocarbon fields

A key element of maturation of the organic matter in source rocks is heat. In conventional petroleum systems, the heat input results from burial and maturation takes place over millions of years. However, intrusions emplaced in organic-rich shale formations add immense amounts of heat at a time scale that is almost instantaneous with respect to geological time scales. Numerous studies have investigated the thermal effects of sills on their organic-rich host rock formations in numerous basins worldwide (Einsele et al., 1980; Svensen et al., 2004; Fjeldskaar et al., 2008; Svensen et al., 2009; Aarnes et al., 2010; Aarnes et al., 2011; Iyer et al., 2013; Galerne and Hasenclever, 2019), but none of them investigated producing petroleum systems. In this section, we address the thermal impact of sills emplaced within the organic-rich shale formations of the Vaca Muerta and Agrio formations, and how this additional heat was beneficial for the petroleum system in the Neuquén Basin.

The case study used here is the producing oil fields of the Río Grande Valley, southern Mendoza Province, south of the Bardas Blancas village (see location in Figure 2). The Río Grande Valley fields are typical Type I igneous petroleum systems, with sills emplaced in the Vaca Muerta and Agrio source rock formations of the basin. Note as well that the sills in these fields are the main reservoir rocks (see section 4.1). The valley is a morphologic depression with N-S orientation, bounded to the West by the basement-cored anticline of the Sierra Azul – Puntilla del Huincán and to the East by the Palauco, Cara Cura and Reyes ranges (Figure 4E)(Kozlowski et al., 1993a). The volcanic activity in the study area mainly occurred during the Late Oligocene-Middle Miocene Molle Eruptive Cycle (MEC) and the Late Miocene-Pliocene Huincán Eruptive Cycle (HEC), defined by Bettini (1982) and Combina and Nullo (2011). These eruptive cycles resulted in thick lava flow sequences, as well as numerous andesitic to basaltic sills dominantly emplaced in the source rock formations of the Mendoza Group.

Spacapan et al. (2018) performed basin models to test the thermal effects of the sills in the Río Grande Valley oil fields. The test consisted of comparing two end

member scenarios: a scenario that only accounts for regional burial but not for sill emplacement, and conversely a scenario that accounts for both regional burial and sill emplacement. The models with and without intrusions show drastic differences in temperature and maturation patterns.

In the model without intrusion, the shallowest maturation depth at present day is the base of the Huitrín Formation, with values of 0.55 to 0.7 %Ro, indicating early oil generation in Vaca Muerta and Agrio formations (Figure 5). In addition, only a very limited percentage of organic matter is transformed to hydrocarbons (TR 30% on average) in the Vaca Muerta Formation (Figure 5).

In the model with intrusions, however, the Vaca Muerta and Agrio formations reach the main oil to dry gas maturation windows (Figure 5). The highest degrees of maturity and the highest transformation ratios (80 % to 100 %) are concentrated in the surroundings of the sills. Further from the intrusions, the Vaca Muerta and Agrio formations exhibit lower degrees of maturation and lower transformation ratios, ranging 2-25 % (Figure 5). These results show that the source-rock maturation in the Río Grande Valley fields was dominated by the igneous intrusions, and that the maturation of the source rock formations was constrained to the intruded domains. Without sills, the source rock formations would be immature to marginally mature.

The models of Spacapan et al. (2018) also show that the thermal impact of sill-complexes depends on the sill-complex architecture. Parameters such as number of sills, sill spacing, sill thickness, sill composition and timing of emplacement, greatly affect the temperature distribution in the basin. The emplacement of several sills vertically superposed enhances source-rock maturation between the sills, and the extent of the maturation aureole is enhanced by the local number of intrusions (Figure 5). In addition, the coeval emplacement of several sills has larger thermal impact than successive sill emplacement, where each sill has time to cool down before the emplacement of the next sill (Spacapan et al., 2018). Also, the host rock background temperature, prior to the sill emplacement, has a significant impact on the extent and degree of host rock maturation. Therefore, the knowledge of the burial history of the organic-rich formations is essential for quantifying the thermal and maturation impacts of the sill-complex.

Because the seismic imaging of the sill-complex in the Río Grande Valley fields is challenging (see section 7.1), the mapping of the sills was done through correlation between wells along E-W and N-S transects (Figure 5A). This mapping evidences that

the sill-complex of the RGV is not continuous, but consists of several local sill-clusters with gaps of intrusions between them (Spacapan et al., 2020a). Their average lateral extension is more than 4.5 km in E-W direction, and they can extend over 11.5 km in N-S direction. Such heterogeneous distribution of sills implies heterogeneous maturation of the source rock in the Río Grande Valley petroleum system.

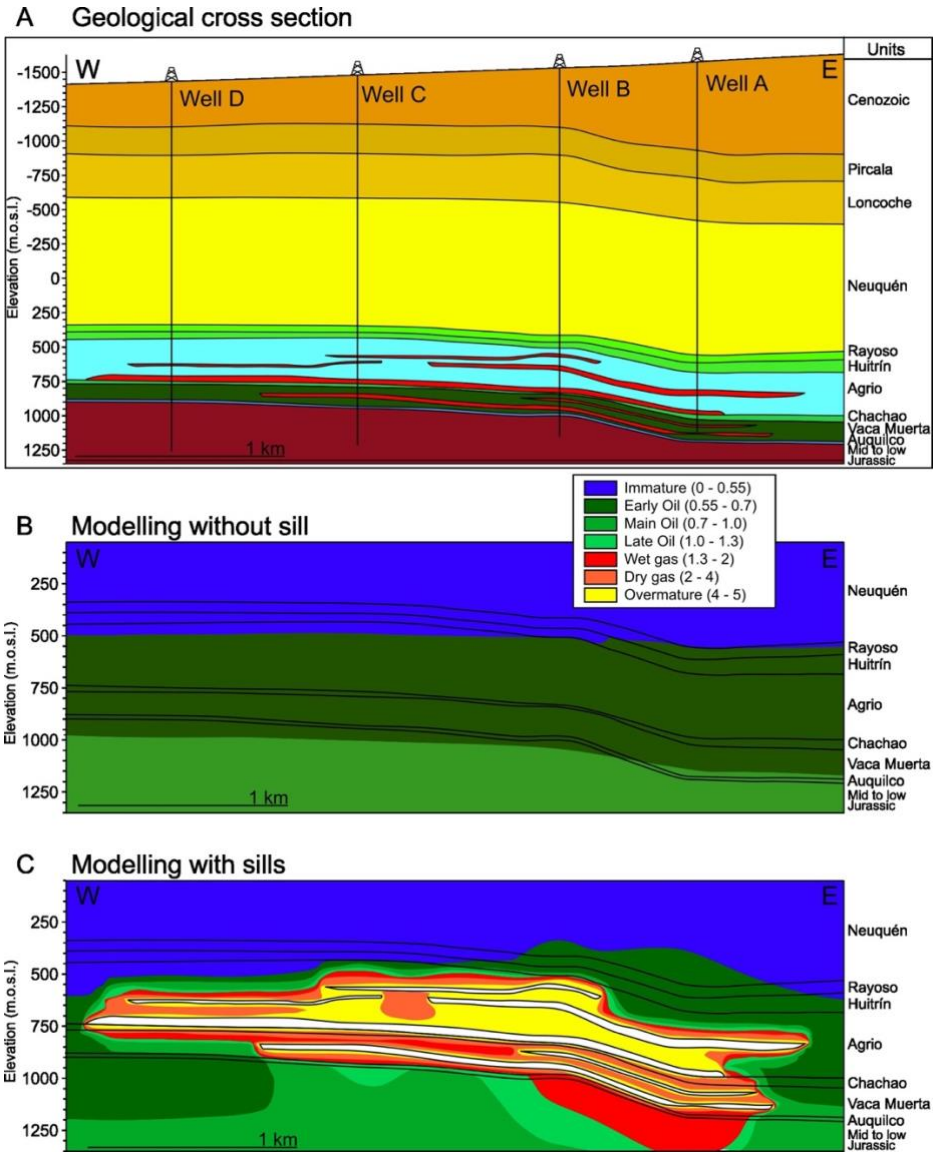

Figure 5. Summary figure illustrating maturation induced by igneous intrusions in the Río Grande Valley oil field (Spacapan et al., 2018). See location in Figure 4E. A. Geological cross section across Río Grande Valley oil field constructed from four wells. Cross section contains two and four sills emplaced in Vaca Muerta Formation and Agrio Formation, respectively. B. Thermal modelling of Río Grande Valley without sill showing low maturation of the Vaca Muerta and Agrio formations. C. Thermal modelling of Río Grande Valley with sills showing substantial maturation of the Vaca Muerta and Agrio formations.

3.2 Maturation documented on field analogue

The key challenges in studying the igneous petroleum system of the Río Grande Valley oil fields are that (1) seismic imaging is poor (see section 7.1)(Rabbel et al., 2018), and (2) geological studies can mostly be done through wireline well data, with very seldom rock samples (Witte et al., 2012; Spacapan et al., 2018; Spacapan et al., 2020a).

In the Neuquén Basin, Andean tectonics brought to surface geological analogues of the igneous petroleum systems of the Río Grande Valley oil fields. The best examples are a 4-km long section at El Manzano, West of Río Grande Valley (Figure 4)(Rabbel et al., 2021), and Sierra de Cara Cura, south of Río Grande Valley (Figure 4)(Palma et al., 2024b). In this section, we will focus on results collected in the Sierra de Cara Cura range.

Sierra de Cara Cura is located in the northern sector of the Neuquén Basin, in southern Mendoza Province (Figure 2). It is part of the southern edge of the Malargüe Fold-and-Thrust Belt. The Cara Cura range is formed by two asymmetric anticlines with a NNE-SSW strike and W vergence (Figure 6A). At Sierra de Cara Cura, the whole stratigraphic section of the basin from basement to Late Cenozoic deposits and an entire 10-15 km long intrusive complex are exposed (Figure 6A). Remarkably, this corresponds to the characteristic extent of the producing subsurface oil fields in the Río Grande Valley (Spacapan et al., 2020a; Spacapan et al., 2020b).

Palma et al. (2024b) performed pyrolisis analyses and organic petrology on samples collected along transects across the exposed Vaca Muerta and Agrio formations (location on Figure 6) for quantifying the thermal impact of the multiple sills on the TOC (Total Organic Content), HI (Hydrogen Index), Tmax (Maximum Temperature) and TR (Transformation Ratio). The pyrolysis data shed light on the thermal impact of the intrusions on the source rock. The data exhibit clear compositional differences between the organic-rich shale in the vicinity of the intrusions (low TOC, low HI, high TR close to 100%, variable Tmax) with respect to the shale away from the intrusions (higher TOC, high IH, low TR, constant Tmax) (Figure 6C,D).

The pyrolysis data of Palma et al. (2024b) show that ~80% of the thickness of the Vaca Muerta Formation is thermally affected by magmatic intrusions, whereas

~40% of the Agrio Formation is thermally affected, based on TR values (Figure 6C,D). The data does not show a clear relationship between sills thickness and aureole thickness. Generally, the aureole thickness is more than twice the sill thickness. Where the vertical distance between two sills is smaller than the aureole thickness, the thermal aureoles overlap. This is consistent with the results of Spacapan et al. (2018), who demonstrate that where sills clusters are located, the thermal aureoles of each individual sill overlap, leading to a non-linear relationship between the intrusion thickness and their thermal effects (see section 3.1; Figure 5).

The results of Palma et al. (2024b) suggest that the best parameter to define the extent of the thermal aureole is the HI, which was used to separate between thermally altered and unaltered samples. This is consistent with former studies in the northern Neuquén Basin, because HI values appear rather homogeneous in the unaltered Agrio and Vaca Muerta Formations, and so HI anomalies can be more confidently interpreted in terms of local thermal effects (Spacapan et al., 2020a; Rabbel et al., 2021). Conversely, TOC content in the Vaca Muerta and Agrio Formation can be quite variable, and so identifying the thermal effects of igneous sills based on TOC can be challenging. The unaltered samples show %Ro values of ~0.67, i.e., below the peak of the oil window (Figure 6F). In the aureole, the high TR values close to 100% suggest that most of the organic matter has been transformed to hydrocarbons. Also, altered samples show a carbonized organic matter (Figure 6C,D). The Tmax value is not a suitable parameter to determine the size of thermal aureole generated during the emplacement of sills (Palma et al., 2024b).

Note that the pyrolysis analyses were carried out on samples collected in the field. In most former studies of the thermal impacts of igneous intrusions on organic-rich shale, pyrolysis analyses were carried out on subsurface samples, either cores or cuttings, which are supposed to be unaffected by surface weathering. The pyrolysis results presented by Rabbel et al. (2021) and Palma et al. (2024b) are qualitatively very similar to those obtained from subsurface samples (Iyer et al., 2018; Spacapan et al., 2018; Spacapan et al., 2019; Spacapan et al., 2020a): the TOC content systematically decreases, and the HI index systematically increases, toward the intrusions with similar values. This shows that pyrolysis analyses on field shale samples, if properly collected, provide meaningful results that are not much affected by weathering. Such a result opens the door for more field-based sampling campaigns to study the thermal evolution of organic-rich shale, which is much less costly than well

samples. For a more quantitative comparison between field and borehole samples, one needs to account for the burial history of both our study area and the areas where well data have been analysed.

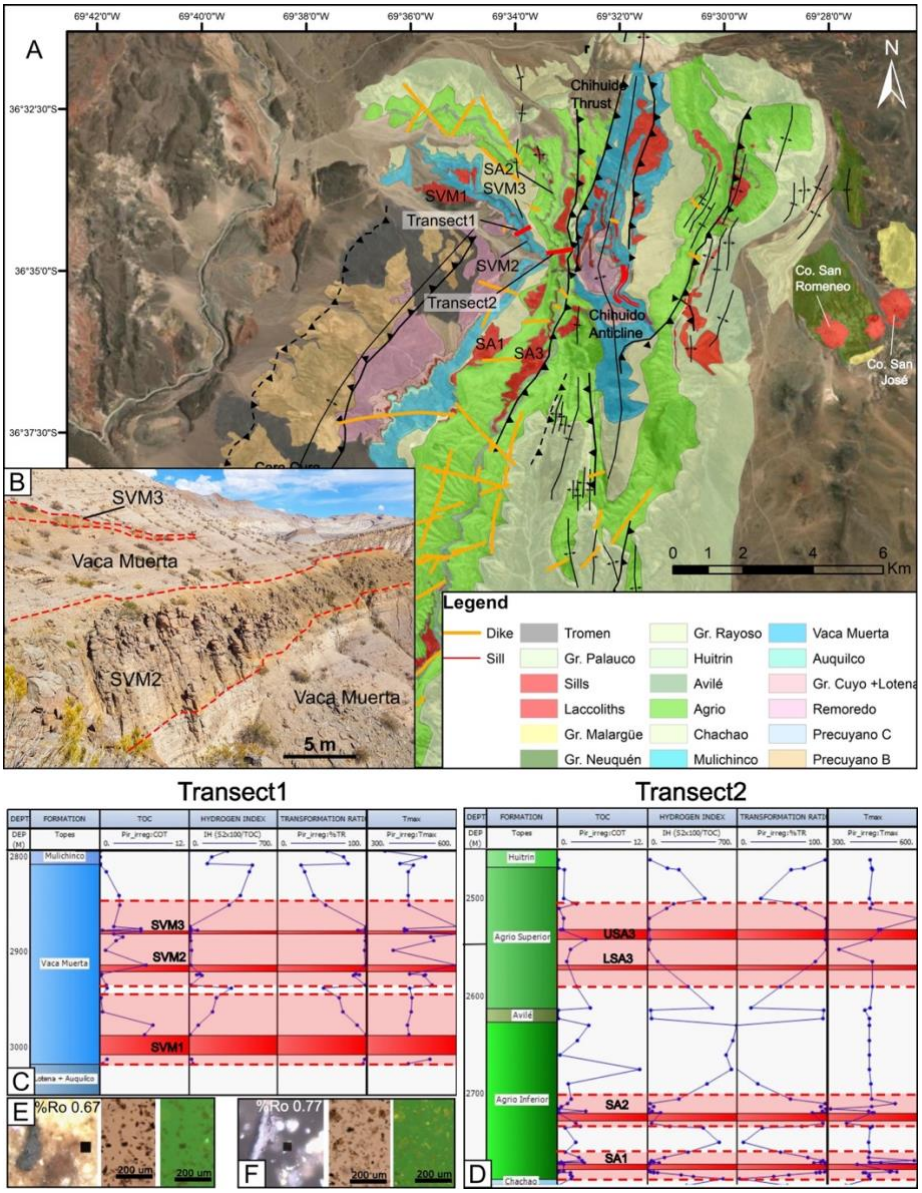

Figure 6. Summary figure illustrating maturation of igneous intrusions from the Cara Cura range field analogue (Palma et al., 2024b). A. Geological map of the Cara Cura range. Map indicates sill names (SVM1, SVM2, SVM3, SA1, SA2 and SA3) and geochemical transects od C and F. B. Field photograph of sills SVM2 and SVM3 emplaced in Vaca Muerta Formation. C. Plot of profiles of TOC, TR, HI and Tmax measured across Vaca Muerta Formation (Transect1, see location in A). D. Plot of profiles of TOC, TR, HI and Tmax measured across Agrio Formation (Transect2, see location in A). Red dashed lines represent the estimated boundary of the thermal aureole around the sills. E and F. Images from organic petrology.

Vitrinite reflectance (%Ro; left), thermal alteration index of organic matter (TAI) in transmitted light (centre) and fluorescence light (right) in the base of Upper Agrio (E), and in Lower Agrio (F).

4 Structural impacts of igneous intrusions

4.1 Sills as fractured reservoirs

Sills have traditionally been viewed as impermeable features, acting as barriers and baffles against fluid flow (Rateau et al., 2013; de Miranda et al., 2018), potentially leading to overall negative impacts on petroleum systems. However, the sills in the Río Grande Valley have shown that sills may not only have beneficial effects on maturation (Section 3.1) but can also represent fractured hydrocarbon reservoirs of economic relevance. In this section, we describe these fractured reservoirs which have been characterized using both subsurface data from RGV and direct outcrop analogues. Note that the reservoir sills are sealed by the low-permeability shale of their host rock.

Spacapan et al. (2020a) characterised the reservoir properties of the sills. Oil production curves for magmatic sills located in Huitrín, Agrio and Vaca Muerta formations show that they are essentially fracture-dominated reservoirs with a minor influence of matrix porosity, with fast initial production rate rapidly decaying to much lower production rate. Capillary pressure and porosity-permeability plots for magmatic intrusions show the coexistence of essentially two groups of reservoir properties: one of moderate-to-low reservoir quality, and a second one of good reservoir quality. Some degree of variability may arise from the coexistence of intervals with different fracture intensity, aperture, connectivity, degree of cementation and tortuosity, or more likely, a combination of several of these factors.

The analysis of Spacapan et al. (2020a) was based on rock cores from the oil-producing sills. However, the available core material was rather limited to derive a complete picture of the fracture natures and distribution. Rabbel et al. (2021) and Palma et al. (2024b) complemented the analysis of Spacapan et al. (2020a) through the extensive field mapping of seismic-scale outcrop analogues. The outcrop studied by Rabbel et al. (2021) at El Manzano is the westward extension of the subsurface petroleum system of the Río Grande Valley fields, brought to the surface by thrusting. The structural analysis of Rabbel et al. (2021) evidence multiple fracture types driven by a broad spectrum of physical processes and associated with different fracture distributions. In addition to tectonic fractures, these fracture types include cooling

joints, bitumen veins and hydrothermal veins that formed in high-temperature environment, i.e. during the cooling of the sills.

The most prominent fracture type are cooling joints created by thermal contraction of the sill. The exposed sills exhibit complex distributions of cooling joints within the igneous intrusions (Figure 7). The innermost domains of sills exhibit fractures that are perpendicular to the intrusion's walls, typically called columnar joints, as they fracture the sills in columns perpendicular to the contacts with the host rocks (Figure 7)(Bermúdez and Delpino, 2008; Rabbel et al., 2021). Within the columns, one can find fractures that are perpendicular to the columns, and so parallel to the intrusion's contact, named transverse joints (Bermúdez and Delpino, 2008). Along straight sill segments, the cooling joint pattern is regular. Nevertheless, irregularities in sill shape, such as steps or broken bridge, are associated with prominent perturbation of the cooling joint pattern (Figure 7).

Other types of fractures associated with the sills are graphitic bitumen veins and bituminous shale injection structures. These features result from the rapid maturation of the organic matter in the contact aureole of the sills. Such fast maturation lead to fast generation of hydrocarbons, leading to fast fluid pressure build-up. Given that the shale has very low permeability, this fluid pressure build-up could only be released through hydrofracturing or fluidisation of the shale, leading to injection of either organic-rich fluids or fluidised bituminous shale.

Large hydrothermal veins were also found to cut through both the sills and the host rock. The veins occur both at sill tips, and along the more central part of sills and may crosscut, or be crosscut by, bitumen dykes (Figure 7D). The mutual crosscutting relationships demonstrate that these processes are coeval. Commonly, these features are several centimeters to a meter wide, tens to hundreds of meters long, and include arrays of branching veins, and carry fragments of host rock. Millimeter- to centimeter-scale macropores are very common and often filled with bitumen (Figure 7D).

Spacapan et al. (2020a) noticed that the sill clusters of the Río Grande Valley fields are located in tectonically deformed areas. Post-emplacement tectonic stress and deformation eventually lead to the faulting of the sills (Figure 7D). Pre-existing cooling fractures are reactivated, or new faults are created, leading to additional secondary porosity. Larger faults crosscut the entire sedimentary column.

In summary, the fracture distribution within the igneous reservoir rocks of the Río Grande Valley fields exhibits strong lateral changes on the scale of some tens to

hundreds of meters, depending on the number and intensity of processes involved. Such changes involve locally increased fracture density, wider orientation distribution, higher connectivity and a variable length distribution. For modelling these fracture systems, Rabbel et al. (2021) showed that the fracture length is best described using a log-normal distribution, not by a power law.

Note that reservoir quality is strongly influenced by the degree of cement precipitation, which impacts fluid flow and reservoir capability. In the Río Grande Valley fields, core observations allow establishing the following sequence of cement precipitation in fractures: (1) first growth of a zeolite phase, made of large spherulitic zeolites, from the fracture walls to the centre; (2) formation of secondary zeolites, filling the pores generated by dissolution of primary zeolite, and secondary calcite, growing between primary zeolite crystals, occluding partially to totally the fracture porosity. The observations of Spacapan et al. (2020a) are a clear example of how the number, nature and intensity of cement phases controls the probability of fracture porosity occurrence and, hence, the storage capacity and fluid transmissibility of the igneous body.

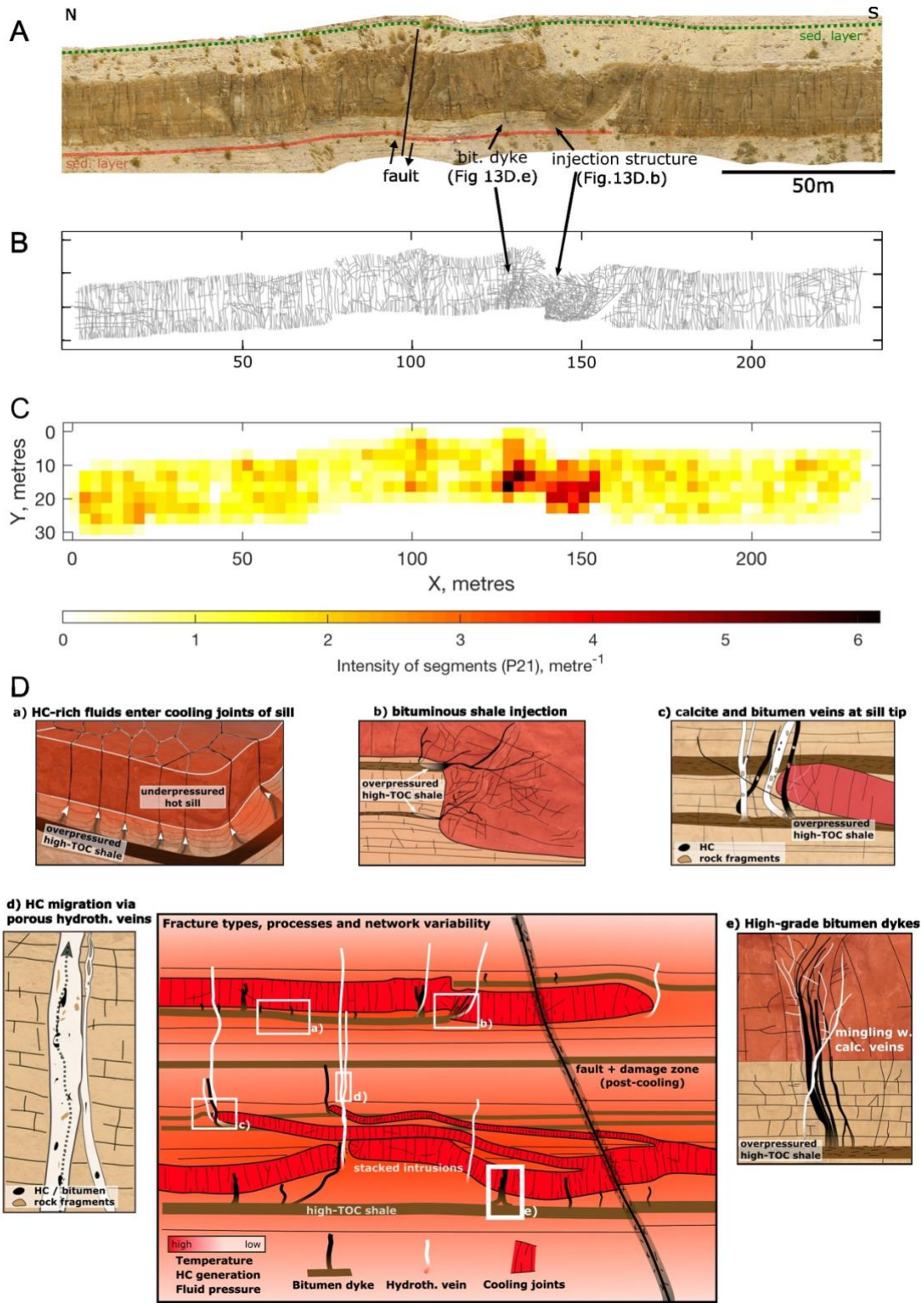

Figure 7. Figure summarising characteristic of igneous fractured reservoirs (Rabbel et al., 2021). A. Orthorectified image of one sill at El Manzano outcrop (see location in Figure 4C). B. 2D fracture mapping of image A. C. Map of fracture intensity (P21) of fracture map of B using open-source FracPaQ toolbox (Healy et al., 2017). D. Schematic summary of fracture types of sill fractured reservoir in organic-rich shale, underlying mechanisms and fracture network variations interpreted from field evidence. Central image visualizes large-scale

features, including intrusion architecture and its relation to spatial fracture network variations. Insets (a–f) highlight specific fracture types and potential implications for igneous reservoirs.

4.2 Gentle doming as structural trap

Doming associated with igneous intrusions in sedimentary basins occurs when magma intrudes into the layers, causing them to bend upwards into a broad, 4-way closure dome-like structure (Pollard and Johnson, 1973; Jackson and Pollard, 1990; Trude et al., 2003; Hansen and Cartwright, 2006; Jackson et al., 2013b; Magee et al., 2014). In hydrocarbon-bearing basins, these dome structures can trap oil and gas (Schmiedel et al., 2017), creating effective structural traps.

The Cerro Bayo de la Sierra Negra intrusive complex, located in the central part of the Neuquén Basin (see El Trapial in Figure 2), is a prime example of how an intrusive complex can influence hydrocarbon-bearing sedimentary basins. This intrusive complex, also known as Cerro Bayo-Trapial, constitutes the shallow plumbing system of an eroded Lower Miocene volcanic complex (González and Aragón, 2000). It is surrounded by the large oil fields of El Trapial and Chihuido de la Sierra Negra (Lombardo et al., 2024). The main structural trap at El Trapial is a large-scale dome of the Mesozoic strata. In this section, we will describe in detail the link between the dome and the intrusive complex.

At the surface, the intrusive complex consists of a swarm of radial dykes and a few sills emplaced in the red sedimentary rocks of the Neuquén Group. The dykes converge toward the central part of the complex, which consists of a gentle subcircular hill (Cerro Bayo) with a diameter of roughly 3 km, culminating at approximately 1360 meters above sea level. An initial interpretation of Cerro Bayo was that it consists of a plug feeding a Christmas tree laccolith (González and Aragón, 2000), but Lombardo et al. (2024) show that the Cerro Bayo hill is made of gently tilted strata of the Neuquén Group, which are heavily intruded by the radial dykes.

The subsurface structure of the Cerro Bayo de la Sierra Negra intrusive complex was revealed through the integration of high-quality 3D seismic data, numerous well logs, and field observations. Seismic data revealed key features, including sills, dykes, and faults. Sills were identified as sub-horizontal, high-impedance reflections, often concentrated in the Quintuco-Vaca Muerta interval

(Figure 8C). Annular faults were recognized in seismic data and exhibit inward-dipping reverse fault patterns. The mapped subsurface sill complex exhibits a subcircular distribution, with a radius of ~10 kilometres.

The El Trapial dome results from the superimposition of two different scales of doming: a large-scale dome (~10 km radius), and several smaller-scale domes (~3 km radius) clustered around the central axis (Figure 8). The large-scale dome affects all the Mesozoic formations, including the Jurassic Tordillo Formation and the formations below. The small-scale domes are associated with annular inward-dipping reverse faults that accommodate their growth, which are rooted in the Vaca Muerta Formation and only affect shallower formations (Figure 8). The amplitude of the El Trapial dome is estimated to be approximately 500 meters, with the shallow, small-scale domes contributing around 200 meters of uplift. The remaining 300 metres of uplift are rooted deeper.

There is a perfect correlation between the dome structure and the intrusive complex. The centre and the extent of the dome coincide precisely with the centre and the extent of the intrusive complex (Figure 8B and D). In addition, Lombardo et al. (2024) show that the amplitude and distribution of the shallow, small-scale domes correlate with the distribution of the sills emplaced within the Vaca Muerta Formation. Such correlation shows that the doming has resulted from the emplacement of the plumbing system of the Cerro Bayo de la Sierra Negra volcanic complex at different crustal levels.

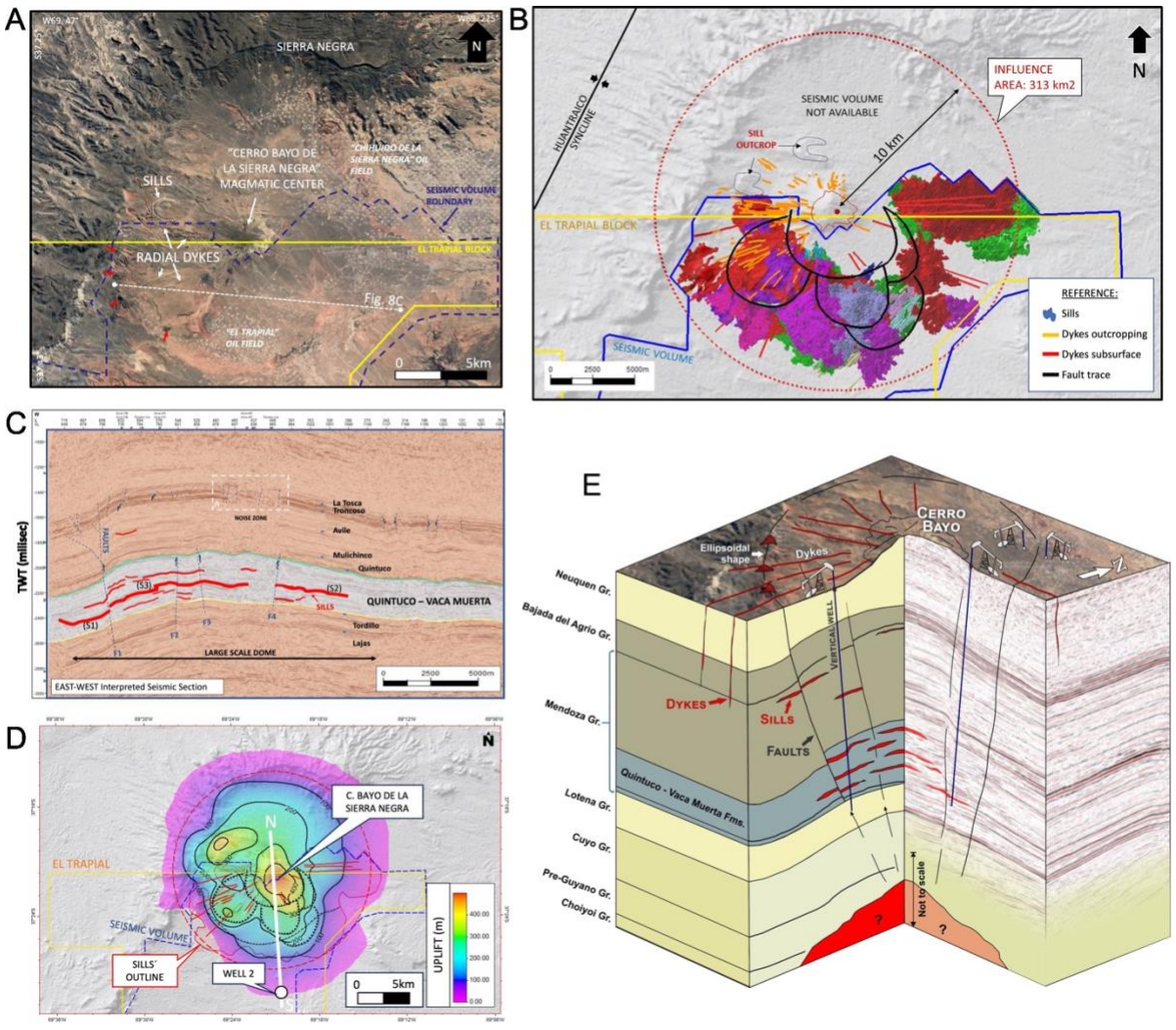

Figure 8. Synthetic figure illustrating El Trapial dome structure induced by Cerro Bayo de la Sierra Negra intrusive complex (Lombardo et al., 2024). A. Satellite image of Cero Bayo de la Sierra Negra intrusive complex, showing radial dyke swarm (red), exposed sills (white dashed lines) and oil fields (each white dot on satellite image is a well pad. Black line locates seismic section of C. B. Map of igneous intrusions mapped in subsurface data. The bodies in colors represent all the sills at subsurface identified on the seismic volume though the different attributes described on this contribution. The orange and red lines represent the dykes at surface and subsurface, respectively. The dashed red circle represents the outer boundary of all the igneous bodies. C. Interpreted East-West seismic section in time (see location in A) crossing the dome structure of Cerro Bayo complex. Notice igneous sills intruding predominantly the Quintuco-Vaca Muerta section. D. Map of estimated uplift of El Trapial dome structure. E. 3D block diagram of the El Trapial dome associated with the Cerro Bayo de la Sierra Negra intrusive complex.

4.3 Faulted laccolith-induced doming as fractured reservoir

The emplacement of laccoliths leads to the formation of dome-structures, deforming and potentially, fracturing the overburden rocks (Corry, 1988; Trude et al., 2003; Magee et al., 2014; Agirrezabala, 2015). These rocks, including the laccolith itself, may act as traps, fractured reservoirs, or migration path for hydrocarbons, depending on the mechanics of laccolith fluid emplacement. The El Trapial dome case study described in Section 4.2 is a perfect trap because the intrusion-induced dome is gentle, typically associated with intrusions of low thickness-to-diameter ratios, such as wide thin sills (Pollard and Johnson, 1973; Galland and Scheibert, 2013). However, intrusions of significantly higher thickness-to-diameter ratios, such as laccoliths, are common (Corry, 1988; Cruden et al., 2018). The inflation of laccoliths is expected to significantly deform their overburden, triggering fracturing, stretching, and even faulting of the overburden (so-called "punched laccolith" mechanism) (Koch et al., 1981; Wilson et al., 2016; Schmiedel et al., 2019). The resulting structures are expected to significantly affect permeability architecture of the deformed sedimentary strata (Delpino et al., 2014a).

In this section, we present a case study of an intrusion-induced dome associated with a thick laccolith at Pampa Amarilla (see location in Figure 2)(Galland et al., 2022), where integrated field mapping and subsurface data interpretation allowed for a 3D modelling of this subsurface laccolith through a structural reconstruction. The Pampa Amarilla dome structure is located in the Malargüe fold-and-thrust belt in the northern Neuquén Basin, southern Mendoza province, Argentina, ~50 km south of Malargüe city and 20 km east of Bardas Blancas town (Figure 2). In the study area, Upper Cretaceous continental deposits of the Neuquén Group crop out regionally, except for a sub-circular outcrop of deeper marine sediments from the mid Cretaceous to Lower Cretaceous formations of the Huitrín and Agrio Formations, respectively (Figure 9A). In the subsurface, beneath the sub-circular outcrop, the presence of a thick igneous body has been known since 1937, following the drilling of well PA.x-2 (Pampa Amarilla), which encountered over 100 m of andesite without reaching the bottom of the intrusion. During the drilling of this well, several hydrocarbon manifestations occurred while crossing the overburden rocks and the igneous body.

High-quality seismic data enabled a good reconstruction of the subsurface structure to the north, west, and south of the Pampa Amarilla dome (Figure 9B). However, the eastern part lacked 3D seismic coverage, and seismic data loses coherence at the dome's location due to imaging difficulties related to the structural complexity of the dome. Additionally, well logs and cutting description of two wells (PA.x-2 and PA.x-6, see locations in Profile L390, Figure 9C) were included in the study to determine the depths of stratigraphic formation tops and to apply a simple vertical geometric scaling of the seismic data.

Integrating field, borehole, and seismic data, Galland et al. (2022) produced a structural model of both the dome and the underlying intrusion (Figure 9C), which shows that the Pampa Amarilla dome formed due to the emplacement of a ~400 m thick subsurface laccolithic intrusion, with a thickness-to-length ratio T/D~0.13. Furthermore, the dome exhibits a trapdoor structure, with faulting along the western, northwestern, and southwestern edges, and gentle tilting of the overburden to the east (Figure 9D). The trapdoor tilting of the laccolith's overburden was the main mechanism controlling the thickening of the laccolith.

The reconstructed subsurface Pampa Amarilla laccolith is elliptical in map view, with a 3 km-long east-west axis and a 2 km-long north-south axis. Along east-west cross section, the laccolith is wedge shaped with maximum thickness near its western edge and gradual thinning towards the east (Figure 9C). According to these results and considering that numerous laccolithic intrusions exhibit similar T/D values to that of the Pampa Amarilla laccolith (Cruden and Weinberg, 2018), this study suggests that numerous laccoliths on Earth grew by faulting of their overburden. This result implies that the established mechanical models of laccolith emplacement based on elastic bending of the overburden (Pollard and Johnson, 1973; Kerr and Pollard, 1998; Bunger and Cruden, 2011; Galland and Scheibert, 2013) may apply only to a few thin laccoliths or thick sills.

The study Galland et al. (2022) highlights the necessity and value of integrating field geological measurements with subsurface (3D seismic and borehole) data for structural reconstructions of subsurface laccolith intrusions and for delineating the damage zones generated in potential hydrocarbon reservoir rocks (Figure 9D). In the case of Pampa Amarilla laccolith and dome, the faulted edges of the dome are the main exploration targets as fractured reservoirs.

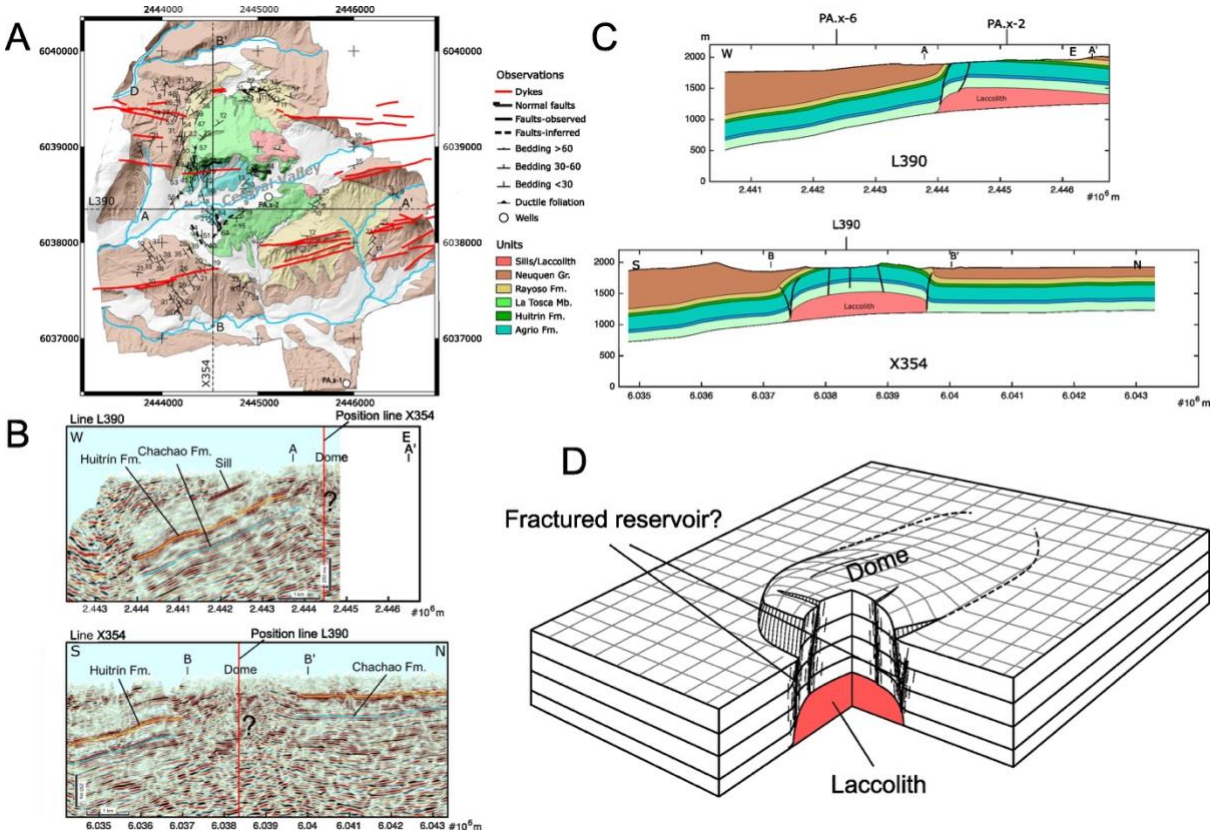

Figure 9. Figure illustrating laccolith-induced faulted dome as potential fractured reservoir, using Pampa Amarilla laccolith case study (Galland et al., 2022). A. Geological map of the Pampa Amarilla dome (see location in Figure 2) showing structural field measurements, seismic profiles (in B) and geological cross sections (in C). The coordinate system of the map is the Campo Inchauspe / Argentina 2 EPSG:22192. B. EW (L390, top) and NS (X354, bottom) seismic profiles across the Pampa Amarilla dome (see locations of A-A' and B-B' on map in A) with interpreted tops of the Huitrín (orange lines) and Chachao (light blue lines) formations. Note that the seismic data is incoherent at the location of the dome. C. Geological cross sections A-A' (L390, top) and B-B' (X354, bottom), located on geological map of A. The locations of wells PA.x-2 and PA.x-6 are indicated on Profile L390. D. Sketch summarizing the structure of the Pampa Amarilla laccolith and faulted, trapdoor dome, locating potential fractured reservoir.

5 Impacts of igneous intrusions on hydrocarbon migration

5.1 Syn-cooling fluid migration

Sections 3.1 and 3.2 describe the thermal effects of igneous sills on organic-rich shale formation, and in particular on the maturation of the organic matter. Fast maturation triggers fast generation of hydrocarbons and associated fluid pressure build-up. Rabbel et al. (2023) show that the hydrocarbon generation during the cooling of the intrusions leads to significant hydrocarbon migration under high grade conditions.

Rabbel et al. (2023) collected geological observations from several localities in the Neuquén Basin (El Manzano, see section 4.1; Cuesta del Chihuido; see locations in Figure 2). These authors systematically observed occurrence of veins with solid, strongly graphitized bitumen, as well as cooling joints filled with solid bitumen or organic-rich shale (Figure 10). These observations evidence transport of hydrocarbon-rich fluids and liquefied sediments into the sills in a high-temperature (probably >350°C), high-pressure environment. These phenomena happen within years to several decades after solidification.

The hydrocarbons generated in such a short time scale cannot migrate by Darcy porous flow through very low-permeability shale. Instead, the resulting pressure build-up is so high that hydrocarbons migrate by in-situ fracturing of the shale, the so-called primary migration (Kobchenko et al., 2011; Kobchenko et al., 2014; Rabbel et al., 2020). This process is responsible for the bitumen veins observed in the field, which can be injected both within the shale host rock and the intrusions (see Section 4.1). In addition, elevated pore pressures also resulted in local shale fluidization under the sills (Figure 10).

Observations of high-grade bituminous material in cooling joints inside the sills suggest that sills become permeable long before complete cooling (Rabbel et al., 2023). However, numerical studies of hydrothermal circulations induced by the cooling of a sill commonly assume that sills are impermeable barriers (Fjeldskaar et al., 2008; Iyer et al., 2017). Consequently, these simulations modelled high fluid overpressures below the sills, leading almost systematically to the nucleation of hydrothermal vent complexes at the tips of the sills as a mechanism of fluid pressure dissipation.

767 Nevertheless, no hydrothermal vent complex is observed in the Neuquén Basin, and
768 another mechanism is expected to be at work.
769 The field observations from the Neuquén Basin motivated novel numerical
770 modelling of hydrothermal circulations that account for sills becoming permeable
771 during cooling (Rabbel et al., 2023). The modelling results show that three distinct
772 phases of fluid flow occur around the cooling sills (Figure 10). (1) before solidification,
773 the sill is still impermeable, fluid pressure builds up under the sill, and fluid flow is
774 parallel to the sill contacts. (2) Cooling of the sill leads to the generation of cooling
775 joints, which make the sill permeable. Fluid flow suddenly change to vertical, while the
776 fluids can cross the newly permeable sill. This step considerably reduces fluid
777 overpressure under the sill in comparison to models with impermeable sills. (3) A
778 plume of hydrocarbon slowly rises above the sill, instead of hydrothermal vent
779 complexes generating at the tips of the sills like in models with impermeable sills
780 (Fjeldskaar et al., 2008; Iyer et al., 2017).
781 These models show that the flow of methane through the sill occurs at
782 temperatures >400°C, which meet the conditions for hydrothermal graphitization, in
783 good agreement with the field observations. This result shows that flow of
784 hydrocarbons into newly formed cooling joints is likely not a viable migration/charge
785 mechanism for sill reservoirs in the Río Grande Valley fields (see section 4.1), as the
786 intrusions are too hot for survival of liquid hydrocarbons. This suggests instead that
787 the charge of the sill reservoirs occur later when the sill has cooled down (see Section
788 5.2), and the hydrocarbons likely migrated from the large maturation aureoles at the
789 scale of the sill complexes (see Section 3.1).
790

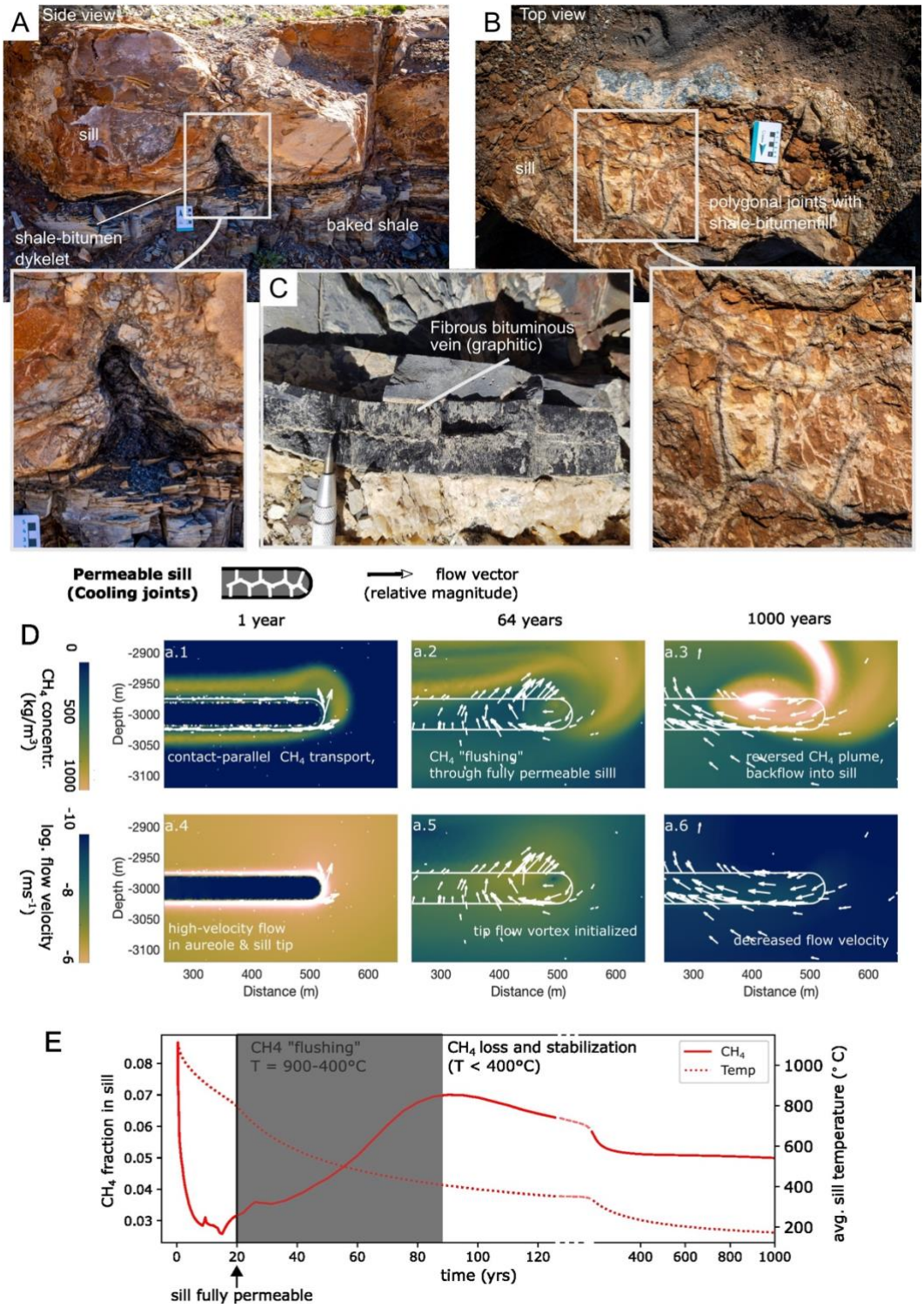

Figure 10. Summary figure illustrating syn-cooling fluid migration (modifed from Rabbel et al., 2023). A. Field photograph of upwelling dikelets of liquefied shale and bitumen entering the cooling joint network of a thin sill at Cuesta del Chihuido (ca. 30 cm thick, side view). B. Field photograph of top view of sill from A demonstrating black bituminous fill in polygonal cooling joints. C. Field photograph of graphitic, fibrous bituminous vein near a sill at El Manzano outcrop. D. Cross section maps from numerical simulations of hydrothermal circulations associated with a cooling sill emplaced in otganic-rich shale. Top row: methane concentrations

after 1 year (left), 64 years (centre) and 1000 years after sill emplacement. Bottom row: flow velocity of hydrothermal fluids. Arrows indicate flow directions. E. Plot of methane fraction in sill (solid line) and average sill temperature (dashed line) through time computed from numerical simulations.

5.2 Post-cooling fluid migration

In the northern part of the Neuquén Basin, middle Miocene to Pliocene arc volcanism is represented by the igneous La Brea Formation, which consists of exhumed massive shallow, andesite subvolcanic intrusions (Baldauf et al., 1997; Nullo et al., 2002; Araujo et al., 2019). The La Brea magmatic suite illustrates a clear link between igneous intrusions and hydrocarbons, as 'La Brea' means "tar" in Spanish. The reason is that bitumen seeps have been documented near one of these intrusions, Cerro Alquitrán, back in 1833 (Yrigoyen, 1983) and represent a historical landmark in the hydrocarbon geology of the Neuquén Basin. Other nearby intrusions, such as Cerro La Paloma, are also associated with large bitumen seeps (Dessanti, 1959; Galland et al., 2024).

The Cerro Alquitrán is an exhumed 10.7±0.5 million-year-old subvolcanic intrusion, located at the foothills of the Andes mountains, Argentina (Nullo et al., 2002) (Figure 2). It is an intrusion of andesitic composition emplaced through the Mesozoic and Cenozoic sedimentary formations of the northern Neuquén Basin (Nullo et al., 2002; Boll et al., 2014). The shape of the intrusion is inferred to exhibit a thick laccolithic to plug shape (Dessanti, 1959). The Cerro Alquitrán intrusion is located in the eastern border of the Neuquén basin, where thin and proximal late Jurassic to Paleocene strata were deposited. As a consequence, the Vaca Muerta and Agrio formations at the location of Cerro Alquitrán are not rich in organic matter and did not experience burial maturation.

The peculiarity of Cerro Alquitrán is the presence of large natural bitumen seeps clustering around the igneous body (Figure 11) (Dessanti, 1959). The major surface bitumen seeps occur in various forms, from tar pits to long bitumen flows (Figure 11B). The surface of the bitumen flows often exhibits ropy structures that mimic basaltic pahoehoe lava flows. On map view, the overall distribution of the major seeps follows the edge of the intrusion (Figure 11C), suggesting relationship between the intrusion and fluid migration pathways.

The andesite hill of Cerro Alquitrán exhibits sub-circular shape on map view (Figure 11C). The contacts of the intrusion are nowhere exposed, making it challenging to constrain its overall shape. Nevertheless, it is likely that the intrusive contacts are relatively close to the outer edges of the outcropping andesite, suggesting a rounded massive intrusion type laccolith or plug. This hypothesis is supported by the structure of the neighbouring Cerro La Paloma intrusion, where vertical intrusion contacts are well exposed (Galland et al., 2024). The igneous body exhibits a concentric structural architecture, with three main structural patterns (Figure 11). The most prominent structures are brecciated andesite (Figure 11), distributed along bands (Figure 11C). Locally, kinematic indicators within the breccia highlight that the inner part of the intrusion moved upward with respect to the outer part. Structures of less intensity are fracture bands (Figure 11D), which contain thousands of fractures that are sub-perpendicular to the top surface of the fracture band (Figure 11). Finally, the core of the andesite body consists of massive andesitic rock affected by a very few fractures (Figure 11). The concentric distribution and systematic outward-dipping nature of the structures in the andesite suggest that the fracturing and brecciation resulted from syn-emplacement brittle deformation of the andesite due to fast shearing near the intrusive contacts.

There are clear relationships between the andesite structures and the bitumen seeps. Both at Cerro Alquitrán and Cerro La Paloma, the main bitumen are located near the intrusive contact, and where the andesite is the most fractured and brecciated. At Cerro La Paloma, a string of seeps is parallel to the intrusive contact, and the bitumen seeps from the brecciated andesite, not from the host rock of the contact itself (Galland et al., 2024). Locally, it is possible to observe the breccia impregnated with the bitumen that seeps out (Figure 11).

Organic geochemical analyses demonstrate that the bitumen seeping out at Cerro Alquitrán and Cerro La Paloma is not of local origin (Galland et al., 2023; Galland et al., 2024). Instead, it is expected that it has migrated from a regional kitchen 10-20 km to the west of the area. The presence of numerous sills emplaced in the organic-rich shale formations between the source of the bitumen and its seeping location suggest that subsurface network of igneous intrusions might have channelled, at least partly, regional fluid migration.

All in all, the demonstrative Cerro Alquitrán case study highlights the great relevance of igneous intrusions on subsurface fluid migration long time after the cooling of the magma.

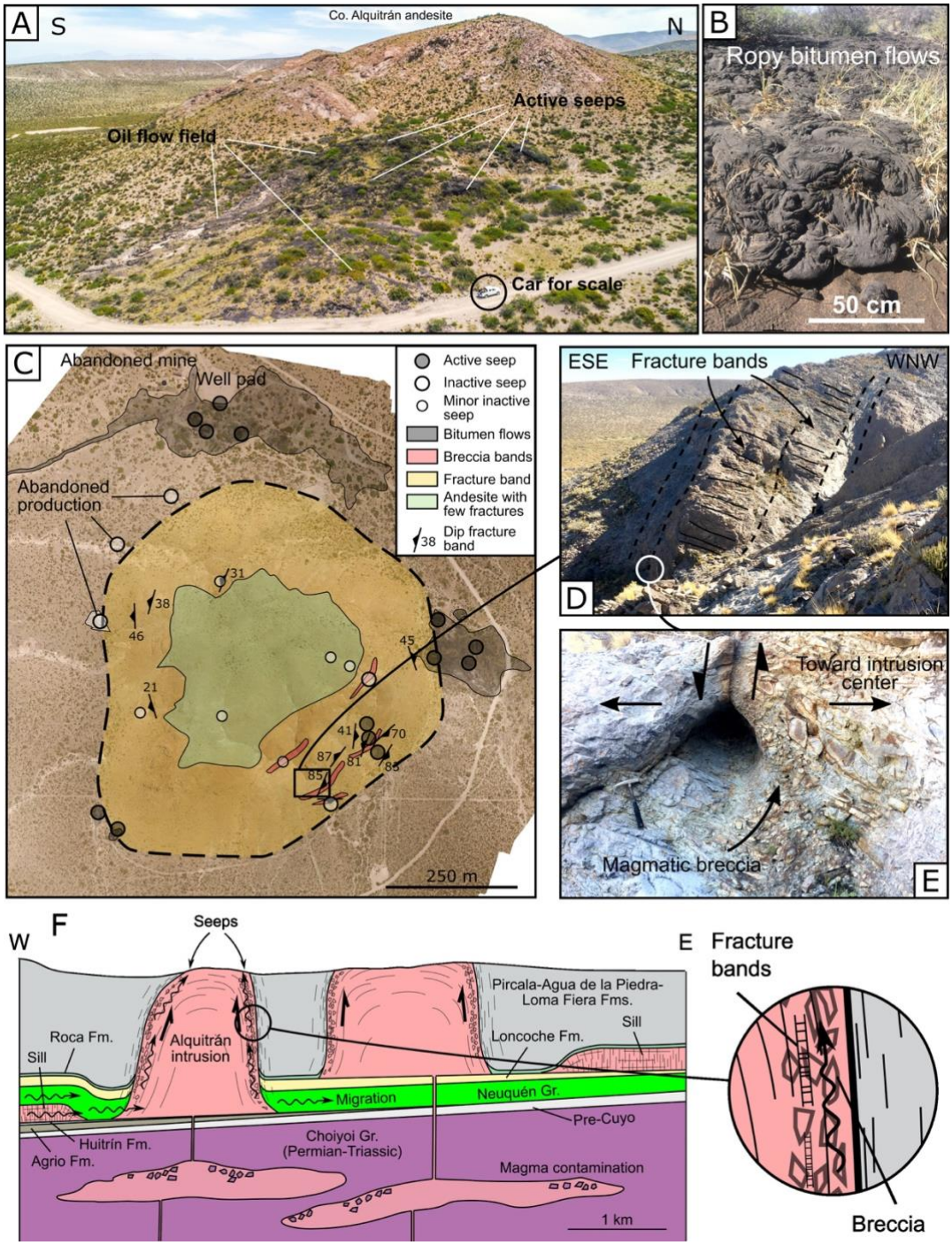

Figure 11. Figure illustrating post-magma emplacement hydrocarbon migration, using Cerro Alquitrán laccolith case study (Galland et al., 2023; Galland et al., 2024). A. Drone photograph of eastern seep illustrating the extent of the bitumen seep. B. Field photograph of bitumen ropy flow complex. C. Map of Cerro Alquitrán intrusion locating zones of breccia bands (red),

fracture bands (yellow) and poorly fractured andesite (green), as well as bitumen seeps. D. Field photograph of steep outward-dipping fracture bands near the SE edge of Cerro Alquitrán andesite. E. Sub-vertical breccia with fault gauge indicating upward movement of the interior of the intrusion. F. Schematic model of structure of Cerro Alquitrán and surrounding intrusions and its implications for hydrocarbon migration.

5.3 Reservoir compartmentalisation

Sections 4.1 and 5.2 show that igneous intrusions can represent high-permeability fluid pathways and fractured reservoirs. Conversely, other studies suggest that igneous intrusions can also be low-permeability barriers (Senger et al., 2017), leading to seal (de Miranda et al., 2018) or compartmentalisation of reservoirs (Rateau et al., 2013; Schofield et al., 2015).

The Volcán Auca Mahuida, Risco Alto and Las Manadas oil fields provide an example of how intrusive bodies emplaced in conventional reservoir rocks can have adverse effects. This sector is located on the Auca Mahuida volcano, in the northeastern Neuquén Basin (Figure 2 and Figure 12A). This eruptive center, part of the Payenia Volcanic Province (Pleistocene-Holocene)(Rossello et al., 2002; Ramos and Folguera, 2011), has interacted with a complex tectonic and sedimentary history, significantly impacting the formations it was emplaced through (Basaldúa and Cristallini, 2022). The structural complexity associated with this volcano and the petroleum significance of the region have motivated numerous studies and models aimed at explaining its evolution (Ventura et al., 2013; Delpino et al., 2014b; Pallares et al., 2016; Longo, 2017). In this area, conventional hydrocarbon reservoirs consist of sandstones from the Rayoso (Barremian-Aptian), Centenario (Upper Valanginian-Lower Aptian), Mulichinco (Lower Valanginian-Upper Valanginian), and Quintuco (Late Berriasian-Early Valanginian) formations, with the Mulichinco Formation being the primary reservoir. Meanwhile, the source rock corresponds to the Vaca Muerta Formation (Figure 12C).

Chiacchiera et al. (2022) analyzed data (well logs, borehole images, fluid testing, and a VSP Walkaway) from nine wells to investigate the effects of dykes on a sector northeast of the main crater of the Auca Mahuida volcano (Figure 12B). While some areas of the volcano have seismic data, the fields near the top crater lack such data, mainly due to the complex topography and the significant thickness of basaltic

cover. Transects were performed, and variations in fluid types (liquid hydrocarbons, gas, and water) were analyzed to identify hydraulic disconnections (Chiacchiera et al., 2022).

Chiacchiera et al. (2022) concluded that subsurface dykes exhibit NE-SW and E-W orientations with dips of 60°-70° towards the south and southwest. These orientations coincide with surface faults and those described in the literature, suggesting that intrusions propagated through pre-existing structural discontinuities (Spacapan et al., 2016), affecting hydrocarbon connectivity (Senger et al., 2017).

Another impact associated with igneous intrusions is reservoir compartmentalization. Structural and fluid analyses revealed that, within the same stratigraphic levels, neighboring wells contain different fluids, indicating a lack of connectivity between them (Chiacchiera et al., 2022). This led to the identification of four hydraulically independent blocks (Figure 12B). A similar impact was observed at other stratigraphic levels in the same oilfield (Delpino et al., 2014b). This type of compartmentalization corresponds to the Box-Work type described by Holford et al. (2013) and Eide et al. (2016). As igneous bodies in the Mulichinco Formation do not exhibit fracturing that could allow them to act as reservoirs, they instead act as physical barriers to fluid flow. From a petrophysical perspective, intrusions and their associated hydrothermal activity may have reduced the permeability of the Mulichinco Formation, which could explain the high-water saturation in the sandstones surrounding the laccolith in fluid tests.

The analysis of these complex processes enhances the understanding of the interaction between intrusive bodies and productive sedimentary basins. However, further investigation is needed regarding the intersection zones between dykes and sills, as well as sill doming within reservoirs, to determine whether these structures can generate traps in other areas. Finally, VSP Walkaway (Figure 12D) data, such as those from Sigismondi (2012), provide evidence of intrusions in underlying source rocks, which could have reservoir potential when present in these lithologies, as previously discussed in this contribution.

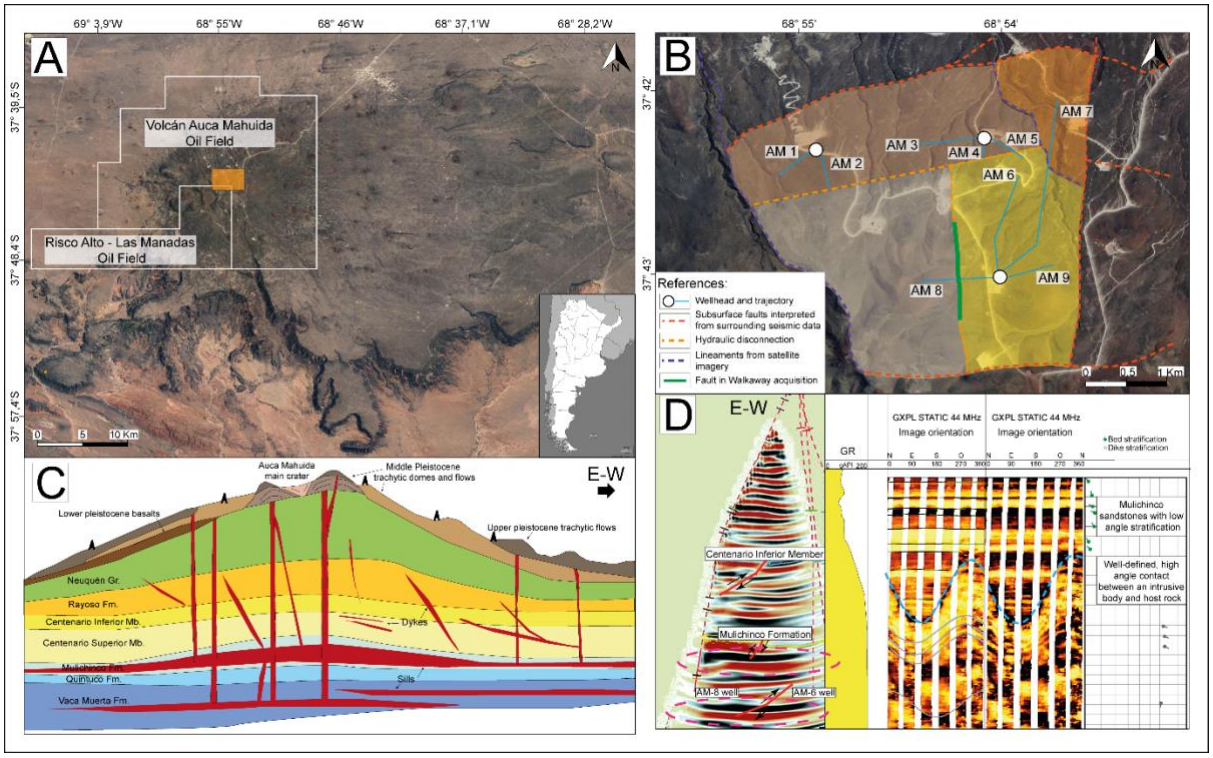

Figure 12. A. Satellite image of the Auca Mahuida volcano, with oilfields involved in this study outlined in white. B. Image of the study area, where the four hydraulically disconnected blocks discussed in this work are highlighted in different colors (Image obtained from Google Earth). C. Schematic cross-section of the upper portion of the Auca Mahuida volcano, showing formations intersected, created with well data and modified from Delpino et al. (2014b). D. Left: VSP Walkaway in the E-W direction, showing faults indicated by red lines. Intrusive bodies highlighted within dashed ellipses. Taken and modified from Roth (2017). Right: A fragment of an image log from well AM-8, showing an intrusion.

6 Bitumen veins and volcanism

The Neuquén Basin hosts hundreds of peculiar veins of solid hydrocarbon (bitumen), which resembles coal (Parnell and Carey, 1995; Cobbold et al., 2014). However, this material is not coal, as the veins are mostly steep dykes, which crosscut (and therefore post-date) the strata (Figure 13). The veins presumably intruded their host rocks, while the organic material within them was liquid oil or asphalt. Later the material solidified, probably by loss of volatile components. Generally, throughout the northern Neuquén Basin, many of the bitumen veins occur within, above, or even just below the Vaca Muerta Formation (Cobbold et al., 2014). Many workers have suggested that the Vaca Muerta Formation was the main source rock for the bitumen veins (e.g., Parnell and Carey, 1995; Cobbold et al., 1999). The idea is that the bitumen resulted from heating of organic-rich shale, producing oil that migrated into veins and subsequently solidified. Parnell and Carey (1995) described evidence for progressive opening of the veins, as a result of overpressure or tectonic stress. Note that some bitumen sills, as well as dykes, occur within shale of the Agrio Formation. Thus there is a possibility that the Agrio shale was also a source rock for some of the bitumen.

In the Mendoza Province, many bitumen veins are sills, parallel to sedimentary strata (Zanella et al., 2015). In contrast, in the provinces of Neuquén and southernmost Mendoza, most bitumen veins are steep, crosscutting dykes (Figure 13). At the surface, individual dykes tend to be continuous, over distances of hundreds of metres or even kilometres (Figure 13E), and they also tend to be parallel, when in swarms (Figure 13A). Many of the bitumen dykes crosscut structures in the Agrio fold belt, which has developed since Late Cretaceous times (Cobbold and Rossello, 2003). Also the dykes crosscut all sedimentary formations, from Jurassic to Palaeocene in age.

The origin of the bitumen veins remains controversial. Early workers stated that the bitumen veins were always “linked to volcanic centres” and that heating was due mainly to magmatic activity, rather than to burial alone (Keidel, 1910; Groeber, 1923). Conversely, Parnell and Carey (1995) favoured a model of progressive heating during Eocene burial. More recently, Cobbold et al. (2014) synthetised all published data with new data, and suggest that early geologists were right, based on the following arguments.

First, in the provinces of Neuquén and southern Mendoza, most of the bitumen veins occur around Tromen volcano, within 70 km of its crater (Figure 13A). A few other veins crop out on the SE flank of Auca Mahuida Volcano (Cobbold et al., 2014), or along the Colorado River were Plio-Pleistocene volcanism occurred (Figure 13B). Around Tromen volcano, many bitumen dykes appear to be radial and point towards the current summit or previous craters of Tromen (Figure 13A). These radial arrangements of the bitumen dykes appear to correlate with the relief and with locally abnormal directions of current greatest horizontal stress to the SE of Tromen volcano, according to data from borehole breakouts (Guzmán et al., 2007). In addition, with distance from the crater of Tromen, some of the radiating bitumen dykes tend to become progressively thinner and even to bifurcate. Their greatest thicknesses (as much as 9.5 m) tend to occur near the foot of the volcano, especially within host rocks that are resistant to fracturing.

Second, the maturity of the bitumen varies regionally. In the domain that is the furthest from Tromen volcano, the bitumen is systematically less mature than in some parts of domains closer to Tromen (Cobbold et al., 2014). In addition, at Curacó Mine (Figure 13E,F), the bitumen within the veins reached higher temperature than the surrounding organic-rich shale (Cobbold et al., 2014). Thus the evidence is for injection of hot oil, forming the dykes.

The correlation between the main volcanic centres and the distribution of the bitumen veins, and the documented anomalously elevated temperatures of the bitumen within the bitumen veins, highlight the potential effect of magmatic activity on the formation of the bitumen veins. Cobbold et al. (2014) concluded that many bitumen veins, in the provinces of northern Neuquén and southernmost Mendoza, formed in Pliocene or Pleistocene times, when large volcanoes (Tromen and Auca Mahuida) were active.

Nevertheless, the exact mechanism of how magmatic activity controlled the formation of the bitumen veins remain poorly understood. Cobbold et al. (2014) proposed that heat advection by hydrothermal fluids generated oil, which intruded adjacent rocks as veins. This mechanism implies regional, distributed effect of magmatic activity. Conversely, geological observations at the locality of El Manzano (Figure 7D)(Rabbel et al., 2021) and at a large bitumen mine near Malargüe (La Valenciana mine; Zanella et al., 2015) suggest that bitumen veins can form in the contact metamorphic aureoles of igneous sills emplaced into organic-rich shale

formations. More research is needed to fully understand the origin of these peculiar geological objects.

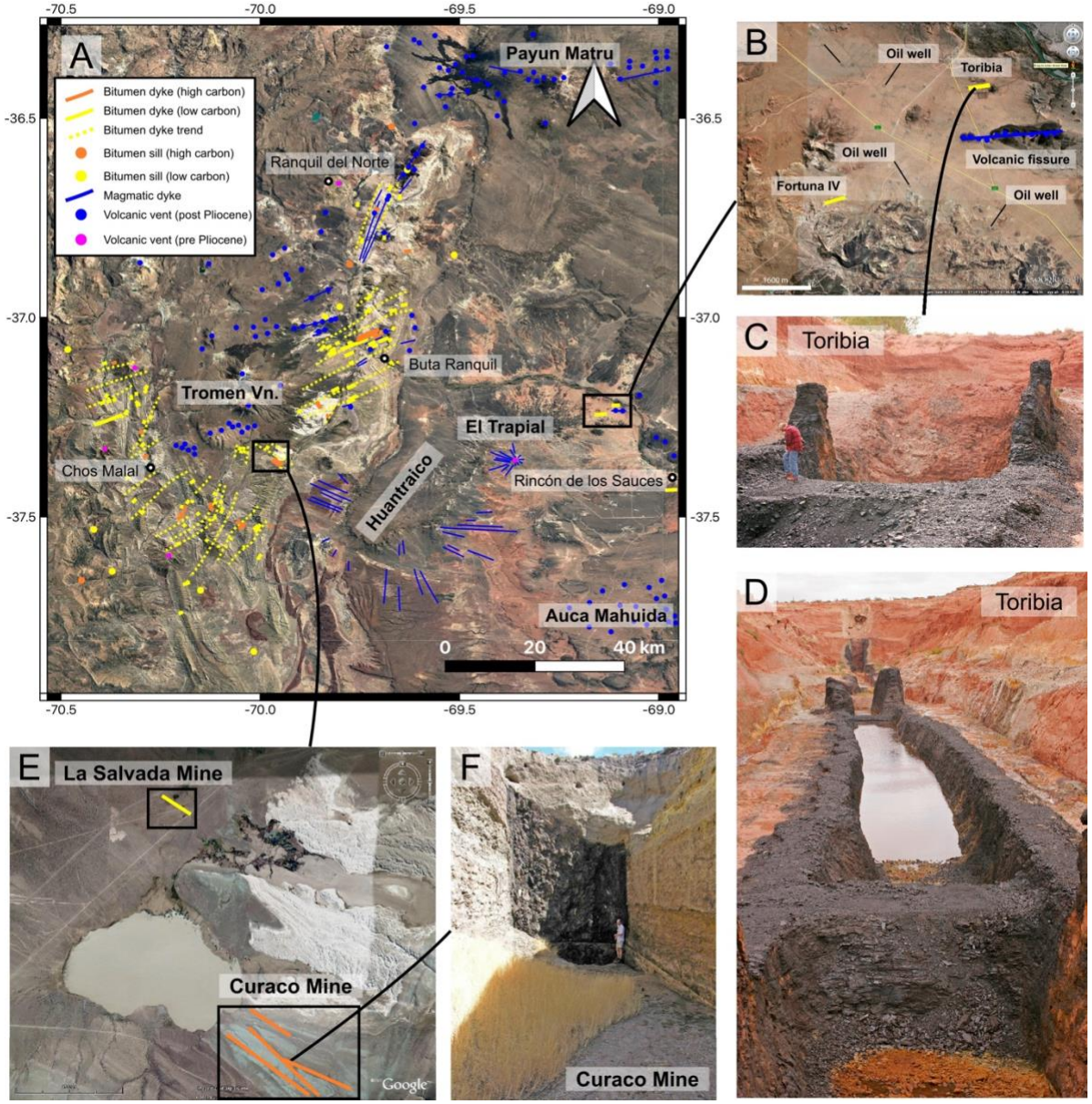

Figure 13. A. Satellite image showing the distribution of bitumen dykes and sills in Central Neuquén Basin. Modified from Cobbold et al. (2014). Black squares locate Toribia bitumen mine (B-D) and La Salvada and Curacó bitumen mines. B. Satellite image of area around Toribia and Fortuna IV bitumen mines. C and D. Field photographs of Toribia Mine. E. Satellite image of area around Auquilco Lake. F. Field photograph of Curacó Mine.

7 Geophysical imaging in volcanic basins

Igneous systems emplaced in sedimentary basins show a wide range of different rock properties and distributions. Acoustic impedance of magmatic rocks is typically much higher than for siliciclastic sedimentary rocks, but can be in the same range as acoustic impedance of carbonates and evaporites. Igneous intrusions are commonly discordant and steeply dipping, and volcanic deposits exhibit highly heterogeneous lithologies. Conventional geophysical imaging techniques are commonly poorly adapted to these complexities, making geophysical imaging of volcanic and subvolcanic systems challenging. In the following sections, we list some case study examples from the Neuquén Basin that highlights how geological data can help improving geophysical imaging of volcanic systems emplaced in sedimentary basins.

7.1 Seismic modelling of sill complexes

3D seismic reflection data are often the primary source for the mapping and characterization of large-scale intrusive complexes (Planke et al., 2005; Jackson et al., 2013a; Magee et al., 2013; Schofield et al., 2015; Schmiedel et al., 2017; Bischoff et al., 2020; Kroeger et al., 2022). A key factor for the advances in seismic mapping of intrusions is that they commonly represent prominent high amplitude reflectors which are easy to map geophysically (Planke et al., 2005; Planke et al., 2015). However, a variety of problems are related to the seismic imaging of igneous intrusions in sedimentary basins. With respect to a typical seismic wavelength, sills often represent thin geological layers of high seismic velocity (Planke et al., 2015). Importantly, recent studies indicate that many sills are too thin to be recognised in seismic images and up to 88% of sills could be missing when interpreting seismic data in volcanic basins (Magee et al., 2015, Schofield et al., 2015). This makes the validation of observations from seismic data difficult in many cases.

Seismic modelling of field analogues is therefore of high importance for improving seismic interpretation of intrusive complexes, because it creates a vital link between geological field observations at the outcrop scale and their expression in seismic data (Lecomte et al., 2016). Realistic seismic modelling requires (1) high-resolution, seismic-scale geological interpretations to provide structural input for the

model geometry, (2) strong constraints on the elastic properties of both intrusions and their host rocks, and (3) use of an adequate modelling technique that correctly implements the 2(3)D resolution and illumination conditions in the subsurface (Lecomte et al., 2016).

Rabbel et al. (2018) presented a study of the hydrocarbon-producing andesitic sills of the Río Grande Valley (see sections 3.1 and 4.1), to illustrate an integrated approach to seismic modelling of field analogues of intrusive complexes. These authors integrated (1) geological interpretation of an andesitic sill complex emplaced in organic-rich shale of the Agrio Formation, exposed along a 4-km long, 400-m high outcrop (Figure 4C and Figure 14B) at the El Manzano locality (see location in Figure 2) and (2) borehole data through sills emplaced in organic-rich shale from the neighbouring Río Grande Valley oil fields to populate the elastic properties of both the intrusions and the host rock (Figure 14A and C).

The seismic models of Rabbel et al. (2018) produced complex interference patterns and their link to the interplay of intrusion geometry and host rock layering that cause them. Such waveform patterns include splitting and transgressive reflections, braided reflections and reflection offsets that could be mistaken for small-scale faults. Comparison to real seismic data shows that these waveforms may be used as indicators for the presence of multiple, potentially stacked and interconnected sills, or intruded intervals that may otherwise not be identified. The individual sills causing such patterns may be less than 10 metres thick in some cases.

Nevertheless, the results of Rabbel et al. (2018) show that each individual sill is not resolved in the seismic model, and only thick sills that are layer-discordant and cause a strong impedance contrast to the surrounding host rock can be mapped with high confidence. The other sills are challenging to detect and are merged in frequency-dependent interference of reflections from host rock layers and intrusions. Features at the scale within the 1/30-wavelength limit of detectability may cause characteristic interference patterns, especially when closely stacked.

Former seismic modelling studies have accounted either for homogeneous host rock (Rohrman, 2007; Magee et al., 2015; Eide et al., 2018) or for a single sill intrusion (Kjenes et al., 2024). In addition, these studies assume systematic high-impedance contrast between the intrusions and their host rock. However, the borehole data presented by Rabbel et al. (2018) show that the impedance contrast can be much lower, if not inverted, in the Río Grande Valley fields. In order to test the relevance a

realistic layered host rock and impedance contrast values, Rabbel et al. (2018) compared seismic models with homogeneous and layered host rocks of realistic impedance measured from borehole (Figure 14). This comparison shows that the seismic model with layered host rock of realistic impedance contrast with the intrusions is much more realistic with respect to the real seismic data from the Río Grande Valley fields (compare Figure 14G and C). The study of Rabbel et al. (2018) thus shows that detailed calibration of geometry and properties of both intrusions and host rock is the key for realistic seismic modelling of sill complexes in sedimentary basins.

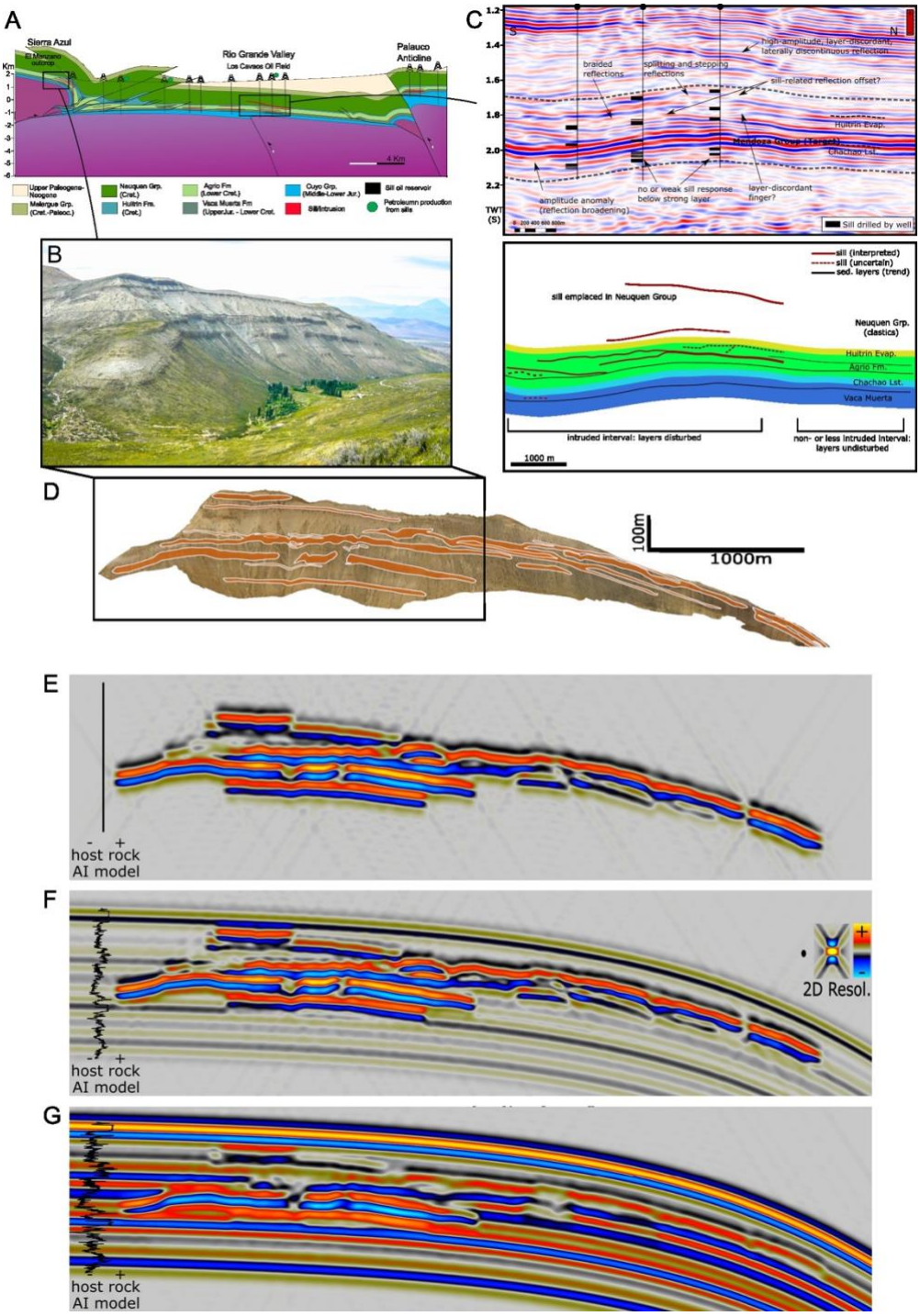

Figure 14. Figure summarising seismic modelling of a sill complex (modified from Rabbel et al., 2018). A. Characteristic geological cross section through the Río Grande oil field and the Sierra Azul, locating the El Manzano outcrop. B. Field photograph of the El Manzano sill complex outcrop. C. Top: Characteristic seismic profile (top) of sill complex in the Río Grande oil fields. Sills (black rectangles) were identified in borehole data. Bottom: interpretation of seismic profile above. D. Orthorectified image of the El Manzano outcrop with interpreted sills. Box locates photograph of B. E. Seismic model of the El Manzano sill complex with homogeneous host rock. F. Seismic model of the El Manzano sill complex with layered host

rock. The acoustic properties of host rock are typical of layered siliciclastic deposits with low acoustic impedance. G. Seismic model of the El Manzano sill complex with layered host rock. The acoustic properties of host rock are those measured in borehole of in the Río Grande Valley oil fields, including shales, carbonates, and gypsum of the Mendoza Group.

7.2 Seismic imaging of subvertical dykes

The seismic data, due to its acquisition characteristics, has primarily been used to image sub-horizontal igneous bodies like volcanic stratigraphy, sills and thin laccoliths (Planke et al., 2000; Thomson and Hutton, 2004; Planke et al., 2005; Bischoff et al., 2020; Bischoff et al., 2021). Conversely, imaging vertical features such as dykes has received less attention because sub-vertical features are harder to detect in reflection seismic volumes (Magee and Jackson, 2020). However, dykes are crucial in volcanic plumbing systems because: (1) their 3D geometry indicates magma transport dynamics from deep to shallow crustal levels, (2) they highlight zones of varying magma flux, and (3) they significantly impact fluid flow in volcanic basins, affecting reservoir compartmentalization (see section 5.3)(Orchuela et al., 2003; Chiacchiera Lobos, 2019) and/or seal by-pass (Senger et al., 2013; Senger et al., 2017). Imaging dykes is further complicated by their thinness, often below the seismic detection threshold.

Lombardo et al. (submitted) proposed a seismic analysis workflow for imaging and extracting subvertical dykes emplaced in sedimentary formations. The case study described by Lombardo et al. (submitted) is the eastern part of the extensive Lower Miocene Huantraico volcanic complex, located in the central Neuquén Basin, Argentina (Figure 15). The remnants of the Huantraico Volcanic Complex consist of a gently folded volcanic plateau (the Huantraico Syncline) and a radial dyke swarm of ~40 km in diameter emplaced in the Mesozoic sedimentary substratum of the volcanic plateau (Figure 15)(Ramos and Barbieri, 1988). The radial dykes are basaltic in composition and reach several kilometers in length and between 10 and 15 m in thickness. Most of the exposed dykes were emplaced in the red sedimentary rocks of the Neuquén Group, such that dykes appear as prominent brown ridges in the red landscape (Figure 15).

The data used by Lombardo et al. (submitted) uses large subsurface data set (3D seismic reflection data, borehole data) gathered during the development of the El

Trapial oil field (see section 4.2)(Lombardo et al., 2024). The workflow described by Lombardo et al. (submitted) is based on seismic reflection data using an on-shore, zero-phase, time-migrated, 3D seismic reflection survey (340 km^2), a post stack seismic inversion volume (P-impedance). Vertical igneous intrusions in sedimentary sequences disrupt the host rock stratigraphy and interrupt the lateral continuity of the layers. If this perturbation is big enough it is expected to affect the continuity of the reflectors of the sedimentary host-rock, resulting in a subtle but measurable seismic response (Figure 15)(Magee and Jackson, 2020).

The workflow consists of extracting two complementary attributes from the 3D seismic data. The first attribute is “Amplitude Contrast”, which is a measure of amplitude similarity or difference between adjacent traces in 2D or 3D seismic volumes. High attribute value means high amplitude contrast, and can indicate faults or fracture corridors, or dykes and dyke swarms. The presence of a vertical dyke locally distorts the horizon reflected amplitude, creating a traceable anomaly on map view (Figure 15).

The second attribute results from successive implementation of "Variance" and "Ant Tracking". The first step involves calculating an attribute which enhances the spatial discontinuities in the seismic volume (Variance). Variance is a commonly used seismic edge detection attribute that measures variability between seismic traces waveforms in three dimensions. It is designed to highlight discontinuities of layers, such as faults and any other sharp contrast in the seismic volume (Figure 15). The second step consists of delineating the discontinuities highlighted by the Variance attribute using Ant Tracking, which suppresses the noise and enhances the lateral continuity of the features. Running Ant Tracking on Variance volume data thus enhances subtle structural discontinuities and accentuates planar features, favoring their extraction from the input 3D volume.

This workflow applied to the data from the Huantraico Volcanic Complex (Figure 15) highlights linear features on map view in Amplitude Contrast maps and vertical planar features on Ant Tracking volume. The extraction from the Ant Tracking volume (Figure 15) highlights that these anomalies correspond to planar subvertical structures that extend across part of the Mesozoic stratigraphy in the study area, and in part can be traced to dykes at the surface where outcrops allow. Outcropping dykes exhibit the same distribution as those of the subsurface linear discontinuities highlighted by the

seismic workflow of Lombardo et al. (submitted), strongly suggesting that these discontinuities correspond to dykes in the subsurface.

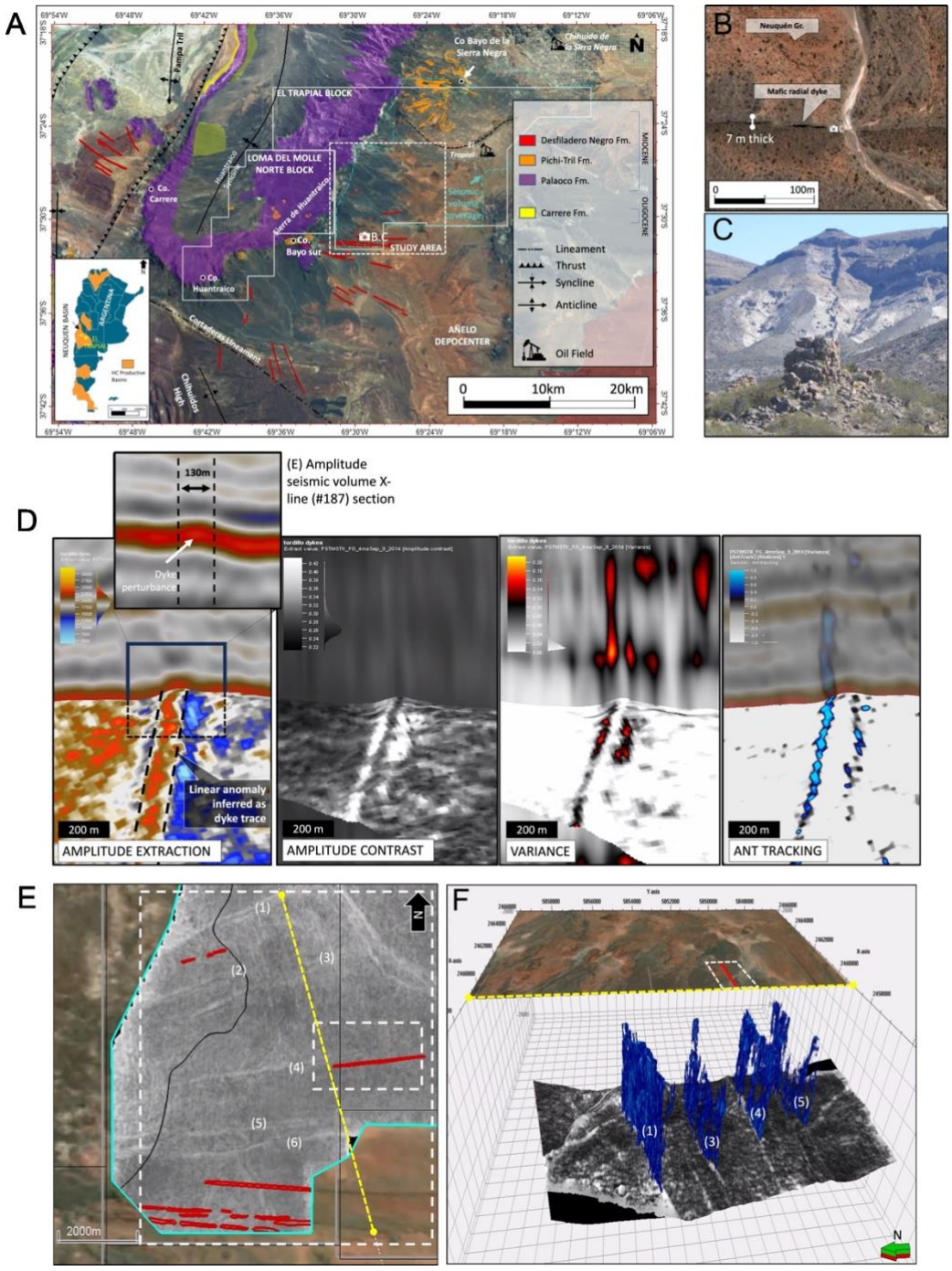

Figure 15. Figure summarising seismic imaging of dykes (Lombardo et al., under review). A. Satellite image of southern Huantraico region, including geology of Cenozoic volcanic deposits, outcropping radial dykes, location of 3D seismic cube (polygon with blue dashed line), locations of B and C, and El Trapial and Loma del Molle blocks (solid white lines); modified from Ramos and Barbieri (1988), Kay and Copeland (2006), Garrido et al. (2012) and Turienzo et al. (2020). B. Detailed satellite image of vertical dyke, located in A. C. Field

photograph of a characteristic vertical dyke. D. Left: Amplitude extraction, representing the raw and unprocessed amplitude over the Tordillo reflector. The inset displays a detailed vertical seismic section of the amplitude volume, showing a bell-shaped perturbation of the Tordillo reflector. Centre left: Amplitude contrast, providing better shape delineation. Centre right: Variance. Right: Ant tracking applied on Variance volume, showing good performance in feature delineation. The vertical section is a combination of the Amplitude volume and the Ant Tracking volume. E. Amplitude Contrast map extracted over Tordillo reflector and dykes cropping out at surface interpreted on satellite image (red lines). Amplitude Contrast map highlights linear features (numbered) interpreted as dykes. F. Oblique view of a 3D block diagram integrating map of Amplitude Contrast extracted over Tordillo reflector, dyke extractions from the Ant Tracking volume (blue planar features) and satellite image (vertical scale exaggerated x20 for visualization purpose).

7.3 Sub-volcanic seismic imaging

Numerous sedimentary basins host significant piles of extrusive lava flows. Such sequences have highly heterogeneous geological structures that cause high impedance contrasts between the layers that make up the sequence. However, the rough interfaces of the individual lava flows significantly degrades the seismic signal (Maresh et al., 2006; Nelson et al., 2015; Schuler et al., 2015). This results in major challenges in imaging the internal structure of the basalt sequence, constraining its total thickness and limiting the ability to quantify the sub-basalt geology (Sanford et al., 2023).

The Loma del Molle Norte (LDMN) block, which includes the Huantraico Volcanic Complex, features complex volcanic geology and topography (see Section 7.2). Large areas of the LDMN block include the eruptive products of the Lower Miocene Huantraico Volcanic Complex, preserved in the gently folded Huantraico Syncline. The volcanic cover forms a plateau approximately 600 metres higher than the surrounding terrains. Under this volcanic cover, laccoliths and sills could potentially serve as the structural and trapping mechanism for conventional oil and gas reservoirs, similar to those found in the El Trapial Field (see Section 4.2) and Auca Mahuida Volcano (see Section 5.3). However, no commercial accumulations of conventional oil and gas have been discovered yet. The presence of the Vaca Muerta

formation with good organic facies drives the detailed study of the Loma del Molle Norte intrusive complex.

At the surface, the plumbing system of the Huantraico Volcanic Complex is exposed outside the volcanic plateau, i.e. where the volcanic cover has been eroded, and consists of a swarm of radial dykes and a few sills emplaced in the red sedimentary rocks of the Neuquén Group (Figure 16A)(see Section 7.2). The dykes converge toward the central part of the complex, near the middle of the volcanic plateau (yellow star in Figure 16A).

3D seismic data has been acquired 20 years ago, focusing on conventional reservoirs. However, the structure of both the plumbing system and the sedimentary host rock below the volcanic cover was not revealed through conventional seismic processing (Figure 16C). Motivated to better understand the drilling risks of the volcanic complex, a 24 Hz Full Waveform Inversion (FWI) was done to better resolve the near-surface and deep velocity complexities (Figure 16D). Therefore, iterative ray-based reflection tomography and well calibration were performed to provide a good starting velocity model for FWI inversion and improved seismic imaging at the reservoir level.

Reprocessed seismic data revealed key features, including laccoliths, sills, dykes, and faults (Figure 16E), and better delineates their geological extension. Sills were identified as sub-horizontal, high-impedance reflections. The single-iteration Least-Square Migration with curvelet-domain application improves the illumination issues, reduces migration artifacts, and provides an image with better continuity for structural and quantitative studies compared to conventional Pre-Stack Depth Migration (PSDM).

Ultimately, the FWI image provides a more detailed image of the subsurface compared to the migration image by highlighting fine structural details such as dykes and laccoliths (Figure 16E), which can be hardly observed in the migration image.

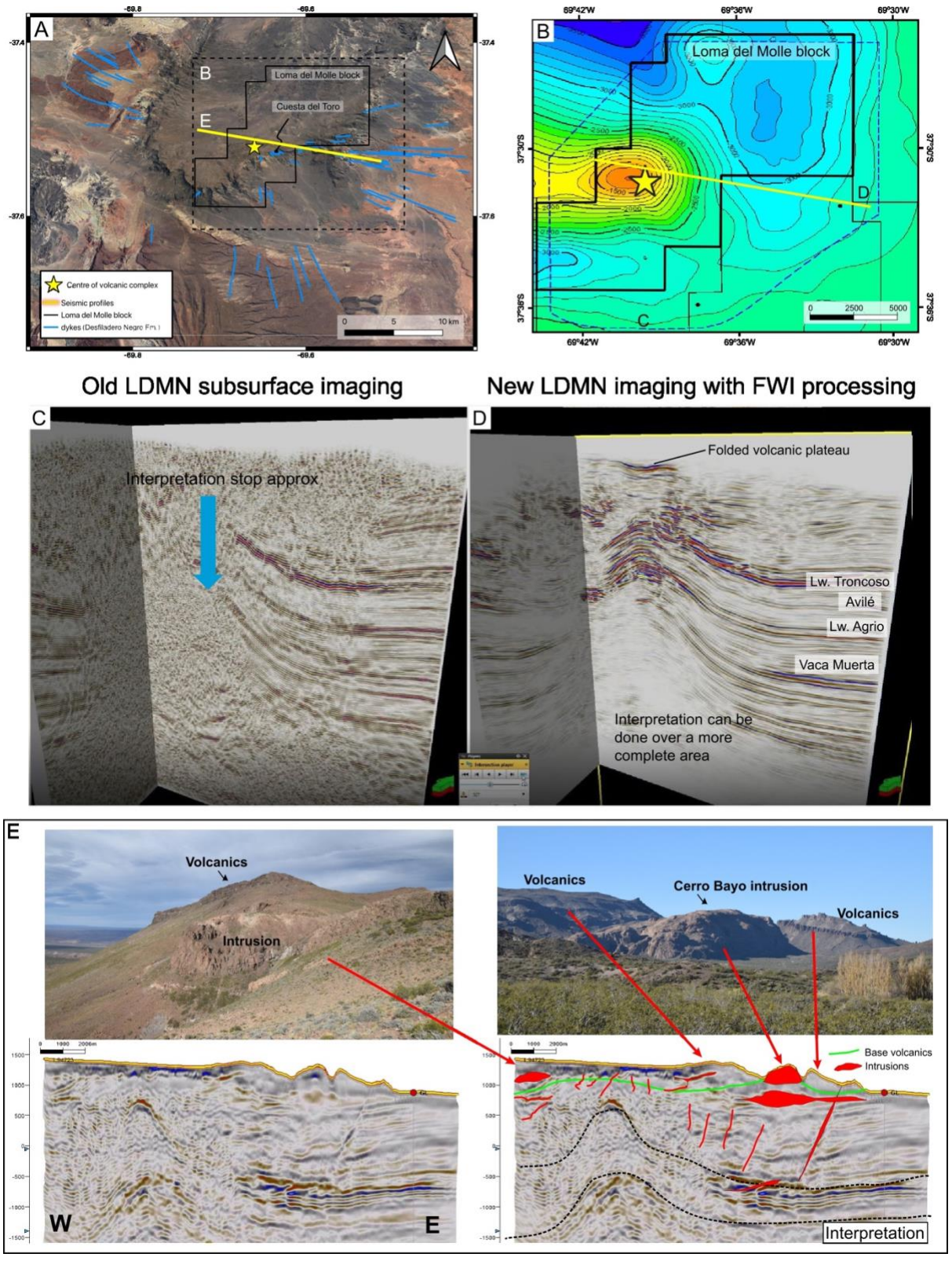

Figure 16. A. Satellite image of Huantraico Volcanic complex locating radial dykes (blue lines), the boundary of the Loma del Molle Norte block (black solid polygon), the extent of the map of B, the centre of the volcanic complex (yellow star) and the location of seismic section of E (yellow line). Dark rocks correspond to Lower Miocene volcanic plateau. B. Depth map of Top Mulichinco Formation computed from 3D seismic data (see location in A). C. Seismic profile

from old LDMN seismic data. D. Seismic profile at same location as that of C after FWI processing. E. Ground truthing of seismic data with field observations.

7.4 Imaging igneous intrusions using remote geophysical methods

Even though igneous intrusions commonly exhibit significantly higher acoustic impedance than their sedimentary host rock (e.g., Magee et al., 2018), the literature highlights that seismic imaging of igneous intrusions in sedimentary basins can be challenging (Mark et al., 2018; Rabbel et al., 2018). Examples in the Neuquén Basin support this statement, such as the sill complex in the Río Grande Valley oil fields or the Pampa Amarilla laccolith, which only appear as local perturbances of the stratigraphic reflectors (Figure 9B and Figure 14C; see Section 7.1)(Rabbel et al., 2018; Galland et al., 2022). Conversely, mapping igneous intrusions by well correlation may be valuable, but well data provide only 1D data and are very costly.

Nevertheless, a combination of different geophysical methods (seismic, gravity, magnetics, magneto telluric, etc) in combination with outstanding outcrop control within the Neuquén Basin may allow to fully reveal the impact of volcanic plumbing systems on the petroleum system. As new data is collected, this can be used to not only study the sedimentary structure but also to reveal the distribution and geometries associated with volcanic plumbing systems.

The magnetotelluric (MT) method explores the Earth's subsurface conductivity by measuring time-varying electric and magnetic fields. The audiomagnetotelluric (AMT) method, an extension of MT with a higher frequency range (1 Hz to 1 MHz), is particularly useful for imaging the shallowest hundreds of meters (Simpson and Bahr, 2005). In recent years, electromagnetic methods have been widely used to characterize cover geology, estimate basement depth, and constrain igneous intrusive bodies (Tabod et al., 2006; Zhao et al., 2019; Subbarao et al., 2023; Jiang et al., 2024).

In this section, we present the results from an exploratory controlled-source AMT (CSAMT) survey, which uses artificially generated signals from a controlled-source transmitter (10 Hz to 100 kHz). We performed the AMT survey across the well-constrained Pampa Amarilla dome structure (see Section 4.3 and Figure 9) (Galland et al., 2022), to assess the potential of the method for resolving shallow intrusion geometry.

The CSAMT profile consisted of 12 survey sites, spaced 500–1000 m apart (Figure 17A). AMT responses were distorted by cultural and geological noise, mitigated using tensor decomposition and strike analysis (Groom and Bailey, 1989; McNeice and Jones, 2001; Caldwell et al., 2004). This technique also determines subsurface dimensionality, classifying AMT data as 1D (horizontally homogeneous layers), 2D (layering varying in two directions), or 3D (complex variations in all directions).

The acquired data were of high quality, except for AMT stations 1 and 9, which exhibited distortions. Frequencies above 1000 Hz showed high distortion, indicating reduced reliability in shallow zones, while frequencies below 1000 Hz provided more reliable deep subsurface data. Geoelectric strike analysis indicated a complex structure with conductivity variations in all directions. Noise and static shift distortions were corrected using WinGLink software, yielding final phase and apparent resistivity curves. For 2D modeling, an initial grid incorporated prior geological and geophysical constraints (Figure 9C; Section 4.3)(Galland et al., 2022). Resistivities and thicknesses of geological units were estimated based on LLD/NS log records from the PA.x-6 borehole (Roch S.A.) and seismic line L390 (see well and seismic line locations in Figure 17A): Vaca Muerta Formation (thickness: 225 m; resistivity: 80 Ω m), Agrio Formation (thickness: 250 m; resistivity: 60 Ω m), Neuquén Group (outcropping; resistivity: 38 Ω m), laccolith (thickness: 400 m; resistivity: 1600 Ω m).

The best-fitting model was selected based on correlations between observed and inverted data (Figure 17C). Two distinct domains were identified: a resistive eastern domain and a conductive western domain. Skin depth analysis revealed that deeper electrical structures were better resolved in the eastern domain than in the western domain. The AMT model identified eight geoelectric units correlated with major geological formations based on boreholes PA.x-6 and PA.x-2 (Figure 17D):

- Neuquén Group: shallow western sector (geoelectric zones b, h, d), with resistivities between <16 and 150 Ω·m.
- Agrio, Chachao, and Vaca Muerta formations: 600–1000 m depth (geoelectric zone g), resistivities <16 Ω·m.
- Laccolith: Eastern sector, depths >400 m (geoelectric zone e), resistivities 500–1000 Ω·m, correlating with dioritic andesites (PA.x-2 borehole).

The geological units in the western geoelectric domain dip ~30° to the west (Figure 17C), in agreement with the seismic and geological interpretation (Galland et al., 2022). In the central sector, an abrupt lateral resistivity change was interpreted as a high-angle normal fault, consistent with western bounding fault of the trapdoor dome of the Pampa Amarilla Laccolith (Galland et al., 2022).

The 2D AMT model reveals a high-resistivity, tabular body (500–1000 Ω·m) in the eastern sector, corresponding to the laccolith. The modelled top surface is ~400 m below ground level, aligning with the structural reconstruction of Galland et al. (2022) (Figure 17C), who inferred an asymmetrical shape with a 400 m thickness in the west, tapering eastward. However, the AMT model suggests a uniform thickness with a base extending to ~900 m or deeper (method limitations apply). The AMT model also suggests that the intrusive body extends ~500 m further west than the structural interpretation of Galland et al. (2022) (Figure 17C).

All in all, the AMT inversion is in good agreement with the integrated seismic/structural study of the Pampa Amarilla laccolith (Section 4.3) (Galland et al., 2022). This shows the relevance and robustness of AMT survey to constrain subsurface distribution of igneous intrusions in sedimentary basins. In addition, the AMT data reveal some difference with respect to the structural interpretation of Galland et al. (2022), suggesting that combining geophysics and structural approach may be complementary, and so provide better results.

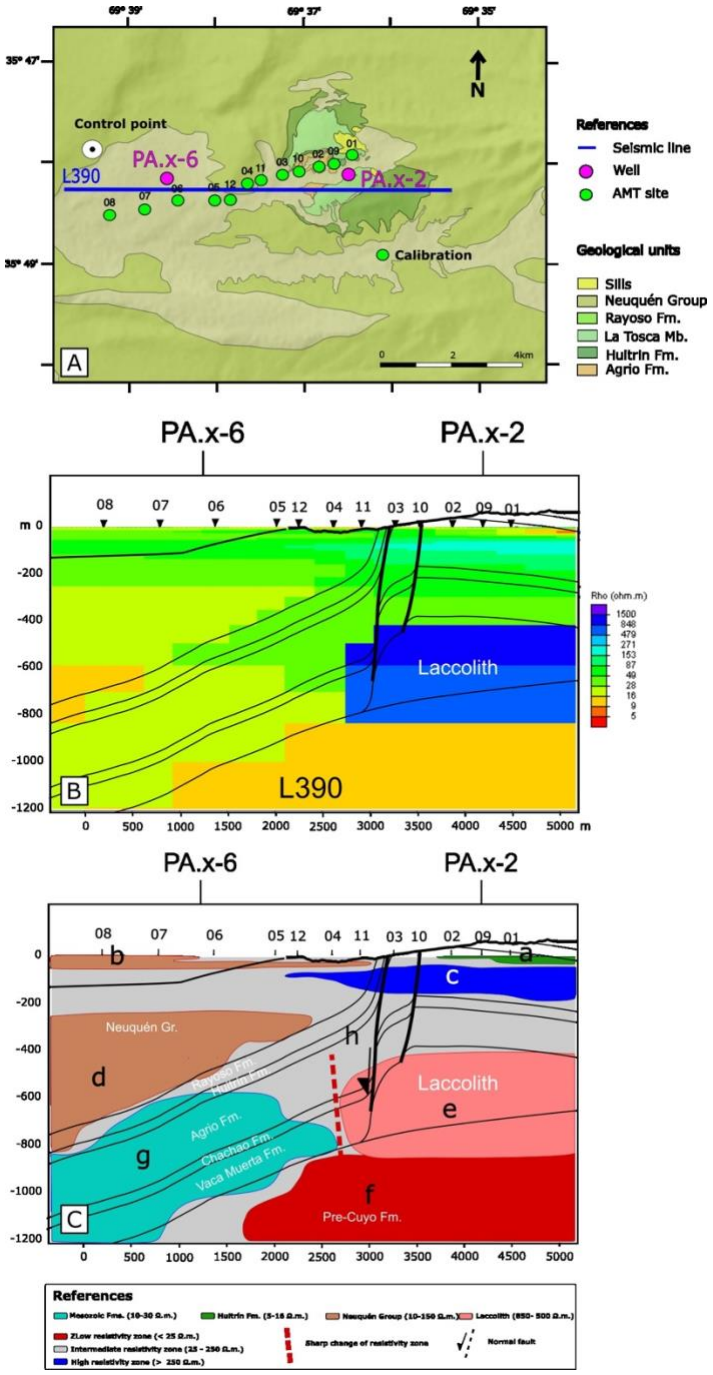

Figure 17. A. Simplified geological map of Pampa Amarilla dome locating the measurement stations (green dots), the section L390 (blue line), and wells PA.x-6 and PA.x-2 (pink dots), modified from Galland et al. (2022) and Figure 9. Cross section L390 has a similar orientation as that of AMT profile. B. AMT 2D inverted model by software WinGLink, with superimposed geological cross section of upper Figure 9C (Galland et al., 2022). C. Interpreted AMT model highlighting geoelectrical domains (letters, see text for explanation), with superimposed geological cross section of upper Figure 9C.

8 Concluding remarks and future research directions

8.1 The Neuquén Basin, a world class case study

The Neuquén Basin is a unique volcanic basin that offers (1) substantial industry subsurface data of buried igneous petroleum systems and (2) outstanding seismic-scale outcrops of exhumed igneous petroleum systems. As such, the Neuquén Basin represents a unique case study for advancing our understanding of magma-sedimentary rock interactions, and more precisely of the impacts of volcanism on the petroleum system.

Many case study examples described in this paper could not have been possible without academia-industry collaborations (see sections 3.1, 4.1, 4.2, 4.3, 5.3 and 7). The added value of such collaborations is that industry partners gave access to substantial subsurface data (seismic, borehole) that are not affordable for academic institutions, whereas the scientific problems provided by industry partners are of high academic values to understand fundamental processes of magma-sedimentary rock interactions. Our review thus highlights that high-quality academic research and applied research are not excluding each other, and that working hand-in-hand can boost research frontiers and quality.

Both the published subsurface data from producing hydrocarbon fields associated with volcanic systems and the easy access to outstanding outcrops make the Neuquén Basin a very valuable educational object for training academia and industry geoscientists on the relevance of volcanic basins.

8.2 Implications for igneous petroleum systems

Our review shows that the classification of Delpino and Bermúdez (2009) based on Type I and Type II igneous petroleum systems, is somehow too restrictive. Type I igneous petroleum systems, i.e. when igneous intrusions are emplaced into a source rock, mostly addresses hydrocarbon generation with respect to the thermal state of the system. Conversely, Type II igneous petroleum systems, i.e. when igneous intrusions are emplaced in other rock formations, mostly addresses the local mechanical effects of igneous intrusions on fluid migrations or storage. However, the El Trapial oil field (section 4.2) and Pampa Amarilla laccolith-induced doming (section 4.3) examples fall in-between Type I and Type II igneous petroleum systems. In both

cases, the igneous intrusions were emplaced into the source rock of the Vaca Muerta Formation, but the structural effects on reservoir properties are effective in other rock formations (potential Chachao limestone fractured reservoir at Pampa Amarilla, Galland et al., 2022; conventional Troncoso sandstone reservoir in El Trapial field, Lombardo et al., 2024). The Type I and Type II defined by Delpino and Bermúdez (2009) only account for local effects of igneous intrusions, i.e. in the contact aureole or the intrusion itself. Our review paper shows that volcanic systems can have larger effects that extend beyond the contact aureole.

Finally, the generation of bitumen dykes in the Neuquén Basin (Section 6) suggests that volcanism can affect hydrocarbon generation and migration over large areas of the basin.

8.3 Implications for improving geophysical imaging in volcanic basins

Numerous volcanic basins worldwide are not eroded and are only accessible through geophysical imaging. Major issues of interpreting geophysical data are (1) low resolution that is not sufficient to capture the metre- to decametre-scale processes, which are characteristic of most igneous intrusions and magma/sedimentary rock interactions, and (2) the non-uniqueness of the interpretation.

Examples described in Section 7 highlight the added value of integrating outcrop data to improve the robustness and the geological relevance of geophysical data interpretation. In addition, the geophysical-scale outcrops of volcanic plumbing systems emplaced in sedimentary sequences throughout the basin can be used to calibrate geophysical methods, either through forward geophysical modelling (see Section 7.1), or ground-truthing of geophysical data inversion (see Section 7.4). Outcrops of the Neuquén Basin thus offer world-class opportunities to improve geophysical imaging of buried volcanic basins.

8.4 Future research questions

This review highlights several, still unresolved, research directions on the effects of volcanism on hydrocarbon-bearing sedimentary basins.

- It is necessary to understand in which conditions igneous intrusions are high-permeability, fractured reservoirs or low-permeability, seal or compartmentalising layers. This not only has profound implications for fluid flow within the basin it is also important regarding potential carbon storage.
- The high-permeability intrusions documented in this paper highlight local migration of hydrocarbons (see Cerro Alquitrán, Section 5.2). Nevertheless, in numerous basins, igneous sill complexes are extensive, sometime across the entire basin that hosts them. It is thus important to understand to which extent extensive sill complexes control and impact basin-scale subsurface fluid migration, which would be key for basin models;
- Section 6 highlights a correlation between the distributions of bitumen veins throughout the Neuquén Basin and volcanism, however the detailed mechanism of how volcanic activity can stimulate the generation of bitumen veins remains to be revealed.

Further research in the Neuquén Basin has the potential to provide the necessary data to address these fundamental questions.

8.5 Other applications of magma/sedimentary rock interactions

The research conducted in the Neuquén Basin addresses fundamental processes of magma/sedimentary rock interactions and fluid migrations. So far, the main application of this knowledge in the Neuquén Basin has been focused on hydrocarbon industry, as the basin has been a major producer of oil and gas for decades. This focus has, on the flip side, provided valuable detailed subsurface data-sets, without which many of the fundamental research questions on the effects of the volcanic system in the sedimentary basin setting would still remain unanswered. This built up knowledge on, e.g. fluid migration, reservoir structure, magma-sediment interactions, thermal stimulation of fluid migration, that has been facilitated through these Neuquén Basin studies, can also be applied to other processes involving fluid flow and trapping, such as ground water exploration, CO_2 storage in both volcanic and sedimentary rocks, exploration of critical minerals (e.g. graphite in contact aureoles of sills emplaced in organic-rich shale, REE in bitumen veins, etc). Thus the legacy of the Neuquén Basin as a window into the impacts of volcanism on hydrocarbon-bearing sedimentary

basins, extends beyond the basin and towards a world-class case study and reference point.

Acknowledgements

The authors thank Chevron Argentina for providing the seismic data presented in Sections 4.2, 7.2 and 7.3, ROCH S.A. for providing the seismic and borehole data presented in Section 4.3, and YPF for providing subsurface data presented in Sections 3.1 and 7.1. D. A. Jerram is partly funded through the Research Council of Norway's 'Beyond Elasticity' project (grant 334654) at the NJORD Centre, UNiversity of Oslo.

References

Aarnes, I., Svensen, H., Connolly, J.A.D., Podladchikov, Y.Y., 2010. How contact metamorphism can trigger global climate changes: Modeling gas generation around igneous sills in sedimentary basins. Geochimica et Cosmochimica Acta 74, 7179-7195, doi: 10.1016/j.gca.2010.09.011.

Aarnes, I., Svensen, H., Polteau, S., Planke, S., 2011. Contact metamorphic devolatilization of shales in the Karoo Basin, South Africa, and the effects of multiple sill intrusions. Chemical Geology 281, 181-194, doi: 10.1016/j.chemgeo.2010.12.007.

Abdelmalak, M.M., Rossetti, L.M., Millett, J.M., Planke, S., Jerram, D.A., Faleide, J.I., Polteau, S., 2025. Breakup Magmatism in the South Atlantic: Mechanisms and Implications. Earth-Sci. Rev. 264, 105088, doi: https://doi.org/10.1016/j.earscirev.2025.105088.

Agirrezabala, L.M., 2015. Syndepositional forced folding and related fluid plumbing above a magmatic laccolith: Insights from outcrop (Lower Cretaceous, Basque-Cantabrian Basin, western Pyrenees). Geol. Soc. Am. Bull., doi: 10.1130/b31192.1.

Araujo, V.S., Frisicale, M.C., Sánchez, N., Turienzo, M., Lebinson, F., Dimieri, L.V., 2019. The relationship between Cenozoic shallow igneous bodies and thrust systems of the mountain front of the Cordillera Principal, Mendoza province, Argentina. J. S. Amer. Earth. Sci. 92, 531-551, doi: https://doi.org/10.1016/j.jsames.2019.03.027.

Baldauf, P., Stephens, G., Nullo, F.E., Combina, A.M., Kunk, M., 1997. Tertiary uplift, magmatism and sedimentation of the Andes, Southern Mendoza Province, Argentina, Geological Society of America, Abstracts with Program.

Barrionuevo, M., Giambiagi, L., Mescua, J., Suriano, J., de la Cal, H., Soto, J.L., Lossada, A.C., 2019. Miocene deformation in the orogenic front of the Malargüe fold-and-thrust belt (35°30′–36° S): Controls on the migration of magmatic and hydrocarbon fluids. Tectonophysics, doi: https://doi.org/10.1016/j.tecto.2019.06.005.

Basaldúa, A.D., Cristallini, E.O., 2022. Evolución y estructuración dómica del subsuelo del campo volcánico Auca Mahuida, Neuquén; Asociación Geológica Argentina. Revista de la Asociación Geológica Argentina 79, 1–17.

Bauer, K., Schulze, A., Ryberg, T., Sobolev, S.V., Weber, M.H., 2003. Classification of lithology from seismic tomography: A case study from the Messum igneous complex, Namibia. J. Geophys. Res. 108, doi: https://doi.org/10.1029/2001JB001073.

Bermúdez, A., Delpino, D.H., 2008. Concentric and radial joint systems within basic sills and their associated porosity enhancement, Neuquén Basin, Argentina, in: Thomson, K., Petford, N. (Eds.), Structure and Emplacement of High-Level Magmatic Systems, pp. 185-198, doi: 10.1144/sp302.13.

1487 Bettini, F., 1982. Complejos efusivos terciarios presentes en las Hojas 30c y 32b
1488 (Puntilla del Huincán y Chos Malal), del sur de Mendoza y Norte del Neuquén,
1489 Argentina, Actas V Congreso Latinoamericano de Geología, pp. 79-114.

1490 Bischoff, A.P., Bankher, K.A., Alashi, E.A., Arola, T., Brinji, H.S., Németh, K.,
1491 Martinkauppi, A., Jabrte, A.H., Kortunov, E., Alzahrani, I.S., Martinkauppi, I., Melibari,
1492 R.A., 2025. Geothermal resources in the northern Harrat Rahat volcanic field, Saudi
1493 Arabia: A drilling and field data assessment. Geothermics 128, 103272, doi:
1494 https://doi.org/10.1016/j.geothermics.2025.103272.

1495 Bischoff, A.P., Barrier, A., Beggs, M., Nicol, A., Cole, J.W., 2020. Volcanoes Buried in
1496 Te Riu-a-Māui/Zealandia Sedimentary Basins. New Zealand Journal of Geology and
1497 Geophysics - IAVCEI Special Issue: Cenozoic Volcanism in New Zealand, doi:
1498 https://doi.org/10.1080/00288306.2020.1773510.

1499 Bischoff, A.P., Nicol, A., Beggs, M., 2017. Stratigraphy of architectural elements in a
1500 buried volcanic system and implications for hydrocarbon exploration. Interpretation 5,
1501 SK141-SK159, doi: 10.1190/INT-2016-0201.1.

1502 Bischoff, A.P., Planke, S., Holford, S., Nicol, A., 2021. Seismic Geomorphology,
1503 Architecture and Stratigraphy of Volcanoes Buried in Sedimentary Basins, in: Károly,
1504 N. (Ed.), Updates in Volcanology. IntechOpen, Rijeka, p. Ch. 4, doi:
1505 10.5772/intechopen.95282.

1506 Boll, A., Alonso, J., Fuentes, F., Vergara, M., Laffitte, G.A., Villar, H.J., 2014. Factores
1507 controlantes de las acumulaciones de hidrocarburos en el sector norte de la Cuenca
1508 Neuquina, entre los Ríos Diamante y Salado, Provincia de Mendoza, Argentina, IX
1509 Congreso de Exploración y Desarrollo de Hidrocarburos, Mendoza, pp. 3-44.

1510 Brisson, I., Veiga, R.D., 1998. La estratigrafía y estructura de la Cuenca Neuquina:
1511 Gira de campo, unpublished report. Repsol YPF, Buenos Aires, p. 1—58.

1512 Brisson, I.E., Fasola, M.E., Villar, H., 2020. Organic Geochemical Patterns of the Vaca
1513 Muerta Formation, in: Minisini, D., Fantin, M., Lanusse Noguera, I., Leanza, H.A.
1514 (Eds.), Integrated Geology of Unconventionals: The Case of the Vaca Muerta Play,
1515 Argentina. American Association of Petroleum Geologists, pp. 297-328.

1516 Bunger, A.P., Cruden, A.R., 2011. Modeling the growth of laccoliths and large mafic
1517 sills: Role of magma body forces. J. Geophys. Res. 116, B02203, doi:
1518 10.1029/2010jb007648.

1519 Caldwell, T.G., Bibby, H.M., Brown, C., 2004. The magnetotelluric phase tensor.
1520 Geophys. J. Int. 158, 457-469, doi: 10.1111/j.1365-246X.2004.02281.x.

1521 Chevallier, L., Gibson, L.A., HNhleko, L.O., Woodford, A.C., Nomquphu, W., Kippie, I.,
1522 2004. Hydrogeology of fractured-rock aquifers and related ecosystems within the

Qoqodala dolerite ring and sill complex, Great Kei catchment, Eastern Cape, Water Res. Com., S. Afr. Water Research Commission, p. 127.

Chevallier, L., Goedhart, M., Woodford, A., 2001. The influence of dolerite sill and ring complexes on the occurrence of grounwater in the Karoo fractured aquifers: a morpho-tectonic approach, Water Res. Com., S. Afr., p. 143.

Chiacchiera Lobos, S.A., 2019. Controles estructurales y mágmaticos en reservorios de la Formación Mulichinco en el yacimiento Volcán Auca Mahuida, Provincia de Neuquén, Argentina. Universidad Nacional de Río Negro, Neuquén.

Chiacchiera, S.A., Ribas, S., Orts, D., 2022. Controles estructurales y magmáticos en reservorios de la Formación Mulichinco en el yacimiento Volcán Auca Mahuida, provincia de Neuquén, Argentina, XI Congreso de Exploración y Desarrollo de Hidrocarburos. Instituo Argentino del Petroleo y del Gas, Mendoza, p. 291—311.

Cobbold, P.R., Diraison, M., Rossello, E.A., 1999. Bitumen veins and Eocene transpression, Neuquén basin, Argentina. Tectonophysics 314, 423-442.

Cobbold, P.R., Rossello, E.A., 2003. Aptian to recent compressional deformation, foothills of Neuquén Basin, Argentina. Mar. Pet. Geol. 20, 429-443.

Cobbold, P.R., Ruffet, G., Leith, L., Loseth, H., Rodrigues, N., Leanza, H.A., Zanella, A., 2014. Radial patterns of bitumen dykes around Quaternary volcanoes, provinces of northern Neuquén and southernmost Mendoza, Argentina. J. S. Amer. Earth. Sci. 56, 454-467, doi: https://doi.org/10.1016/j.jsames.2014.09.015.

Combina, A.M., Nullo, F., 2011. Ciclos tectónicos, volcánicos y sedimentarios del Cenozoico del sur de Mendoza-Argentina (35°-37° S y 69° 30'W). Andean geology 38, 198-218.

Corry, C.E., 1988. Laccoliths: mechanisms of emplacement and growth.

Courtillot, V.E., Renne, P.R., 2003. On the ages of flood basalt events. Comptes Rendus Geoscience 335, 113-140, doi: https://doi.org/10.1016/S1631-0713(03)00006-3.

Cruden, A.R., McCaffrey, K.J.W., Bunger, A.P., 2018. Geometric Scaling of Tabular Igneous Intrusions: Implications for Emplacement and Growth, in: Breitkreuz, C., Rocchi, S. (Eds.), Physical Geology of Shallow Magmatic Systems: Dykes, Sills and Laccoliths. Springer International Publishing, Cham, pp. 11-38, doi: 10.1007/11157_2017_1000.

Cruden, A.R., Weinberg, R.F., 2018. Chapter 2 - Mechanisms of Magma Transport and Storage in the Lower and Middle Crust—Magma Segregation, Ascent and Emplacement, in: Burchardt, S. (Ed.), Volcanic and Igneous Plumbing Systems. Elsevier, pp. 13-53, doi: https://doi.org/10.1016/B978-0-12-809749-6.00002-9.

D'Elia, L., García, M., Feinstein, E., Villarreal, A., Juan, F., Klocker, F., Berdini, O., Poiré, D., Franzese, J., 2023. Characterization of a naturally fractured ignimbrite reservoir: Subsurface model validated from worldwide analogue outcrops and production data. Mar. Pet. Geol. 158, 106558, doi: https://doi.org/10.1016/j.marpetgeo.2023.106558.

de Miranda, F.S., Vettorazzi, A.L., Cunha, P.R.C., Aragão, F.B., Michelon, D., Caldeira, J.L., Porsche, E., Martins, C., Ribeiro, R.B., Vilela, A.F., Corrêa, J.R., Silveira, L.S., Andreola, K., 2018. Atypical igneous-sedimentary petroleum systems of the Parnaíba Basin, Brazil: seismic, well logs and cores. Geol. Soc. London. Spec. Pub. 472, 341, doi: 10.1144/SP472.15.

de Saint-Blanquat, M., Habert, G., Horsman, E., Morgan, S.S., Tikoff, B., Launeau, P., Gleizes, G., 2006. Mechanisms and duration of non-tectonically assisted magma emplacement in the upper crust: The Black Mesa pluton, Henry Mountains, Utah. Tectonophysics 428, 1-31, doi: 10.1016/j.tecto.2006.07.014.

Delpino, D., Bermúdez, A., Vitulli, N., Loscerbo, C., 2014a. Sistema de petróleo no convencional relacionado con lacolitos eocenos de intraplaca. Área Altiplanicie del Payún, Cuenca Neuquina, IX Congreso de Exploración y Desarrollo de Hidrocarburos. Argentinean Oil and Gas Institute (IAPG), Mendoza, pp. 223-242.

Delpino, D., Santiago, E., Carrizo, N., Mendez, M.A., Zurita, D., 2014b. Miembro Centenario Inferior: Un nuevo reservorio en el yacimiento Volcán Auca Mahuida-Risco Alto-Las Manadas, Cuenca Neuquina, Argentina, IX Congreso de Exploración y Desarrollo de Hidrocarburos. Instituto Argentino del Petróleo y del Gas, p. 65—72.

Delpino, D.H., Bermúdez, A.M., 2009. Petroleum systems including unconventional reservoirs in intrusive igneous rocks (sills and laccoliths). The Leading Edge 28, 804-811, doi: 10.1190/1.3167782.

Dessanti, R.N., 1959. Geologia del Cerro Alquitran y alrededores, Departamento de San Rafael (Prov. de Mendoza). Museo de La Plata, Notas XIX, Geológia 71, 301-325.

Dyhr, C.T., Holm, P.M., Llambías, E.J., 2013a. Geochemical constraints on the relationship between the Miocene–Pliocene volcanism and tectonics in the Palaoco and Fortunoso volcanic fields, Mendoza Region, Argentina: New insights from 40Ar/39Ar dating, Sr–Nd–Pb isotopes and trace elements. J. Volcanol. Geotherm. Res. 266, 50-68, doi: https://doi.org/10.1016/j.jvolgeores.2013.08.005.

Dyhr, C.T., Holm, P.M., Llambías, E.J., Scherstén, A., 2013b. Subduction controls on Miocene back-arc lavas from Sierra de Huantraico and La Matancilla and new 40Ar/39Ar dating from the Mendoza Region, Argentina. Lithos 179, 67-83, doi: https://doi.org/10.1016/j.lithos.2013.08.007.

1596 Eide, C.H., Schofield, N., Jerram, D.A., Howell, J.A., 2016. Basin-scale architecture of
1597 deeply emplaced sill complexes: Jameson Land, East Greenland. J. Geol. Soc. 174,
1598 23-40, doi: 10.1144/jgs2016-018.

1599 Eide, C.H., Schofield, N., Lecomte, I., Buckley, S.J., Howell, J.A., 2018. Seismic
1600 Interpretation of Sill-Complexes in Sedimentary Basins: The 'Sub-Sill Imaging
1601 Problem. J. Geol. Soc. 175, 193-209.

1602 Einsele, G., Gieskes, J.M., Curray, J., Moore, D.M., Aguayo, E., Aubry, M.-P., Fornari,
1603 D., Guerrero, J., Kastner, M., Kelts, K., Lyle, M., Matoba, Y., Molina-Cruz, A., Niemitz,
1604 J., Rueda, J., Saunders, A., Schrader, H., Simoneit, B., Vacquier, V., 1980. Intrusion
1605 of basaltic sills into highly porous sediments, and resulting hydrothermal activity.
1606 Nature 283, 441-445, doi: 10.1038/283441a0.

1607 Farooqui, M.Y., Hou, H., Li, G., Machin, N., Neville, T., Pal, A., Shrivastva, C., Wang,
1608 Y., Yang, F., Yin, C., 2009. Evaluating volcanic reservoirs. Oilfield Review 21, 36-47.

1609 Feinstein, H., de la Cal, H., Villarreal, A., Berdini, O., 2022. Yacimiento San Martín:
1610 reservorio de hidrocarburos en rocas volcánicas naturalmente fracturadas de la Serie
1611 Tobífera, Cuenca Austral, Tierra del Fuego, Argentina, X Congreso de Exploración y
1612 Desarrollo de Hidrocarburos. Instituo Argentino del Petroleo y del Gas, Mendoza, pp.
1613 21-36.

1614 Fennell, L.M., Folguera, A., Naipauer, M., Gianni, G., Rojas Vera, E.A., Bottesi, G.,
1615 Ramos, V.A., 2017. Cretaceous deformation of the southern Central Andes:
1616 synorogenic growth strata in the Neuquén Group (35° 30′–37° S). Basin Res. 29, 51-
1617 72, doi: https://doi.org/10.1111/bre.12135.

1618 Fjeldskaar, W., Helset, H.M., Johansen, H., Grunnaleite, I., Horstad, I., 2008. Thermal
1619 modelling of magmatic intrusions in the Gjallar Ridge, Norwegian Sea: implications for
1620 vitrinite reflectance and hydrocarbon maturation. Basin Res. 20, 143-159, doi:
1621 10.1111/j.1365-2117.2007.00347.x.

1622 Galerne, C.Y., Hasenclever, J., 2019. Distinct Degassing Pulses During Magma
1623 Invasion in the Stratified Karoo Basin—New Insights From Hydrothermal Fluid Flow
1624 Modeling. G3 20, 2955-2984, doi: https://doi.org/10.1029/2018GC008120.

1625 Galland, O., de la Cal, H., Mescua, J., Rabbel, O., 2022. 3-dimensional trapdoor
1626 structure of laccolith-induced doming and implications for laccolith emplacement,
1627 Pampa Amarilla, Mendoza Province, Argentina. Tectonophysics 836, 229418, doi:
1628 https://doi.org/10.1016/j.tecto.2022.229418.

1629 Galland, O., Hallot, E., Cobbold, P.R., Ruffet, G., de Bremond d'Ars, J., 2007.
1630 Volcanism in a compressional Andean setting: A structural and geochronological study
1631 of Tromen volcano (Neuquén province, Argentina). Tectonics 26, TC4010, doi:
1632 10.1029/2006TC002011.

Galland, O., Scheibert, J., 2013. Analytical model of surface uplift above axisymmetric flat-lying magma intrusions: Implications for sill emplacement and geodesy. J. Volcanol. Geotherm. Res. 253, 114-130, doi: http://dx.doi.org/10.1016/j.jvolgeores.2012.12.006.

Galland, O., Spacapan, J.B., Rabbel, O., Mair, K., Soto, F.G., Eiken, T., Schiuma, M., Leanza, H.A., 2019. Structure, emplacement mechanism and magma-flow significance of igneous fingers – Implications for sill emplacement in sedimentary basins. J. Struct. Geol. 124, 120–135, doi: https://doi.org/10.1016/j.jsg.2019.04.013.

Galland, O., Villar, H., Mescua, J., Jerram, D.A., Messager, G., Medialdea, A., Midtkandal, I., Palma, J.O., Planke, S., Augland, L.E., Zanella, A., 2024. Structural control of igneous intrusions on fluid migration in sedimentary basins: the case study of large bitumen seeps at Cerro Alquitrán and Cerro La Paloma, northern Neuquén Basin, Argentina, in: Kilhams, B., Watson, D., Holford, S. (Eds.), The Impacts of Igneous Systems on Sedimentary Basins and Their Energy Resources. Geological Society, London, Special Publications, doi: https://doi.org/10.1144/SP547-2023-115.

Galland, O., Villar, H.J., Mescua, J., Jerram, D.A., Midtkandal, I., Palma, J.O., Planke, S., Zanella, A., 2023. The long-term legacy of subvolcanic intrusions on fluid migration in sedimentary basins: The Cerro Alquitrán case study, northern Neuquén Basin, Argentina. Basin Res. 35, 1840-1855, doi: https://doi.org/10.1111/bre.12782.

Garrido, A.C., Kramarz, A., Forasiepi, A., Bond, M., 2012. Estratigrafía, mamíferos fósiles y edad de las secuencias volcanosedimentarias eoceno-miocenas de la sierra de Huantraico-sierra Negra y cerro Villegas (provincia del Neuquén, Argentina). Andean geology 39, 482-510.

Gilbert, G.K., 1877. Report on the geology of the Henry Mountains. U.S. Geogr. Geol. Surv. Rocky Mountain Region (Powel), p. 160.

González, P.D., Aragón, E., 2000. El Cerro Bayo de la Sierra Negra, Neuquén: ejemplo de un lacolito tipo Arbol de Navidad. Revista de la Asociacion Geologica Argentina 55, 363-377.

Groeber, P., 1923. Origen del petróleo de Barrancas. Deducciones que sugiere su estudio. Boletín de la Direccion General de Minas, Geología e Hidrología, Serie F (Informes Preliminares y Comunicaciones) 6, 3—14.

Groeber, P., 1946. Observaciones geológicas a lo largo del meridiano 70° 1. Hoja Chos Malal. Revista de la Sociedad Geológica Argentina 1, 177-208.

Groom, R.W., Bailey, R.C., 1989. Decomposition of magnetotelluric impedance tensors in the presence of local three-dimensional galvanic distortion. J. Geophys. Res. 94, 1913-1925, doi: https://doi.org/10.1029/JB094iB02p01913.

1669 Gu, L., Ren, Z., Wu, C., Zhao, M., Qiu, J., 2002. Hydrocarbon Reservoirs in a Trachyte
1670 Porphyry Intrusion in the Eastern Depression of the Liaohe Basin, Northeast China.
1671 AAPG Bull. 86, 1821-1832, doi: 10.1306/61EEDD8C-173E-11D7-
1672 8645000102C1865D.

1673 Gulisano, C.A., Gutiérrez Pleimling, A.R., 1995. Field Guide the Jurassic of the
1674 Neuquén Basin: B, Mendoza Province. Secretaría de Minería de la Nación (ISSN
1675 0328-2317) and Asociación Geológica Argentina (ISSN 0328-3933).

1676 Gürer, D., Galland, O., Corfu, F., Leanza, H.A., Sassier, C., 2015. Structure and
1677 evolution of volcanic plumbing systems in fold-and-thrust belts: A case study of the
1678 Cerro Negro de Tricao Malal, Neuquén Province, Argentina. Geol. Soc. Am. Bull., doi:
1679 10.1130/b31341.1.

1680 Guzmán, C.G., Cristallini, E.O., Bottesi, G.L., 2007. Contemporary stress orientations
1681 in the Andean retroarc between 34°S and 39°S from borehole breakout analysis.
1682 Tectonics 26, doi: 10.1029TC001958.

1683 Hansen, D.M., Cartwright, J.A., 2006. The three-dimensional geometry and growth of
1684 forced folds above saucer-shaped igneous sills. J. Struct. Geol. 28, 1520-1535.

1685 Healy, D., Rizzo, R.E., Cornwell, D.G., Farrell, N.J.C., Watkins, H., Timms, N.E.,
1686 Gomez-Rivas, E., Smith, M., 2017. FracPaQ: A MATLAB™ toolbox for the
1687 quantification of fracture patterns. J. Struct. Geol. 95, 1-16, doi:
1688 https://doi.org/10.1016/j.jsg.2016.12.003.

1689 Holford, S.P., Schofield, N., Jackson, C.A.L., Magee, C., Green, P.F., Duddy, I.R.,
1690 2013. Impacts of Igneous Intrusions on Source and Reservoir Potential in Prospective
1691 Sedimentary Basins Along the Western Australian Continental Margin.

1692 Holmberg, E., 1962. Descripción geológica de la hoja 32-d, Chachahuén. Provincias
1693 de Neuquén y Mendoza, Argentina. Dir. Nac. Geol. Y Minería, Boletín 90.

1694 Holmberg, E., 1975. Descripción geológica de la Hoja 32c, Buta Ranquil (Prov.
1695 Mendoza-Neuquén), *Bull. 152*. Serv. Nac. Min. Geol., Buenos Aires, p. 71.

1696 Howell, J.A., Schwartz, E., Spalletti, L.A., Veiga, G.D., 2005. The Neuquén Basin: an
1697 overview, in: Howell, J.A., Schwartz, E., Spalletti, L.A., Veiga, G.D. (Eds.), The
1698 Neuquén Basin, Argentina: A case study in sequence stratigraphy and basin
1699 dynamics. Geological Society, London, Special Publications, pp. 1-14, doi:
1700 https://doi.org/10.1144/GSL.SP.2005.252.01.01.

1701 Hudec, M.R., Jackson, M.P.A., 2007. Terra infirma: Understanding salt tectonics.
1702 Earth-Sci. Rev. 82, 1-28, doi: http://dx.doi.org/10.1016/j.earscirev.2007.01.001.

Iyer, K., Rüpke, L., Galerne, C.Y., 2013. Modeling fluid flow in sedimentary basins with sill intrusions: Implications for hydrothermal venting and climate change. G3 14, 5244-5262, doi: 10.1002/2013GC005012.

Iyer, K., Schmid, D.W., Planke, S., Millett, J., 2017. Modelling hydrothermal venting in volcanic sedimentary basins: Impact on hydrocarbon maturation and paleoclimate. Earth Planet. Sci. Lett. 467, 30-42, doi: https://doi.org/10.1016/j.epsl.2017.03.023.

Iyer, K., Svensen, H., Schmid, D.W., 2018. SILLi 1.0: a 1-D numerical tool quantifying the thermal effects of sill intrusions. Geosci. Model Dev. 11, 43-60, doi: 10.5194/gmd-11-43-2018.

Jackson, C.A.-L., Schofield, N., Golenkov, B., 2013a. Geometry and controls on the development of igneous sill–related forced folds: A 2-D seismic reflection case study from offshore southern Australia. Geological Society of America Bulletin 125, 1874-1890, doi: 10.1130/b30833.1.

Jackson, C.A.L., Schofield, N., Golenkov, B., 2013b. Geometry and controls on the development of igneous sill-related forced-folds: a 2D seismic reflection case study from offshore southern Australia. Geol. Soc. Am. Bull. 125, 1874-1890.

Jackson, M.D., 1997. Processes of laccolithic emplacement in the Southern Henry Mountains, Southeastern Utah, in: Friedman, J.D., Huffman, A.C. (Eds.), Laccolith complexes of Southeastern Utah: time of emplacement and tectonic setting - Workshop proceedings. U.S. Geological Survey Bulletin 2158, pp. 51-59.

Jackson, M.D., Pollard, D.D., 1990. Flexure and faulting of sedimentary host rocks during growth of igneous domes, Henry Mountains, Utah. J. Struct. Geol. 12, 185-206.

Jerram D, A., Mountney N, P., Howell J, A., Long, D., Stollhofen, H., 2000. Death of a sand sea: an active aeolian erg systematically buried by the Etendeka flood basalts of NW Namibia. J. Geol. Soc. 157, 513-516, doi: 10.1144/jgs.157.3.513.

Jerram, D.A., 2021. Introducing Volcanology: A guide to hot rocks. Dunedin Academic Press.

Jerram, D.A., Davis, G.R., Mock, A., Charrier, A., Marsh, B.D., 2010. Quantifying 3D crystal populations, packing and layering in shallow intrusions: A case study from the Basement Sill, Dry Valleys, Antarctica. Geoscphere 6, 537--548, doi: https://doi.org/10.1130/GES00538.1.

Jerram, D.A., Millett, J., Planke, S., 2022. Petroleum prospectivity in volcanic basins: an overview on understanding volcanic facies relationships and rock properties in volcanic margins, XI Congreso de Exploración y Desarrollo de Hidrocarburos. Instituto Argentino del Petroleo y del Gas, Mendoza, p. 143—156.

1738 Jiang, W., Roach, I.C., Doublier, M.P., Duan, J., Schofield, A., Clark, A.H., Brodie, R.C.,
1739 2024. Application of audio-frequency magnetotelluric data to cover characterisation–
1740 validation against borehole petrophysics in the East Tennant region, Northern
1741 Australia. Exploration Geophysics 55, 466–485, doi:
1742 https://doi.org/10.1080/08123985.2023.2246492.

1743 Jiaqi, L., Pujun, W., Yan, Z., Weihua, B., Yulong, H., Huafeng, T., Xiaoyu, C., 2012.
1744 Volcanic Rock-Hosted Natural Hydrocarbon Resources: A Review, in: Karoly, N. (Ed.),
1745 Updates in Volcanology. IntechOpen, Rijeka, p. Ch. 4, doi: 10.5772/54587.

1746 Johannesen, R.M.I., Ólavsdóttir, J., Boldreel, L.O., Eidesgaard, Ó., Senger, K.,
1747 Galland, O., 2025. Revisiting the Stratigraphy and Structure of the Faroe Islands Flood
1748 Basalts for Large-Scale CO2 Storage in Basalt Reservoirs. Basin Res. 37, doi:
1749 https://doi.org/10.1111/bre.70032.

1750 Kay, S.M., Burns, W.M., Copeland, P., Mancilla, O., 2006a. Upper Cretaceous to
1751 Holocene magmatism and evidence for transient Miocene shallowing of the Andean
1752 subduction zone under the northern Neuquén basin, in: Kay, S.M., Ramos, V. (Eds.),
1753 Evolution of an Andean Margin: A Tectonic and Magmatic View from the Andes to the
1754 Neuquén Basin (35° - 39°S lat.). Geol. Soc. Amer. Spec. Pap., pp. 19-60.

1755 Kay, S.M., Copeland, P., 2006. Early to middle Miocene backarc magmas of the
1756 Neuquén basin: Geochemical consequences of slab shallowing and the westwarddrift
1757 of South America, in: Kay, S.M., Ramos, V. (Eds.), Evolution of an Andean Margin: A
1758 Tectonic and Magmatic View from the Andes to the Neuquén Basin (35° - 39°S lat.).
1759 Geological Sociey of America Special Papers, pp. 185-213.

1760 Kay, S.M., Mancilla, O., Copeland, P., 2006b. Evolution of the late Miocene
1761 Chachahuén volcanic complex at 37ºS over the transient shallow subduction zone
1762 under the Neuquén Andes, in: Kay, S.M., Ramos, V. (Eds.), Evolution of an Andean
1763 Margin: A Tectonic and Magmatic View from the Andes to the Neuquén Basin (35° -
1764 39°S lat.). Geological Sociey of America Special Papers, pp. 215-246.

1765 Keidel, J., 1910. La zona del Mesozoico en la falda oriental de la Cordillera entre el
1766 río Diamante y el río Neuquén. Anales del Ministerio de Agricultura Nacional, Seccion
1767 Geología 5, 27—65.

1768 Kerr, A.D., Pollard, D.D., 1998. Toward more realistic formulations for the analysis of
1769 laccoliths. J. Struct. Geol. 20, 1783-1793.

1770 Kilhams, B., Holford, S., Gardiner, D., Gozzard, S., Layfield, L., McLean, C., Thackrey,
1771 S., Watson, D., 2024. The impacts of igneous systems on sedimentary basins and
1772 their energy resources, Geol. Soc. London. Spec. Pub. The Geological Society of
1773 London, pp. 1-11, doi: 10.1144/SP547-2023-213.

1774 Kjenes, M., Eide, C.H., Argüello Scotti, A., Lecomte, I., Schofield, N., Bøgh, A., 2024.
1775 Lithological influence on sill geometry in sedimentary basins: Controls and recognition

in reflection seismic data. Basin Res. 36, e12857, doi: https://doi.org/10.1111/bre.12857.

Kobchenko, M., Hafver, A., Jettestuen, E., Renard, F., Galland, O., Jamtveit, B., Meakin, P., Dysthe, D.K., 2014. Evolution of a fracture network in an elastic medium with internal fluid generation and expulsion. Physical Review E 90, 052801.

Kobchenko, M., Panahi, H., Renard, F., Dysthe, D.K., Malthe-Sørenssen, A., Mazzini, A., Scheibert, J., Jamtveit, B., Meakin, P., 2011. 4D imaging of fracturing in organic-rich shales during heating. J. Geophys. Res. 116, n/a-n/a, doi: 10.1029/2011JB008565.

Koch, F.G., Johnson, A.M., Pollard, D.D., 1981. Monoclinal bending of strata over laccolithic intrusions. Tectonophysics 74, T21-T31, doi: http://dx.doi.org/10.1016/0040-1951(81)90189-X.

Kozlowski, E., Manceda, R., Ramos, V., Ramos, V., 1993a. Estructura, Geología y Recursos Naturales de Mendoza: Relatorio del 12 Congreso Geológico Argentino y 2 Congreso de Exploración de Hidrocarburos, I (18), pp. 235-256.

Kozlowski, E., Manceda, R., VRamos, V., 1993b. Estructura, in: Ramos, V.A. (Ed.), Geología y Recursos Naturales de Mendoza: 12 Congreso Geológico Argentina y 2 Congreso de Exploración de Hidrocarburos, Relatorio, pp. 235-256.

Kroeger, K.F., Bischoff, A.P., Nicol, A., 2022. Petroleum systems in a buried stratovolcano: Maturation, migration and leakage. Mar. Pet. Geol. 141, 105682, doi: https://doi.org/10.1016/j.marpetgeo.2022.105682.

Lecomte, I., Lavadera, P.L., Botter, C., Anell, I., Buckley, S.J., Eide, C.H., Grippa, A., Mascolo, V., Kjoberg, S., 2016. 2 (3) D convolution modelling of complex geological targets beyond–1D convolution. First Break 34, 99-107.

Liu, E., Wang, H., Tonguç Uysal, I., Zhao, J.x., Wang, X.-C., Feng, Y., Pan, S., 2017. Paleogene igneous intrusion and its effect on thermal maturity of organic-rich mudstones in the Beibuwan Basin, South China Sea. Mar. Pet. Geol. 86, 733-750, doi: https://doi.org/10.1016/j.marpetgeo.2017.06.026.

Llambías, E.J., Rapela, C.W., 1988. Las volcanitas de Collipilli, Neuquén (37°S) y su relación con otras unidades paleógenas de la cordillera. Revista de la Asociación Geológica Argentina 44, 224-236.

Lombardo, E.F., Galland, O., Yagupsky, D., Jerram, D.A., 2024. Characterization of a structural trap associated with an intrusive complex: the El Trapial Oil Field, Neuquén basin, Argentina, in: Kilhams, B., Watson, D., Holford, S. (Eds.), Geol. Soc. London. Spec. Pub. Geological Society, London, Special Publications, doi: 10.1144/SP547-2023-98.

Lombardo, E.F., Yagupsky, D., Jerram, D.A., Galland, O., under review. Seismic Imaging of Subvertical Dykes in Sedimentary Basins: A Case Study from the Huantraico Volcanic Complex, Neuquén Basin, Argentina. Global and Planetary Change.

Longo, L.M., 2017. Caracterización de la estructura del complejo volcánico Auca Mahuida mediante datos aeromagnéticos y gravimétricos. Universidad Nacional de La Plata.

Magee, C., Hunt-Stewart, E., Jackson, C.A.L., 2013. Volcano growth mechanisms and the role of sub-volcanic intrusions: Insights from 2D seismic reflection data. Earth and Planetary Science Letters 373, 41-53, doi: doi: 10.1016/j.epsl.2013.04.041.

Magee, C., Jackson, C.A.L., 2020. Seismic reflection data reveal the 3D structure of the newly discovered Exmouth Dyke Swarm, offshore NW Australia. Solid Earth 11, 579-606, doi: 10.5194/se-11-579-2020.

Magee, C., Jackson, C.A.L., Schofield, N., 2014. Diachronous sub-volcanic intrusion along deep-water margins: insights from the Irish Rockall Basin. Basin Res. 26, 85-105, doi: 10.1111/bre.12044.

Magee, C., Maharaj, S.M., Wrona, T., Jackson, C.A.L., 2015. Controls on the expression of igneous intrusions in seismic reflection data. Geosphere 11, 1024-1041, doi: 10.1130/GES01150.1.

Magee, C., Stevenson, C.T.E., Ebmeier, S.K., Keir, D., Hammond, J.O.S., Gottsmann, J.H., Whaler, K.A., Schofield, N., Jackson, C.A.L., Petronis, M.S., O'Driscoll, B., Morgan, J., Cruden, A., Vollgger, S.A., Dering, G.M., Micklethwaite, S., Jackson, M.D., 2018. Magma Plumbing Systems: A Geophysical Perspective. Journal of Petrology 59, 1217-1251, doi: 10.1093/petrology/egy064.

Maresh, J., White, R.S., Hobbs, R.W., Smallwood, J.R., 2006. Seismic attenuation of Atlantic margin basalts: Observations and modeling. Geophysics 71, B211-B221, doi: 10.1190/1.2335875.

Maretto, H., Carbone, O., Gazzera, C., Schiuma, M., 2002. Los Reservorios de la Formación Tordillo, in: Schiuma, M., Hinterwimmer, H., Vergani, G. (Eds.), Rocas Reservorio de las Cuencas Productivas Argentinas. V Congreso de Exploración y Desarrollo de Hidrocarburos. Instituto Argentino del Petroleo y del Gas, Mar del Plata, Argentina, pp. 335–358.

Mark, N.J., Schofield, N., Pugliese, S., Watson, D., Holford, S., Muirhead, D., Brown, R., Healy, D., 2018. Igneous intrusions in the Faroe Shetland basin and their implications for hydrocarbon exploration; new insights from well and seismic data. Mar. Pet. Geol. 92, 733-753, doi: https://doi.org/10.1016/j.marpetgeo.2017.12.005.

Masarik, M.C., 2002. Los Reservorios de las Formaciones Agrio y Huitrín: Introducción, in: Schiuma, M., Hinterwimmer, H., Vergani, G. (Eds.), Rocas Reservorio de las Cuencas Productivas Argentinas. V Congreso de Exploración y Desarrollo de Hidrocarburos. Instituto Argentino del Petroleo y del Gas, Mar del Plata, Argentina, pp. 427–431.

McHilroy, D., Flint, S., Howell, J.A., Timms, N.E., 2005. Sedimentology of the tide-dominated Jurassic Lajas Formation, Neuquén Basin, Argentina, in: Viega, G.D., Spalletti, A., Howell, J.A., Schwarz, E. (Eds.), The Neuquén Basin, Argentina: A Case Study in Sequence Stratigraphy and Basin Dynamic. Geological Society, London, Special Publications, p. 83—107.

McNeice, G.W., Jones, A.G., 2001. Multisite, multifrequency tensor decomposition of magnetotelluric data. GEOPHYSICS 66, 158-173, doi: 10.1190/1.1444891.

Minisini, D., Fryklund, B., Gerali, F., Fantín, M., 2020. The first economical unconventional play outside North America: Context, history, and

“coopetition”, in: Minisini, D., Fantín, M., Lanusse Noguera, I., Leanza, H.A. (Eds.), Integrated geology of unconventionals: The case of the Vaca Muerta Play, Argentina. The American Association of Petroleum Geologists, Tulsa, Ohklahoma USA, pp. 1–24, doi: 10.1306/13682221M1203264.

Morley, C.K., 2018. 3-D seismic imaging of the plumbing system of the Kora Volcano, Taranaki Basin, New Zealand: The influence of syn-rift structure on shallow igneous intrusion architecture. Geosphere 14, 2533-2584, doi: 10.1130/GES01645.1.

Muirhead, J.D., Airoldi, G., Rowland, J.V., White, J.D.L., 2012. Interconnected sills and inclined sheet intrusions control shallow magma transport in the Ferrar large igneous province, Antarctica. Geol. Soc. Am. Bull. 124, 162-180, doi: 10.1130/b30455.1.

Nelson, C.E., Hobbs, R.W., Rusch, R., 2015. On the Use of Fractal Surfaces to Understand Seismic Wave Propagation in Layered Basalt Sequences. Pure Appl. Geophys. 172, 1879-1892, doi: 10.1007/s00024-014-0986-5.

Neumann, E.-R., Callegaro, S., Jacobsen, S.B., Hyung, E., Svensen, H.H., Larsen, B.T., Eriksen, Z.T., 2025. Geodynamic evolution of the first basaltic volcanism (B1) in the Oslo Rift (Southeast Norway). Lithos 512-513, 108133, doi: https://doi.org/10.1016/j.lithos.2025.108133.

Nullo, F.E., Stephens, G.C., Otamendi, J., Baldauf, P.E., 2002. El volcanismo del Tertiario superior del sur de Mendoza. Revista de la Asociación Geológica Argentina 57, 119-132.

Orchuela, I., Lara, M.E., Suarez, M., 2003. Productive Large Scale Folding Associated with Igneous Intrusions: El Trapial Field, Neuquen Basin, Argentina, AAPG International Conference, Barcelona, Spain.

Pallares, C., Quidelleur, X., Gillot, P.-Y., Kluska, J.-M., Tchilinguirian, P., Sarda, P., 2016. The temporal evolution of back-arc magmas from the Auca Mahuida shield volcano (Payenia Volcanic Province, Argentina). J. Volcanol. Geotherm. Res. 323, 19-37, doi: https://doi.org/10.1016/j.jvolgeores.2016.04.043.

Palma, J.O., Burchardt, S., Schmiedel, T., Guerriero, L., Jerram, D.A., Mair, K., Leanza, H.A., Galland, O., 2024a. Stratigraphy and structure of Chachahuén volcanic complex, southern Mendoza province, Argentina. J. S. Amer. Earth. Sci. 140, 104900, doi: https://doi.org/10.1016/j.jsames.2024.104900.

Palma, J.O., Rabbel, O., Spacapan, J.B., Ruiz, R., Galland, O., 2024b. The Cara Cura intrusive complex, Neuquén Basin, Argentina: a field analogue of a whole igneous petroleum system, in: Kilhams, B., Watson, D., Holford, S. (Eds.), The Impacts of Igneous Systems on Sedimentary Basins and Their Energy Resources. Geological Society, London, Special Publications, doi: https://doi.org/10.1144/SP547-2023-119.

Parnell, J., Carey, P.F., 1995. Emplacement of bitumen (asphaltite) veins in the Neuquén Basin, Argentina. AAPG Bull. 79, 1798-1815.

Petford, N., McCaffrey, K., 2003. Hydrocarbons in crystalline rocks. Geological Society, London, Special Publications, London.

Planke, S., Rasmussen, T., Rey, S.S., Myklebust, R., 2005. Seismic characteristics and distribution of volcanic intrusions and hydrothermal vent complexes in the Vøring and Møre basins, in: Doré, A.G., Vining, B.A. (Eds.), Petroleum Geology: North-West Europe and Global Perspectives—Proceedings of the 6th Petroleum Geology Conference. Geological Society, London, London, pp. 833-844.

Planke, S., Svensen, H., Myklebust, R., Bannister, S., Manton, B., Lorenz, L., 2015. Geophysics and Remote Sensing, in: Breitkreuz, C., Rocchi, S. (Eds.), Advances in Volcanology. Springer Berlin Heidelberg, pp. 1-16, doi: doi: 10.1007/11157_2014_6.

Planke, S., Symonds, P.A., Alvestad, E., Skogseid, J., 2000. Seismic volcanostratigraphy of large-igneous basaltic extrusive complexes on rifted margins. J. Geophys. Res. 105, 19335-19351.

Pollard, D.D., Johnson, A.M., 1973. Mechanics of growth of some laccolithic intrusions in the Henry Mountains, Utah, II. Bending and failure of overburden layers and sill formation. Tectonophysics 18, 311-354.

Polteau, S., Corfu, F., Svensen, H., Planke, S., 2010. Rapid emplacement of the Karoo Basin sill complex during the Toarcian revealed by U-Pb dating of zircons, Vienna.

Poppe, S., Galland, O., de Winter, N.J., Goderis, S., Claeys, P., Debaille, V., Boulvais, P., Kervyn, M., 2020. Structural and Geochemical Interactions Between Magma and Sedimentary Host Rock: The Hovedøya Case, Oslo Rift, Norway. G3 21, doi: 10.1029/2019GC008685.

Rabbel, O., Galland, O., Mair, K., Lecomte, I., Senger, K., Spacapan, J.B., Manceda, R., 2018. From field analogues to realistic seismic modelling: a case study of an oil-producing andesitic sill complex in the Neuquén Basin, Argentina. J. Geol. Soc., doi: 10.1144/jgs2017-116.

Rabbel, O., Hasenclever, J., Galerne, C.Y., Galland, O., Mair, K., Palma, O., 2023. Impact of permeability evolution in igneous sills on hydrothermal flow and hydrocarbon transport in volcanic sedimentary basins. Solid Earth 14, 625-646, doi: 10.5194/se-14-625-2023.

Rabbel, O., Mair, K., Galland, O., Grühser, C., Meier, T., 2020. Numerical Modeling of Fracture Network Evolution in Organic-Rich Shale With Rapid Internal Fluid Generation. J. Geophys. Res. 125, e2020JB019445, doi: https://doi.org/10.1029/2020JB019445.

Rabbel, O., Palma, J.O., Mair, K., Galland, O., Spacapan, J.B., Senger, K., 2021. Fracture networks in shale-hosted igneous intrusions: Processes, distribution and implications for igneous petroleum systems. J. Struct. Geol. 150, 104403, doi: https://doi.org/10.1016/j.jsg.2021.104403.

Ramos, V.A., Barbieri, M., 1988. El volcanismo cenozoico de Huantraico: edad y relaciones isotopicas iniciales, provincia del Neuquen. Asociacion Geologica Argentina 43, 210-223.

Ramos, V.A., Folguera, A., 2011. Payenia volcanic province in the Southern Andes: An appraisal of an exceptional Quaternary tectonic setting. J. Volcanol. Geotherm. Res. 201, 53-64, doi: https://doi.org/10.1016/j.jvolgeores.2010.09.008.

Ramos, V.A., Vujovich, G., Martino, R., Otamendi, J., 2010. Pampia: A large cratonic block missing in the Rodinia supercontinent. J. Geodyn. 50, 243-255, doi: https://doi.org/10.1016/j.jog.2010.01.019.

Rateau, R., Schofield, N., Smith, M., 2013. The potential role of igneous intrusions on hydrocarbon migration, West of Shetland. Petroleum Geoscience 19, 259-272, doi: 10.1144/petgeo2012-035.

Rodriguez Monreal, F., Villar, H.J., Baudino, R., Delpino, D., Zencich, S., 2009. Modeling an atypical petroleum system: A case study of hydrocarbon generation, migration and accumulation related to igneous intrusions in the Neuquén Basin, Argentina. Mar. Pet. Geol. 26, 590-605, doi: http://dx.doi.org/10.1016/j.marpetgeo.2009.01.005.

Rohrman, M., 2007. Prospectivity of volcanic basins: Trap delineation and acreage de-risking. AAPG Bull. 91, 915-939, doi: 10.1306/12150606017.

Rossello, E.A., Cobbold, P.R., Diraison, M., Arnaud, N., 2002. Auca Mahuida (Neuquén basin, Argentina): A Quaternary shield volcano on a hydrocarbon-producing substrate, 5th ISAG, Extended Abstracts, Toulouse, pp. 549-552.

Roth, R.L., 2017. Volcán Auca Mahuida—ADQUISICIÓN ZVSP - WALKAWAY (p. 1.6) - Internal Report. YPF.

Sanford, O.G., Hobbs, R.W., Brown, R.J., Schofield, N., 2023. Uncertainties in Ray-Tracing Tomography Models Used for Sub-Basalt Seismic Imaging. Pure Appl. Geophys. 180, 145-156, doi: 10.1007/s00024-022-03199-2.

Schiuma, M.F., 1994. Intrusivos del valle del Río Grande, provincia de Mendoza, su importancia como productores de hidrocarburos, Facultad de Ciencias Naturales y Museo. Universidad Nacional de La Plata, La Plata.

Schmiedel, T., Galland, O., Haug, Ø.T., Dumazer, G., Breitkreuz, C., 2019. Coulomb failure of Earth's brittle crust controls growth, emplacement and shapes of igneous sills, saucer-shaped sills and laccoliths. Earth Planet. Sci. Lett. 510, 161-172, doi: https://doi.org/10.1016/j.epsl.2019.01.011.

Schmiedel, T., Kjoberg, S., Planke, S., Magee, C., Galland, O., Schofield, N., Jackson, C.A.-L., Jerram, D.A., 2017. Mechanisms of overburden deformation associated with the emplacement of the Tulipan sill, mid-Norwegian margin. Interpretation 5, SK23-SK38, doi: 10.1190/int-2016-0155.1.

Schmitt, R.R., Andrews, G.D.M., Moore, J.G., Paronish, T., Workman, S., Gumowski, L.M., Brown, S.R., Crandall, D., Neubaum, J., 2023. Self-sealing mafic sills for carbon and hydrogen storage, Enabling Secure Subsurface Storage in Future Energy Systems. Geological Society of London, p. 0, doi: 10.1144/SP528-2022-43.

Schofield, N., Holford, S.P., Millett, J., Brown, D.J., Jolley, D., Passey, S.R., Muirhead, D., Grove, C., Magee, C., Murray, J., Hole, M., Jackson, C.A.L., Stevenson, C.T., 2015. Regional magma plumbing and emplacement mechanisms of the Faroe-Shetland Sill Complex: implications for magma transport and petroleum systems within sedimentary basins. Basin Res., doi: 10.1111/bre.12164.

Schuler, J., Christie, P.A.F., White, R.S., 2015. Effect of flood basalt stratigraphy on the phase of seismic waveforms recorded offshore Faroe Islands. Geophysics 80, D265-D279, doi: 10.1190/geo2014-0308.1.

Schutter, S.R., 2003. Occurrences of hydrocarbons in and around igneous rocks. Geol. Soc. London. Spec. Pub. 214, 35-68, doi: 10.1144/gsl.sp.2003.214.01.03.

Schwarz, E., Howell, J.A., 2005. Sedimentary evolution and depositional architecture of a lowstand sequence set: the Lower Cretaceous Mulichinco Formation, Neuquén Basin, Argentina. Geol. Soc. London. Spec. Pub. 252, 109-138, doi: 10.1144/gsl.sp.2005.252.01.06.

Senger, K., Millett, J., Planke, S., Ogata, K., Eide, C.H., Festøy, M., Galland, O., Jerram, D.A., 2017. Effects of igneous intrusions on the petroleum system: a review. First Break 35, 47-56, doi: 10.3997/1365-2397.2017011.

Senger, K., Roy, S., Braathen, A., Buckley, S.J., Bælum, K., Gernigon, L., Mjelde, R., Noormets, R., Ogata, K., Olaussen, S., Planke, S., Ruud, B.O., Tveranger, J., 2013. Geometries of doleritic intrusions in central Spitsbergen, Svalbard: an integrated study of an onshore-offshore magmatic province with implications for CO2 sequestration. Norwegian Journal of Geology 93, 143-166.

Sigismondi, M.E., 2012. Estudio de la deformación litosférica de la cuenca Neuquina: Estructura termal, datos de gravedad y sísmica de reflexión, Facultad de Ciencias Exactas y Naturales. Universidad de Buenos Aires.

Simpson, F., Bahr, K., 2005. Practical magnetotellurics. Cambridge University Press.

Sleveland, A.R.N., Midtkandal, I., Galland, O., Leanza, H.A., 2020. Sedimentary Architecture of Storm-Influenced Tidal Flat Deposits of the Upper Mulichinco Formation, Neuquén Basin, Argentina. Frontiers 8.

Søager, N., Holm, P.M., Llambías, E.J., 2013. Payenia volcanic province, southern Mendoza, Argentina: OIB mantle upwelling in a backarc environment. Chemical Geology 349-350, 36-53, doi: https://doi.org/10.1016/j.chemgeo.2013.04.007.

Spacapan, J.B., D'Odorico, A., Palma, O., Galland, O., Rojas Vera, E., Ruiz, R., Leanza, H.A., Medialdea, A., Manceda, R., 2020a. Igneous petroleum systems in the Malargüe fold and thrust belt, Río Grande Valley area, Neuquén Basin, Argentina. Mar. Pet. Geol. 111, 309-331, doi: https://doi.org/10.1016/j.marpetgeo.2019.08.038.

Spacapan, J.B., D'Odorico, A., Palma, O., Galland, O., Senger, K., Ruiz, R., Manceda, R., Leanza, H.A., 2019. Low resistivity zones at contacts of igneous intrusions emplaced in organic-rich formations and their implications on fluid flow and petroleum systems: A case study in the northern Neuquén Basin, Argentina. Basin Res. 0, doi: 10.1111/bre.12363.

Spacapan, J.B., Galland, O., Leanza, H.A., Planke, S., 2016. Control of strike-slip fault on dyke emplacement and morphology. J. Geol. Soc. 173, 573-576, doi: 10.1144/jgs2015-166.

Spacapan, J.B., Galland, O., Leanza, H.A., Planke, S., 2017. Igneous sill and finger emplacement mechanism in shale-dominated formations: a field study at Cuesta del Chihuido, Neuquén Basin, Argentina. J. Geol. Soc. 174, 422-433, doi: 10.1144/jgs2016-056.

Spacapan, J.B., Palma, O., Galland, O., Manceda, R., Rocha, E., D'Odorico, A., Leanza, H.A., 2018. Thermal impact of igneous sill complexes on organic-rich formations and the generation of a petroleum system: case study in the Neuquén

2031 Basin, Argentina. Mar. Pet. Geol. 91, 519-531, doi:
2032 https://doi.org/10.1016/j.marpetgeo.2018.01.018.

2033 Spacapan, J.B., Ruiz, R., Manceda, R., D'Odorico, A., Rocha, E., Rojas Vera, E.,
2034 Medialdea, A., Cattaneo, D., Palma, J.O., Leanza, H.A., Galland, O., 2020b. Oil
2035 Production from a Sill Complex Within the Vaca Muerta Formation, in: Minisini, D.,
2036 Fantín, M., Noguera, I.L., Leanza, H.A. (Eds.), Integrated geology of unconventionals:
2037 the case of the Vaca Muerta play, Argentina. American Association of Petroleum
2038 Geologists, pp. 529–554, doi: 10.1306/13682240M1203844.

2039 Subbarao, P.B.V., Kumar, P.V.V., Chandrasekharam, D., Deshmukh, V., Singh, A.K.,
2040 2023. Magnetotelluric investigations over geothermal provinces of India: an overview.
2041 Turkish Journal of Earth Sciences 32, 149-162.

2042 Sun, Q., Jackson, C.A.L., Magee, C., Xie, X., 2019. Deeply buried ancient volcanoes
2043 control hydrocarbon migration in the South China Sea. Basin Res. 32, 146-162, doi:
2044 10.1111/bre.12372.

2045 Svensen, H., Corfu, F., Polteau, S., Hammer, Ø., Planke, S., 2012. Rapid magma
2046 emplacement in the Karoo Large Igneous Province. Earth Planet. Sci. Lett. 325-326,
2047 1-9, doi: 10.1016/j.epsl.2012.01.015.

2048 Svensen, H., Planke, S., Chevallier, L., Malthe-Sorenssen, A., Corfu, F., Jamtveit, B.,
2049 2007. Hydrothermal venting of greenhouse gases triggering Early Jurassic global
2050 warming. Earth Planet. Sci. Lett. 256, 554-566.

2051 Svensen, H., Planke, S., Malthe-Sorenssen, A., Jamtvelt, B., Myklebust, R., Eldem,
2052 T.R., Rey, S.S., 2004. Release of methane from a volcanic basin as a mechanism for
2053 initial Eocene global warming. Nature 429, 542-545.

2054 Svensen, H., Planke, S., Polozov, A.G., Schmidbauer, N., Corfu, F., Podladchikov, Y.Y.,
2055 Jamtveit, B., 2009. Siberian gas venting and the end-Permian environmental crisis.
2056 Earth Planet. Sci. Lett. 277, 490-500, doi: http://dx.doi.org/10.1016/j.epsl.2008.11.015.

2057 Sylwan, C.A., 2014. Source rock properties of Vaca Muerta Formation, Neuquina
2058 Basin, IX Congreso de Exploración y Desarrollo de Hidrocarburos, Mendoza, p. 365—
2059 386.

2060 Tabod, C.T., Tokam Kamga, A.P., Manguelle-Dicoum, E., Nouayou, R., Nguiya, S.,
2061 2006. An audio-magnetotelluric investigation of the eastern margin of the Mamfe
2062 Basin, Cameroon, IAEA.

2063 Thomson, K., 2007. Determining magma flow in sills, dykes and laccoliths and their
2064 implications for sill emplacement mechanisms. Bull. Volcanol. 70, 183-201.

2065 Thomson, K., Hutton, D., 2004. Geometry and growth of sill complexes: insights using
2066 3D seismic from the North Rockall Trough. Bull. Volcanol. 66, 364-375.

2067 Trude, J., Cartwright, J., Davies, R.J., Smallwood, J., 2003. New technique for dating
2068 igneous sills. Geology 31, 813-816.

2069 Tunik, M., Folguera, A., Naipauer, M., Pimentel, M., Ramos, V.A., 2010. Early uplift
2070 and orogenic deformation in the Neuquén Basin: Constraints on the Andean uplift from
2071 U-Pb and Hf isotopic data of detrital zircons. Tectonophysics 489, 258-273, doi:
2072 http://dx.doi.org/10.1016/j.tecto.2010.04.017.

2073 Turienzo, M., Sánchez, N., Lebinson, F., Peralta, F., Araujo, V., Irastorza, A., Dimieri,
2074 L., 2020. Basement-cover interaction in the mountain front of the Northern Neuquén
2075 fold and thrust belt (37°10' – 37°40' S), Argentina. J. S. Amer. Earth. Sci. 100, 102560,
2076 doi: https://doi.org/10.1016/j.jsames.2020.102560.

2077 Veiga, R.D., Vergani, G.D., Brissón, I.E., Macellari, C.E., Leanza, H.A., 2020. The
2078 Neuquén Super Basin. AAPG Bull. 104, 2521-2555, doi: 10.1306/09092020023.

2079 Ventura, G., De Ritis, R., Longo, M., Chiappini, M., 2013. Terrain characterization and
2080 structural control of the Auca Mahuida volcanism (Neuquén Basin, Argentina).
2081 International Journal of Geographical Information Science, 1-12, doi:
2082 10.1080/13658816.2012.741241.

2083 Vergani, G.D., Tankard, A.J., Belotti, H.J., Welsink, H.J., 1995. Tectonic evolution and
2084 paleogeography of the Neuquén basin, Argentina, in: Tankard, A.J., Suárez, R.,
2085 Welsink, H.J. (Eds.), Petroleum Basins of South America. American Association of
2086 Petroleum Geology Memoir, pp. 383-402.

2087 Villar, H.J., Legarreta, L., Cruz, C.E., Laffitte, G.A., Vergani, G., 2005. Los cinco
2088 sistemas petroleros coexistentes en el sector sudeste de la Cuenca Neuquina:
2089 definición geoquímica y comparación a lo largo de una transecta de 150 km, VI
2090 Congreso de Exploración y Desarrollo de Hidrocarburos, Mar del Plata, Argentina, pp.
2091 50–67.

2092 Wilson, P.I.R., McCaffrey, K.J.W., Wilson, R.W., Jarvis, I., Holdsworth, R.E., 2016.
2093 Deformation structures associated with the Trachyte Mesa intrusion, Henry Mountains,
2094 Utah: Implications for sill and laccolith emplacement mechanisms. J. Struct. Geol. 87,
2095 30-46, doi: http://dx.doi.org/10.1016/j.jsg.2016.04.001.

2096 Witte, J., Bonora, M., Carbone, C., Oncken, O., 2012. Fracture evolution in oil-
2097 producing sills of the Rio Grande Valley, northern Neuquén Basin, Argentina. AAPG
2098 Bull. 96, 1253-1277, doi: 10.1306/10181110152.

2099 Wu, C., Gu, L., Zhang, Z., Ren, Z., Chen, Z., Li, W., 2006. Formation mechanisms of
2100 hydrocarbon reservoirs associated with volcanic and subvolcanic intrusive rocks:
2101 Examples in Mesozoic–Cenozoic basins of eastern China. AAPG Bull. 90, 137-147,
2102 doi: 10.1306/07130505004.

2103 Yao, Z., He, G., Li, C.-F., Dong, C., 2018. Sill geometry and emplacement controlled
2104 by a major disconformity in the Tarim Basin, China. Earth Planet. Sci. Lett. 501, 37-45,
2105 doi: https://doi.org/10.1016/j.epsl.2018.08.026.

2106 Yrigoyen, M.R., 1983. Yrigoyen, Marcelo R. "Reseña sobre los conocimientos y la
2107 explotación de los hidrocarburos en Argentina antes de 1907. Petrotecnia, 16-36.

2108 Zanella, A., Cobbold, P.R., Ruffet, G., Leanza, H.A., 2015. Geological evidence for
2109 fluid overpressure, hydraulic fracturing and strong heating during maturation and
2110 migration of hydrocarbons in Mesozoic rocks of the northern Neuquén Basin, Mendoza
2111 Province, Argentina. J. S. Amer. Earth. Sci. 62, 229-242, doi:
2112 http://dx.doi.org/10.1016/j.jsames.2015.06.006.

2113 Zhao, W.J., Sha, D.M., Huan, H.F., Gao, T., 2019. Preliminary structure framework and
2114 concealed intrusive rocks in the Qingchengzi ore field in northeast China disclosed by
2115 large-scale two-dimensional audio-magnetotelluric sounding. The Society of
2116 Exploration Geophysicist and the Chinese Geophysical Society GEM, 19–22.

2117